

3.4. Conductometric Analysis of Diluted Solutions

In the previous chapter, it was shown that an asymmetric quaternary ammonium salt having sizes between those of tetramethylammonium and tetraethylammonium exhibits the highest conductivity. In order to understand this phenomenon, the conductometric analysis of the diluted solutions was carried out.

Although the conductometric analysis on quaternary ammonium salts including tetraalkylborates [55, 57, 59, 61, 68, 71, 72], halides [56, 57, 59, 60, 63, 65, 67, 68, 71, 72], perchlorates [56, 57, 59, 62, 66, 68, 72], nitrates [60, 62, 64], picrates [58, 68-70, 72], phenolates [64], carboxylates [64], methanesulfonate [64] and hexachloroantimonate [70] in propylene carbonate have been reported, no such experimental data for quaternary ammonium tetrafluoroborates are available in the literature.

This is also the first example of the conductometric analysis on asymmetric quaternary ammonium salts in propylene carbonate and permits a much closer investigation of the relationship between the cation size and the transport properties of the solution than is possible with symmetric cations.

3.4.1. Experimental

Electrolyte preparation

Quaternary ammonium salts were dissolved in propylene carbonate to make about 10 wt % solutions. The water content in these stock solutions (less than 300 ppm) was measured by a moisture meter (Mitsubishi Kasei Co., CA-06) and the concentrations of the stock solutions were calibrated. Impurities were less than 1 ppm, which were determined by a X-ray fluorescence spectrometer (Rigaku Industrial Corp., 3370E) for Cl and Br, and an atomic absorption spectrometer (Hitachi, Z-9000) for Na, K and Fe.

Measurements

The conductivity and density at $25 \pm 0.1^\circ\text{C}$ were measured by a conductivity meter (Toa Electronics, CM-60S) and a digital density meter (PAAR, DMA 45), respectively.

The stock solutions were successively diluted and the molar concentrations C (mol dm^{-3}) were calculated from concentrations m' (mol kg^{-1} -solution) and densities d (g cm^{-3}) by $C = m'd$. The densities were calculated from $d = d_o + Dm'$, where d_o is the density of solvent and D is a characteristic constant of the electrolyte.

The conductivity measurements were carried out at $25 \pm 0.1^\circ\text{C}$ by a bridge (Toa Electronics, CM-25E) and a standard type conductivity cell with a cell constant 0.1017 cm^{-1} (Toa Electronics, CG-2001PL). The molar conductivities Λ were calculated from the experimental electrolytic conductivities after correction for the electrolytic conductivity of the solvent.

Density, viscosity, relative permittivity and electrolytic conductivity of propylene carbonate are 1.1998 g cm^{-3} , $2.513 \times 10^{-2} \text{ P}$ [59], 64.92 [59] and $9 \times 10^{-8} \text{ S cm}^{-1}$, respectively.

3.4.2. Results and Discussion

Molar conductivities

The electrolytic conductivities and densities of the stock solutions are given in Table 6. The concentration of tetramethylammonium tetrafluoroborate was adjusted to one tenth of others due to its low solubility in propylene carbonate. The molar conductivities over the concentration range of 10^{-2} to 10^{-3} mol dm $^{-3}$ are given in Table 7.

Table 6. Electrolytic conductivities and densities of 10 wt % quaternary ammonium tetrafluoroborate / PC electrolytes at 25°C.

Salt	σ / mS cm $^{-1}$	d / g cm $^{-3}$
Me $_4$ N BF $_4$	1.90*	1.2002*
Me $_3$ EtN BF $_4$	13.15	1.2020
Me $_2$ Et $_2$ N BF $_4$	10.17	1.1993
MeEt $_3$ N BF $_4$	10.07	1.1967
Et $_4$ N BF $_4$	9.67	1.1952

* 1 wt %

Table 7. Molar concentrations and molar conductivities of quaternary ammonium tetrafluoroborates in PC at 25°C.

10 3 C / mol dm $^{-3}$	Λ / S cm 2 mol $^{-1}$	10 3 C	Λ	10 3 C	Λ
Me $_4$ N BF $_4$		Me $_3$ EtN BF $_4$		Me $_2$ Et $_2$ N BF $_4$	
9.9614	31.064	10.1722	31.100	9.7448	30.978
7.4716	31.559	7.6256	31.597	7.3076	31.374
4.9810	32.288	5.0865	32.250	4.8729	32.026
2.4910	33.038	2.5434	32.970	2.4372	32.807
1.7439	33.438	1.7823	33.377	1.7067	33.177
0.9974	33.839	1.0184	33.683	0.9789	33.342
MeEt $_3$ N BF $_4$		Et $_4$ N BF $_4$			
10.0680	30.810	9.9510	30.327		
7.5500	31.305	7.4616	30.776		
5.0345	31.799	4.9743	31.299		
2.5175	32.529	2.4906	31.919		
1.7651	32.877	1.7443	32.382		
1.0084	33.174	0.9958	32.691		

Analysis of conductivity data

The conductivity data were analyzed by means of the Fernández-Prini expansion of the Fuoss-Hsia equation (See Chap. 6). Derived parameters are summarized in Table 8, where $\lambda_o(\text{BF}_4^-)$ is 20.43 (See Chap. 4.3).

Walden products $\lambda_o \eta$ of each ion were plotted against the reciprocal of ionic radii r in Fig. 13. Walden products of all quaternary ammonium ions nearly follow the theoretical behavior calculated from Stokes law. This result suggests that all quaternary ammonium ions examined are able to move without adhesion to propylene carbonate.

Derived ion association constants were plotted against ionic radii of cations as shown in Fig. 14. Although the differences among K_A values were small, they decreased with increasing the cation size as was observed in quaternary ammonium carboxylate/ γ -butyrolactone electrolytes [54]. No remarkable difference among K_A values was observed when BF_4^- was replaced by the more electron withdrawn anion $(\text{CF}_3\text{SO}_2)_2\text{N}^-$ [73].

Table 8. Derived parameters in PC at 25°C.

Salt	Λ_0 /S cm ² mol ⁻¹	K_A /dm ³ mol ⁻¹	σ_Λ	λ_{o^+} /S cm ² mol ⁻¹
Me ₄ N BF ₄	35.02	4.7	0.042	14.6
Me ₃ EtN BF ₄	34.88	3.7	0.044	14.5
Me ₂ Et ₂ N BF ₄	34.58	3.4	0.085	14.2
MeEt ₃ N BF ₄	34.32	2.6	0.034	13.9
Et ₄ N BF ₄	33.78	2.7	0.065	13.4

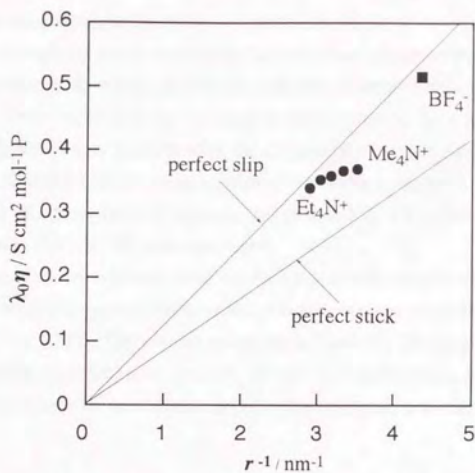


Fig. 13. Walden products as a function of the reciprocal of ionic radii.

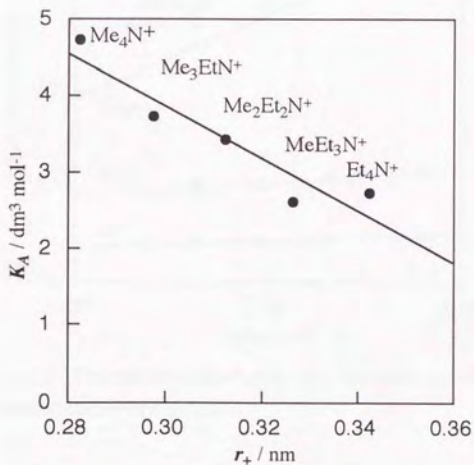


Fig. 14. Effect of cation size on ion association constants.

Estimation of single ion molar conductivities of cyclic cations

Since the single ion limiting molar conductivities of these quaternary ammonium ions are determined chiefly by their sizes not by their shapes [54, 74], those of cations with similar sizes can be easily estimated. Their sizes also can be simply represented by their formula weights FW , because ionic mobilities correlate linearly with the reciprocal of square root of formula weights [75]. The single ion limiting molar conductivities of quaternary ammonium ions were plotted against the reciprocal of square root of formula weights in Fig. 15, where data obtained in γ -butyrolactone [54] and water [74, 76] were also used.

The single ion limiting molar conductivities of dialkylpyrrolidinium, dialkylpiperidinium and spiro ammonium ions were estimated from their formula weights by a linear relationship expressed by $\lambda_o^+ = 38.06 (FW)^{-1/2} + 10.32$. The results are given in Table 9. The single ion limiting molar conductivity decreases by $0.2 \text{ S cm}^2 \text{ mol}^{-1}$ per CH_2 group. A ring formation by the replacement of two methyl groups by a pair of methylene groups doesn't lead to a remarkable increase in conductivity.

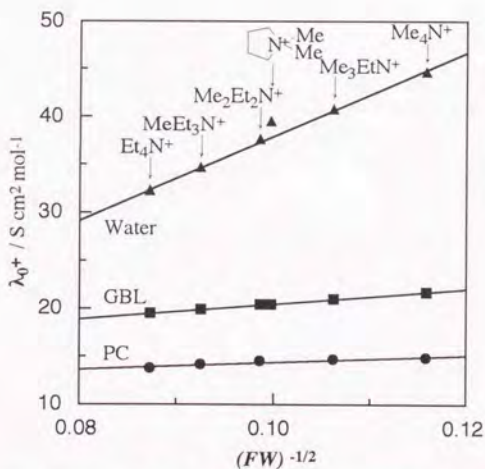


Fig. 15. Correlation between single ion molar conductivities and formula weights.

Table 9. Estimated single ion limiting molar conductivities of cyclic cations.

Cation	$\lambda_0^+ / \text{S cm}^2 \text{mol}^{-1}$
	14.1
	13.9
	13.7
	13.5
	13.5
	13.4
	13.5
	13.5
	13.4

3.5. Summary

In order to find a good electrolyte for electrical double layer capacitors, various quaternary onium salts were prepared, and the electrolytic conductivities and limiting reduction and oxidation potentials of a variety of organic liquid electrolytes based on the quaternary onium salts have been measured.

An electrolyte composed of tetraethylammonium cation, tetrafluoroborate anion and propylene carbonate solvent showed well-balanced performance of high electrolytic conductivity, a wide stable potential window and durability against hydrolysis.

Among quaternary onium salts, triethylmethylammonium, ethylmethylpyrrolidinium and tetramethylenepyrrolidinium tetrafluoroborate salts exhibited higher electrolytic conductivity than the conventional tetraethylammonium salt due to their small ion sizes without losing high dissociation. These electrolytes increased their conductivities until about 2 mol dm^{-3} due to their high solubilities in propylene carbonate. These electrolytes were industrialized by the newly developed synthetic processes.

Furthermore, the conductometric analysis of the diluted solutions of these electrolytes has been carried out to understand the effect of alkyl group. The mobilities (single ion limiting molar conductivities) of quaternary ammonium ions decreased with increasing the cation size. On the other hand, the ion association constants slightly decreased with increasing the cation size due to the electrostatic shielding effect of alkyl groups. It was concluded that the maximum electrolytic conductivity observed at a size between those of tetramethylammonium and tetraethylammonium salts at practical concentrations can be ascribed to the compromise of these two effects.

3.6 References

1. S. Sekido, T. Muranaka, Y. Yoshino and H. Mori, *National Technical Report*, **26**, 220 (1980).
2. A. Nishino, A. Yoshida, I. Tanahashi, I. Tajima, M. Yamasita, T. Muranaka and H. Yoneda, *National Technical Report*, **31**, 318 (1985).
3. T. Morimoto, *Kagaku Kogyo*, **43**, 54 (1992).
4. H. Yoneda, Abstract 37, p. 66, The Electrochemical Society Extended Abstracts, Vol. 93-1, Honolulu, HI, May 16-21, 1993.
5. A. Nishino, in *Proceedings of the Symposium on New Sealed Rechargeable Batteries and Supercapacitors*, B. M. Barnett, E. Dowgiallo, G. Halpert, Y. Matsuda, and Z.-i. Takehara, Editors, PV 93-23, p. 1, The Electrochemical Society Proceedings Series, Pennington, NJ (1993).
6. T. Morimoto, K. Hiratsuka, Y. Sanada and K. Kurihara, *ibid.*, p. 49.
7. B. E. Conway, *J. Electrochem. Soc.*, **138**, 1539 (1991).
8. A. F. Burke, *Preprints of the annual Automotive Technology Development Contractors Coordination Meeting*, Volume II, Dearborn, MI, 1991.
9. Y. Matsuda, M. Morita and K. Kosaka, *J. Electrochem. Soc.*, **130**, 101 (1983).
10. S. Sekido, Y. Yoshino, T. Muranaka and M. Mori, *Denki Kagaku*, **48**, 40 (1980).
11. M. Nawa, T. Nogami and H. Mikawa, *J. Electrochem. Soc.*, **131**, 1457 (1984).
12. H. Yashima, T. Nogami and H. Mikawa, *Synth. Met.*, **10**, 229 (1985).
13. T. Kanbara, T. Yamamoto, K. Tokuda and K. Aoki, *Chem. Lett.*, 2173 (1987).
14. I. Tanahashi, A. Yoshida and A. Nishino, *Denki Kagaku*, **56**, 892 (1988).
15. T. Kanbara, K. Nishimura, T. Yamamoto and K. Tokuda, *J. Power Sources*, **32**, 165 (1990).
16. I. Tanahashi, A. Yoshida and A. Nishino, *J. Electrochem. Soc.*, **137**, 3052 (1990).
17. K. Hiratsuka, Y. Sanada, T. Morimoto and K. Kurihara, *Denki Kagaku*, **59**, 209 (1991).
18. K. Hiratsuka, Y. Sanada, T. Morimoto and K. Kurihara, *Denki Kagaku*, **59**, 607 (1991).
19. M. Morita, M. Goto and Y. Matsuda, *J. Appl. Electrochem.*, **22**, 901 (1992).
20. Y. Sanada, K. Hiratsuka, T. Morimoto and K. Kurihara, *Denki Kagaku*, **51**, 448 (1993).
21. S. Mori, K. Ida and M. Ue, *USP* 4892944 (1990).
22. S. R. C. Hughes and D. H. Price, *J. Chem. Soc. A*, 1093 (1967).
23. H. O. House, E. Feng and N. P. Peet, *J. Org. Chem.*, **35**, 2371 (1971).
24. S. Mori, M. Ue and K. Ida, *JP* 88-30454A (1988).
25. S. Mori, M. Ue and K. Ida, *JP* 88-30453A (1988).
26. B. M. Lowe and H. M. Rendall, *J. Chem. Soc. Faraday Trans. 1*, **67**, 2318 (1971).
27. F. F. Blicke and E. B. Hotelling, *J. Amer. Chem. Soc.*, **76**, 5099 (1954).
28. S. Mori, M. Ue, K. Ida and A. Kominato, *JP* 88-174954A (1988).
29. S. Mori, K. Ida and M. Ue, *JP* 88-115876A (1988).
30. K. Rousseau, G. C. Farrington and D. Dolphin, *J. Org. Chem.*, **37**, 3968 (1972).
31. J. Barthel H. J. Gores and G. Schmeer, *Ber. Bunsenges. Phys. Chem.*, **83**, 911 (1979).

32. M. J. Kelly and W. R. Heineman, *J. Electroanal. Chem.*, **248**, 441 (1988).
33. J. L. Goldman, R. M. Mark, J. H. Young and R. V. Koch, *J. Electrochem. Soc.*, **127**, 1461 (1980).
34. P. Lemoine and M. Gross, *C. R. Acad. Sci. Ser. C*, **290**, 231 (1980).
35. F. Ossola, G. Pistoia, R. Seeber and P. Ugo, *Electrochim. Acta*, **33**, 47 (1988).
36. D. Bauer and M. Breant, in *Electroanalytical Chemistry*, A. J. Bard, Editor, Vol. 8, p. 281, Marcel Dekker, New York (1975).
37. J. Courtot-Coupez and M. L'Her, *Bull. Soc. Chim. Fr.*, 1631 (1970).
38. S. Tobishima and T. Okada, *Electrochim. Acta*, **30**, 1715 (1985).
39. S. Tobishima, J. Yamaki, A. Yamaji and T. Okada, *J. Power Sources*, **13**, 261 (1984).
40. I. Tanahashi, M. Murano and H. Yoneda, *Denshi Tsushin Gakkai, CPM86-111*, 43 (1987).
41. G. Eggert and J. Heitbaum, *Electrochim. Acta*, **31**, 1443 (1986).
42. T. Fujinaga and I. Sakamoto, *J. Electroanal. Chem.*, **67**, 201 (1976).
43. M. Ue, unpublished results.
44. O. Popovych and R. P. Tomkins, in *Nonaqueous Solution Chemistry*, p. 32, Wiley-Interscience, New York (1981).
45. J. Barthel, H. J. Gores, G. Schmeer and R. Wechter, *Topics in Current Chemistry*, **111**, 33 (1983).
46. J. F. Coetzee, in *Recommended Methods for Purification of Solvents and Tests for Impurities*, J. F. Coetzee, Editor, Pergamon Press, Oxford (1982).
47. W. Lange, in *Fluorine Chemistry*, J. H. Simons, Editor, Vol. 1, p. 125, Academic Press, New York (1950).
48. *Catalog Handbook of Fine Chemicals*, Aldrich Chemical Co. (1993).
49. J. Rosenfarb and J. A. Caruso, *J. Solution Chem.*, **5**, 345 (1976).
50. J. Rosenfarb, M. Martin, C. Prakash and J. A. Caruso, *J. Solution Chem.*, **5**, 311 (1976).
51. R. T. Atanasoski, H. H. Law, R. C. McIntosh and C. W. Tobias, *Electrochim. Acta*, **32**, 877 (1987).
52. *γ -Butyrolactone Technical Bulletin*, Mitsubishi Petrochemical Co. (1972).
53. J. F. Coetzee, T. H. Chang, B. K. Deshmukh and T. Fonong, *Electroanalysis*, **5**, 765 (1993).
54. R. E. Mesmer, K. M. Palen and C. F. Baes, Jr., *Inorg. Chem.*, **12**, 89 (1973).
55. R. M. Fuoss and E. Hirsch, *J. Amer. Chem. Soc.*, **82**, 1013 (1960).
56. L. M. Mukherjee and D. P. Boden, *J. Phys. Chem.*, **73**, 3965 (1969).
57. L. M. Mukherjee, D. P. Boden and R. Lindauer, *J. Phys. Chem.*, **74**, 1942 (1970).
58. J. Courtot-Coupez and M. L'Her, *C. R. Acad. Sci. Ser. C*, **271**, 357 (1970).
59. M. L. Jansen and H. L. Yeager, *J. Phys. Chem.*, **77**, 3089 (1973).
60. M. L. Jansen and H. L. Yeager, *J. Phys. Chem.*, **78**, 1380 (1974).
61. N. Matsuura, K. Umemoto and Y. Takeda, *Bull. Chem. Soc. Jpn.*, **48**, 2253 (1975).
62. R. L. Benott, D. Lahaie and G. Boire, *Electrochim. Acta*, **20**, 377 (1975).

63. S. Singh, J. S. Jha and R. Gopal, *Indian J. Chem.*, **14A**, 127 (1976).
64. Z. Pawlak, R. A. Robinson and R. G. Bates, *J. Solution Chem.*, **7**, 631 (1978).
65. S. L. Maiofis, B. K. Filanovskii and M. S. Grilikhes, *Zh. Fiz. Khim.*, **53**, 1263 (1979).
66. Y. Matsuda, H. Nakashima, M. Morita and Y. Takasu, *J. Electrochem. Soc.*, **128**, 2552 (1981).
67. M. Salomon and E. J. Plichta, *Electrochim. Acta*, **29**, 731 (1984).
68. G. Wawrzyniak and T. Jasinski, *Pol. J. Chem.*, **59**, 1181 (1985).
69. J. F. Reardon, *Electrochim. Acta*, **32**, 1595 (1987).
70. P. M. McDonagh and J. F. Reardon, *J. Solution Chem.*, **19**, 301 (1990).
71. P. K. Muhuri and D. K. Hazra, *J. Chem. Soc. Faraday Trans.*, **87**, 3511 (1991).
72. G. Wawrzyniak, L. Chmurzynski and R. Korewa, *Pol. J. Chem.*, **66**, 175 (1992).
73. M. Ue and S. Sekigawa, unpublished results.
74. B. M. Lowe and H. M. Rendall, *J. Chem. Soc. Faraday Trans. 1*, **68**, 2191 (1972).
75. Y. Kiso and T. Hirokawa, *Chem. Lett.*, 891 (1979).
76. T. Kakiuchi, J. Noguchi, M. Kotani and M. Senda, *J. Electroanal. Chem.*, **296**, 517 (1990).

4. Organic Electrolytes for Lithium Batteries

4.1. Introduction

Lithium battery is the most promising high energy density battery system, because of the low equivalent weight and the highest negative electrode potential of lithium metal. For the past three decades, a great deal of effort has been made to develop high energy and/or high power density lithium batteries. The research and development have been stimulated originally by the space and military applications and more recently by consumer applications.

A number of ambient temperature primary lithium battery systems using different cathode and electrolyte materials have been developed as shown in Table 1 [1]. The most successful systems are $\text{Li}/(\text{CF}_x)_n$ and Li/MnO_2 batteries, which were firstly commercialized for consumer usage by Matsushita Electric Industry Co. in 1971 and Sanyo Electric Co. in 1976, respectively [2]. The appearance and construction of these lithium batteries are given in Fig. 1. Their applications are rapidly spreading from professional uses to consumer uses. The coin type cells are used in watches, cameras, calculators and the like, and the great success of automatic cameras have markedly increased the demand of cylindrical type batteries.

The outstanding technical success of primary lithium batteries spurred interest in secondary (rechargeable) lithium batteries. During the last decade, a number of ambient temperature secondary lithium battery systems have been developed, however, their usage was limited to memory backup applications due to the problems including energy density, charge-discharge cycling and cell safety. It was only in 1990 that Sony announced the success of a revolutionary system based on a $\text{Li}_x\text{C}/\text{Li}_y\text{CoO}_2$ system, which is called lithium ion battery or rocking chair type lithium battery. This technology has attracted not only battery manufactures but also chemical companies and keen competition toward industrialization is being played.

Table 1. Characteristics of lithium primary batteries

System	OCV / V	Average voltage / V	Energy density / Wh kg ⁻¹	Usage
Li/SOCl_2	3.6	3.5	390	military, memory backup
$\text{Li}/\text{V}_2\text{O}_5$	3.4	2.8	260	military, medical
$\text{Li}/\text{Ag}_2\text{CrO}_4$	3.3	3.0	220	military, medical
Li/MnO_2	3.0	2.8	160	watch, camera, calculator, backup
Li/SO_2	2.9	2.6	270	military
$\text{Li}/(\text{CF}_x)_n$	2.8	2.6	220	watch, camera, calculator, backup
$\text{LiBi}_2\text{Pb}_2\text{O}_5$	2.3	1.5	130	electronic devices
Li/CuO	2.2	1.5	165	electronic systems
Li/CuS	2.1	1.8	200	medical
LiFeS_2	1.7	1.6	220	watch, electronic devices

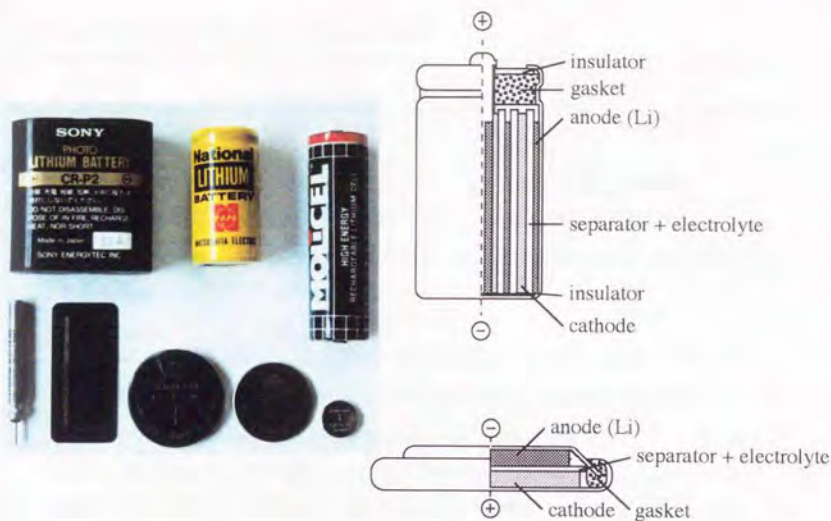


Fig. 1. Appearance and construction of lithium batteries.

In light of advances made in this field, it became clear that the selection of a suitable combination of solvents and solutes and their purification is at the heart of the lithium battery technology. The organic electrolyte for these lithium batteries should be thermodynamically and/or kinetically stable toward lithium metal. Lithium can be plated from many solvents with virtually 100 % efficiency, but it cannot be efficiently stripped, particularly after the deposit has been allowed to stand in contact with the solution. This reversibility is the main issue for rechargeable lithium cells.

There have been numerous studies and reviews regarding the electrochemical properties of nonaqueous electrolytes and their performance in various lithium cells [1-13]. Common electrolyte components thought to be promising are listed in Table 2.

Among many organic electrolytes, $1 \text{ mol dm}^{-3} - \text{LiClO}_4/\text{PC}+\text{DME}$ (1:1 by volume) and $1 \text{ mol dm}^{-3} - \text{LiBF}_4/\text{GBL}$ are popular electrolytes used in Li/MnO_2 and $\text{Li}/(\text{CF}_x)_n$ primary batteries, respectively [1, 2]. The former electrolyte is the most successful example using a high permittivity solvent-low viscosity solvent mixed system. The conductivity change of the $1 \text{ mol dm}^{-3} - \text{LiClO}_4/\text{PC}+\text{DME}$ electrolyte is given in Fig. 2 as a function of solvent composition [14]. The higher conductivity of the solvent mixed system can be understood from the competition between the solvent viscosity, ion solvation and ion aggregation. The recent efforts to develop practical electrolytes still inherit this idea.

Table 2. Promising electrolyte components.

Solvent		Solute
Cyclic carbonate	EC, PC, BC	LiClO_4
Cyclic ester	GBL	LiBF_4 , LiPF_6 , LiAsF_6
Cyclic ether	DO, THF, 2-MTHF	LiCF_3SO_3 , $\text{LiC}_4\text{F}_9\text{SO}_3$
Linear carbonate	DMC, EMC, DEC	$\text{Li}(\text{CF}_3\text{SO}_2)_2\text{N}$, $\text{Li}(\text{CF}_3\text{SO}_2)_3\text{C}$
Linear ester	MF, MA, MP	
Linear ether	DME	

EC; ethylene carbonate, PC; propylene carbonate, BC; butylene carbonate, GBL; γ -butyrolactone, DO; 1,3-dioxolane, THF; tetrahydrofuran, 2-MTHF; 2-methyltetrahydrofuran, DMC; dimethyl carbonate, EMC; ethyl methyl carbonate, DEC; diethyl carbonate, MF; methyl formate, MA; methyl acetate, MP; methyl propionate, DME; 1,2-dimethoxyethane.

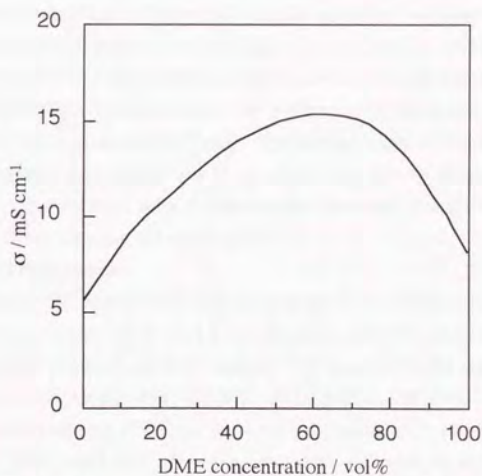


Fig 2. Conductivity of 1 mol dm^{-3} $\text{-LiClO}_4/\text{PC}+\text{DME}$ electrolyte.

4.2. Electrochemical Properties of Organic Electrolytes

The electrolytic conductivity of an organic electrolyte is the important electrochemical property, because it directly affects the internal resistance of a battery, which leads IR drop in working voltage. The measurement of electrochemical window is another screening technique, which must be substantiated by compatibility test with actual electrodes.

4.2.1. Experimental

Electrolyte preparation

LiClO₄ (Japan Carlit Co.), LiBF₄, LiPF₆, LiCF₃SO₃ (Morita Chemical Industries), LiAsF₆ (Lithco), Li(CF₃SO₂)₂N (3M) and LiC₄F₉SO₃ (Tochem Products Co.) were purified by recrystallization, and were then vacuum dried at 100°C. Propylene carbonate, γ -butyrolactone, 1,2-dimethoxyethane and ethyl methyl carbonate (Mitsubishi Petrochemical Co., Battery-grade F-PC, F-GBL, F-DME and F-EMC) were used without further purification. Each lithium salt was dissolved in a solvent (mixture) so as to make 1 mol dm⁻³ solutions.

Measurement

Density of the (mixed) solvents was measured at 25 \pm 0.1°C by a digital density meter (PAAR, DMA 45). Viscosity was determined using a viscosity meter (Tokyo Keiki Co., Visconic ED). Relative permittivity was measured by an LCR meter equipped with a capacitor cell (Ando Electric Co., AG-4311). Electrolytic conductivity and water content of the electrolytes were measured by a conductivity meter equipped with a standard type conductivity cell (Toa Electronics, CM-60S/CGT-511B) and a moisture meter (Mitsubishi Kasei Co., CA-06), respectively.

The limiting reduction and oxidation potentials were measured by linear sweep voltammetry with an automatic polarization system (Hokuto Denko Co., HZ-1A). A pair of 3 ϕ glassy carbon rods (Tokai Carbon Co., GC-10) were used as working and counter electrodes. A silver wire was used as a reference electrode. The sidewall of the working electrode was sealed with a thermo-shrinkable tube to limit the surface area to 7 mm². The surface was polished with alumina powder before use. Measurement was carried out in an argon atmosphere glove box. The limiting reduction and oxidation potentials were defined as the potentials at which the current density exceeded 1 mA cm⁻² when the scan rate was 5 mV s⁻¹.

4.2.2. Results and Discussion

Relevant properties of PC, DME, EMC and their equimolar mixtures utilized in this study are summarized in Table 3, where d_0 , η and ϵ_r are density, viscosity and relative permittivity, respectively. Electrolytic conductivities of 1 mol dm⁻³ solutions of seven popular lithium salts in PC and GBL, and equimolar mixtures of PC/DME, GBL/DME and PC/EMC are given in Table 4. The conductivity ratios among different solvents are listed in Table 5. The electrolytic conductivities of LiCF₃SO₃ and LiC₄F₉SO₃ were remarkably enhanced by replacing PC with GBL or PC/DME beyond expectation from solvent viscosity. It became evident that EMC cannot always increase electrolytic conductivity as observed in the case of DME.

The limiting reduction and oxidation potentials of these electrolytes are given in Table 6. The reduction potential can be limited by both the deposition of lithium and the decomposition of the solvent, where there is still a controversy as to what is happening [1, 2]. The oxidation potential

can be limited by the oxidation of solvent or anion. It became evident that the durability toward oxidation increases in the following order:



It is known that oxidation of ether involves a one electron transfer to yield the radical cation, followed by chemical reactions including polymerization [2]. Ether solvents have long been regarded as a promising solvent for the secondary system due to the good Li cycling efficiency, however, they are no more useful for the recent 4 V lithium cell based on a very oxidizing cathode such as Li_xCoO_2 due to this behavior. Linear carbonates and esters shown in Table 2 are considered to replace the ether solvents as a low viscosity solvent.

Table 3. Physical properties of the solvent at 25°C.

Solvent	ϵ_r / -	η / cP	d_0 / g cm ⁻³
PC	64.9	2.51	1.1998
GBL	41.8	1.73	1.1248
DME	7.2	0.47	0.8612
EMC	2.4	0.65	1.0070
PC/DME	35.5	1.06	1.0229
PC/EMC	27.4	1.25	1.0994

Table 4. Electrolytic conductivities at 1 mol dm⁻³ and 25°C.

Salt	PC	GBL	PC/DME	GBL/DME	PC/EMC
LiBF ₄	3.4	7.5	9.7	9.4	3.3
LiClO ₄	5.6	10.9	13.9	15.0	5.7
LiPF ₆	5.8	10.9	15.9	18.3	8.8
LiAsF ₆	5.7	11.5	15.6	18.1	9.2
LiCF ₃ SO ₃	1.7	4.3	6.5	6.8	1.7
Li(CF ₃ SO ₂) ₂ N	5.1	9.4	13.4	15.6	7.1
LiC ₄ F ₉ SO ₃	1.1	3.3	5.1	5.3	1.3

in mS cm⁻¹.

Table 5. Conductivity ratios among different solvents.

Salt	$\frac{\sigma(\text{GBL})}{\sigma(\text{PC})}$	$\frac{\sigma(\text{PC/DME})}{\sigma(\text{PC})}$	$\frac{\sigma(\text{PC/EMC})}{\sigma(\text{PC})}$
LiClO ₄	1.9	2.9	1.0
LiBF ₄	2.2	2.5	1.0
LiPF ₆	1.9	2.7	1.5
LiAsF ₆	2.0	2.7	1.6
LiCF ₃ SO ₃	2.5	3.8	1.0
Li(CF ₃ SO ₂) ₂ N	1.8	2.6	1.4
LiC ₄ F ₉ SO ₃	3.0	4.6	1.2

Solvent index	$\frac{\eta(\text{PC})}{\eta(\text{GBL})}$	$\frac{\eta(\text{PC})}{\eta(\text{PC/DME})}$	$\frac{\eta(\text{PC})}{\eta(\text{PC/EMC})}$
	1.5	2.4	2.0

Table 6. Limiting reduction and oxidation potentials.

Electrolyte	E_{red} / V vs. SCE	E_{ox}
LiClO ₄ /PC	-3.0	+3.1
LiCF ₃ SO ₃ /PC	-3.0	+3.1
LiBF ₄ /GBL	-3.0	+4.2
LiClO ₄ /PC+DME	-3.0	+2.1
LiPF ₆ /PC+EMC	-3.0	+3.5

4.3. Conductometric Analysis of Diluted Solutions (1)

Propylene carbonate (PC) and γ -butyrolactone (GBL) are important dipolar aprotic solvents used for organic electrolytes in lithium batteries as described before.

The conductometric analysis of the diluted solutions containing these solvent was also performed in order to gain a better understanding about the solvent-solute interactions [15 - 40], which includes LiCl [16, 22, 26, 30, 34], LiBr [16, 26], LiI [22, 25], LiNO₃ [20], LiSCN [33], LiAlCl₄ [15, 24], LiClO₄ [16-20, 23, 26-31, 34-36], LiBF₄ [26, 32], LiPF₆ [26], LiAsF₆ [21, 27-29, 31, 36] and Li(CF₃SO₂)₂N [36] in PC and LiAlCl₄ [15], LiPic [38], LiClO₄ [28, 29, 31, 37], LiBF₄ [39, 40], LiPF₆ [39], LiAsF₆ [28, 29, 31, 39, 40] in GBL.

LiClO₄ has long been used as an electrolyte salt in lithium batteries and its conductometric analysis is already established. However, its undesirable safety characteristic requests a more stable and safer salt [12, 41] and lithium salts having a strong electron withdrawing anion such as LiBF₄, LiPF₆, LiAsF₆, LiCF₃SO₃, Li(CF₃SO₂)₂N and LiC₄F₉SO₃ are now commercially used in lithium batteries. The conductometric studies on these salts in dipolar aprotic solvents are very scarce compared with those of LiClO₄, furthermore, a perusal of the literature shows remarkable deviations in the data.

Since the conductometric parameters in pure solvents are important information for investigating the practical binary or ternary mixed solvent systems, a systematic study on the transport properties of these lithium salts in pure solvents is desirable.

The author has carried out a systematic conductometric analysis on these lithium salts in propylene carbonate and γ -butyrolactone in order to compare the mobility and ionic association tendency of each anion. The corresponding quaternary ammonium salts having the same anions, which are also important solutes for nonaqueous electrolytes in electrical double layer capacitors, were also examined in both solvents for obtaining a more consistent set of the single ion limiting molar conductivities and for comparing the difference between R₄N⁺ and Li⁺ in the association constants with each anion.

In spite of the fact that the radii of ions and solvents are very important information for interpreting the obtained parameters such as single ion limiting molar conductivity and association constant, different values have been adopted by several authors. It seems that incorrect or inconsistent data have been used without precaution. The author has systematically calculated the radii of ions and solvents by using the molecular models constructed from both the crystallographic data and computer-aided molecular dynamics. The mobility and ionic association of each anion were discussed from this consistent set of ionic radii.

4.3.1. Experimental

Electrolyte preparation

LiClO₄, Et₄NClO₄ (Japan Carlit Co.), LiBF₄, Et₄NBF₄, LiPF₆, Et₄NPF₆, LiCF₃SO₃, Et₄NCF₃SO₃ (Morita Chemical Industries), LiAsF₆ (Lithco), Li(CF₃SO₂)₂N (3M), LiC₄F₉SO₃ (Tochem Products Co.), Bu₄NBPh₄ (Aldrich Chemical Co.) and Bu₄NClO₄ (Kodak Chemical Co.) were purified by recrystallization. Me₄N(CF₃SO₂)₂N and Et₄N(CF₃SO₂)₂N were prepared by the titration of bis(trifluoromethylsufonyl)imide [42] with tetramethyl- or tetraethylammonium hydroxide

aqueous solution (SACHEM, Inc.) followed by recrystallization. All the salts were vacuum dried at 100°C. Propylene carbonate and γ -butyrolactone (Mitsubishi Petrochemical Co., Battery-grade F-PC and F-GBL) were used without further purification.

Each salt was dissolved in propylene carbonate and γ -butyrolactone so as to make about 1 mol dm⁻³ solutions. Water content in these mother solutions (20 - 100 ppm) was measured by a moisture meter (Mitsubishi Kasei Co., CA-06) and the concentrations of the solutions were calibrated. The mother solutions were diluted to about 10⁻² mol dm⁻³ by the solvent to make the stock solutions, whose densities at 25°C were measured by a digital density meter (PAAR, DMA 45).

Measurements

The stock solutions were successively diluted and molar concentrations C (mol dm⁻³) were calculated from the concentrations m' (mol kg⁻¹-solution) and the densities d (g cm⁻³) of each solution by $C = m'd$. Densities were calculated from $d = d_0 + Dm'$, where d_0 is the density of solvent and D is a characteristic constant of the electrolyte.

The conductivity measurements were carried out at 25 ± 0.1°C by a bridge (Toa Electronics, CM-25E) and an LCR meter (Ando Electric Co., AG-4311) equipped with a standard type conductivity cell with a cell constant 0.1017 cm⁻¹ (Toa Electronics, CG-2001PL).

Molecular modeling

The sizes and volumes of molecules were calculated from the molecular models constructed by a molecular modeling system CHEMLAB-II (Molecular Design Co.) on a VAX8350 (Digital Equipment Corp.). The MM2 program was used for structure optimization. All graphical diagrams were generated by the CSC Chem3D Plus software (Cambridge Scientific Computing) on a Macintosh Quadra 840AV (Apple Computer, Inc.).

4.3.2. Results and Discussion

Relevant properties of propylene carbonate and γ -butyrolactone used in this work are summarized in Table 7, where d_0 , η , ϵ_r , κ and q are density, viscosity, relative permittivity, electrolytic conductivity and Bjerrum critical distance, respectively.

Molar conductivities

Molar conductivities Λ were calculated from the experimental electrolytic conductivities σ after correction for the electrolytic conductivity of the solvent κ . The molar conductivities over concentration range of 10⁻² to 10⁻³ mol dm⁻³ are given in Table 8.

Table 7. Physical properties of the Solvents at 25°C.

Solvent	d_0 / g cm ⁻³	η / cP	ϵ_r / -	κ / S cm ⁻¹	q / nm
PC	1.1998	2.513 ^a	64.92 ^a	0.9 × 10 ⁻⁷	0.432
GBL	1.1248	1.727 ^b	41.77 ^b	2.5 × 10 ⁻⁷	0.671

^aRef. 19, ^bRef. 29.

Table 8. Molar conductivities in PC and GBL at 25°C.

(a) PC

$10^3 C$ / mol dm ⁻³	Λ / S cm ² mol ⁻¹	$10^3 C$	Λ
LiClO ₄		Et ₄ NClO ₄	
9.73623	24.220	9.07625	29.099
7.29899	24.594	6.80707	29.486
4.86626	25.052	4.53848	30.122
2.43382	25.766	2.26978	30.668
1.70559	26.009	1.59849	31.035
0.97666	26.324	0.90777	31.407
LiBF ₄		Et ₄ NBF ₄	
10.61301	24.461	10.67611	30.302
7.07857	25.430	8.00653	30.751
3.53938	26.406	5.33861	31.396
2.48345	26.963	2.67045	32.040
1.42096	27.348	1.87316	32.464
0.94724	27.617	1.16274	32.733
LiPF ₆		Et ₄ NPF ₆	
9.40520	23.382	9.72876	28.052
7.05574	23.741	7.27841	28.703
4.70396	24.152	4.86499	28.985
2.35176	24.730	2.43270	29.650
1.65190	25.098	1.70461	29.983
0.94429	25.321	0.97365	30.257
LiAsF ₆		Et ₄ NCF ₃ SO ₃	
9.97748	23.093	9.85492	27.185
7.48167	23.566	7.39065	27.604
4.98704	23.924	4.92962	27.996
2.49383	24.504	2.46547	28.721
1.74831	24.687	1.72819	28.996
0.99770	25.018	0.98768	29.372
LiCF ₃ SO ₃		Me ₄ N(CF ₃ SO ₂) ₂ N	
10.37139	20.413	9.91005	25.833
7.77699	21.128	7.43138	26.228
5.18529	21.949	4.95408	26.627
2.59196	23.068	2.47851	27.278
1.81759	23.482	1.73393	27.660
1.03943	24.032	0.99275	27.812
Li(CF ₃ SO ₂) ₂ N		Et ₄ N(CF ₃ SO ₂) ₂ N	
9.74284	20.067	9.56860	24.926
7.30385	20.374	7.17465	25.271
4.87161	20.755	4.78149	25.684
2.44491	21.301	2.39634	26.315
1.70633	21.573	1.67599	26.617
0.97755	21.902	0.95940	26.954
LiC ₄ F ₉ SO ₃		Bu ₄ NClO ₄	
9.52025	17.501	9.67535	24.889
7.13935	18.238	7.25496	25.212
4.75873	18.757	4.83791	25.695
2.38090	19.577	2.41914	26.377
1.66803	19.952	1.70839	26.680
0.95306	20.366	0.97048	27.007
		Bu ₄ NBPh ₄	
		10.15792	14.906
		7.62192	15.234
		5.08312	15.691
		2.54332	16.164
		1.78164	16.395
		1.01809	16.708

(b) GBL

$10^3 C$ / mol dm ⁻³	Λ / S cm ² mol ⁻¹	$10^3 C$	Λ
LiClO ₄		Et ₄ NClO ₄	
9.58965	35.992	10.30569	40.381
7.19114	36.705	7.72942	41.239
4.79394	37.600	5.15404	42.345
2.39794	39.033	2.57562	43.854
1.67993	39.436	1.80477	44.466
0.96142	40.253	1.03370	45.274
LiBF ₄		Et ₄ NBF ₄	
10.17992	36.263	10.00729	42.594
7.63167	37.312	7.50557	43.468
5.00138	38.579	5.00290	44.624
2.54824	40.322	2.50356	46.194
1.78342	41.112	1.75462	46.819
1.01890	42.055	1.00604	47.662
LiPF ₆		Et ₄ NPF ₆	
10.00672	34.812	10.01102	39.232
7.49897	35.452	7.50689	39.943
4.99735	36.269	5.00197	40.954
2.50220	37.447	2.50347	42.321
1.75169	37.963	1.75626	42.875
1.00363	38.560	1.00178	43.672
LiAsF ₆		Et ₄ NCF ₃ SO ₃	
9.55417	34.147	10.07926	37.349
7.16342	34.781	7.55902	38.120
4.77540	35.568	5.04137	39.146
2.38977	36.740	2.51877	40.595
1.67404	37.245	1.76684	41.090
0.95822	37.779	0.98097	42.050
LiCF ₃ SO ₃		Me ₄ N(CF ₃ SO ₂) ₂ N	
10.28191	30.028	8.48166	36.579
7.70482	31.078	6.35377	37.183
5.13958	32.503	4.23678	37.942
2.56961	34.363	2.12115	39.035
1.80497	35.319	1.48687	39.479
1.02848	36.092	0.84810	40.090
Li(CF ₃ SO ₂) ₂ N		Et ₄ N(CF ₃ SO ₂) ₂ N	
9.57643	29.369	10.62500	33.981
7.17987	29.896	7.96138	34.649
4.79140	30.607	5.31058	35.448
2.39301	31.592	2.65547	36.641
1.67870	31.929	1.86516	37.171
0.95909	32.531	1.06482	37.753
LiC ₄ F ₉ SO ₃		Bu ₄ NClO ₄	
10.00281	25.678	8.99496	36.148
7.49758	26.509	6.74637	36.827
4.99905	27.575	4.49761	37.742
2.49967	29.064	2.24946	39.098
1.75464	29.636	1.57690	39.603
1.00154	30.383	0.92512	40.319
		Bu ₄ NBPh ₄	
		10.48329	20.752
		7.86439	21.279
		5.24523	21.896
		2.64101	22.927
		1.83983	23.345
		1.05004	23.856

Analysis of conductivity data

The data were preliminary analyzed in terms of the Shedlovsky equation. However, very small or negative association constants were often obtained, presumably due to the neglect of short range interactions in Onsager limiting law. Therefore, the data were analyzed by means of the Fernández-Prini expansion of the Fuoss-Hsia equation (See Chap. 6).

Derived parameters are summarized in Table 9. The standard errors of estimate were less than 0.1 and standard deviations in Λ_0 and K_A were less than 0.1 and 1, respectively.

Limiting molar conductivities

The ratios of the limiting molar conductivities in GBL to those in PC [Λ_0 (GBL) / Λ_0 (PC)] are also given in Table 9. They ranged from 1.51 to 1.55 for lithium salts and from 1.43 to 1.48 for tetraethylammonium salts, respectively. Since the ratio of the viscosity of GBL to that of PC is 1.46, higher values observed for lithium salts suggest the existence of a slightly stronger Li⁺-solvent interaction in PC than in GBL.

Single ion limiting molar conductivities

Conductivity data of Bu₄NClO₄ and Bu₄NBPh₄ were also analyzed in order to split a limiting molar conductivity into two single ion limiting molar conductivities, λ_0^+ and λ_0^- . λ_0^- (BPh₄⁻) in PC and GBL were calculated from empirically adjusted equation [43]:

$$\lambda_0 = 0.8204 / \eta [5.35 - (0.0103 \epsilon_r + 0.85)] \quad (1)$$

The obtained λ_0^- (BPh₄⁻) gave λ_0^+ (Bu₄N⁺) from Λ_0 (Bu₄NBPh₄), which then generated λ_0^- (ClO₄⁻) from Λ_0 (Bu₄NClO₄). The resulting λ_0^- (ClO₄⁻) = 18.93 S cm² mol⁻¹ in PC was comparable with reported values; 18.78 [17], 18.44 [19], 18.40 [31], 18.89 [36], and the calculated transport number t_0^+ (Et₄NClO₄) = 0.416 was almost the same as the experimentally observed value; 0.417 [44].

Table 9. Derived parameters for PC and GBL electrolytes at 25°C.

Salt	PC			GBL			$\frac{\Lambda_0 \text{ (GBL)}}{\Lambda_0 \text{ (PC)}}$	$\frac{\log K_A \text{ (GBL)}}{\log K_A \text{ (PC)}}$
	Λ_0	K_A	σ_A	Λ_0	K_A	σ_A		
LiClO ₄	27.35	2.8	0.063	42.44	8.4	0.026	1.55	2.0
LiBF ₄	28.83	8.4	0.047	44.64	16.7	0.086	1.55	1.3
LiPF ₆	26.31	2.1	0.019	40.73	5.7	0.049	1.55	2.3
LiAsF ₆	26.00	1.1	0.038	39.91	5.7	0.055	1.53	-
LiCF ₃ SO ₃	25.33	16.1	0.088	38.86	25.0	0.018	1.53	1.2
Li(CF ₃ SO ₂) ₂ N	22.80	1.5	0.036	34.43	3.7	0.034	1.51	3.1
LiC ₄ F ₉ SO ₃	21.45	12.3	0.017	32.65	18.1	0.084	1.52	1.2
Et ₄ NClO ₄	32.43	3.1	0.013	47.77	9.5	0.062	1.47	2.0
Et ₄ NBF ₄	33.96	3.0	0.014	50.19	9.9	0.053	1.48	2.1
Et ₄ NPF ₆	31.33	2.0	0.029	45.99	7.8	0.100	1.47	3.0
Et ₄ NCF ₃ SO ₃	30.39	2.3	0.062	44.30	9.5	0.045	1.46	2.7
Me ₄ N(CF ₃ SO ₂) ₂ N	28.90	1.8	0.007	42.07	4.8	0.069	1.46	2.7
Et ₄ N(CF ₃ SO ₂) ₂ N	27.92	2.0	0.031	39.98	5.6	0.039	1.43	2.4
Bu ₄ NClO ₄	28.02	2.8	0.037	42.48	8.8	0.042	1.52	2.1
Bu ₄ NBPh ₄	17.61	2.4	0.031	25.70	6.3	0.032	1.46	2.1

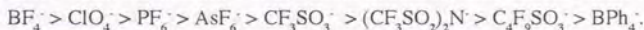
Λ_0 in S cm² mol⁻¹, K_A in dm³ mol⁻¹.

Although no reliable conductivity data in pure GBL exist, the resulting $\lambda_0^{\circ}(\text{ClO}_4^-) = 28.45 \text{ S cm}^2 \text{ mol}^{-1}$ was similar to the reported values; 26.23 [28], 27.20 [31], 27.77 [38], and the calculated $t_0^{\circ}(\text{LiClO}_4) = 0.330$ was close to the experimentally observed value; 0.36 [31]. Furthermore, calculated $t_0^{\circ}(\text{Bu}_4\text{NClO}_4) = 0.330$ was very close to that in PC (0.324) in this work and those in other dipolar aprotic solvents: DMF; 0.326 [45], DMSO; 0.329 [45].

The resulting consistent set of the single ion limiting molar conductivities in PC and GBL are given in Table 10. Deviations in the single ion limiting molar conductivities calculated from the limiting molar conductivities of Et_4N^+ salts and Li^+ salts were at most 0.03 and 0.11 $\text{S cm}^2 \text{ mol}^{-1}$ in PC and GBL, respectively. The ratios of the single ion limiting molar conductivities in GBL to those in PC [$\lambda_0(\text{GBL})/\lambda_0(\text{PC})$] ranged from 1.43 to 1.51 except for Li^+ , Bu_4N^+ and BPh_4^- .

The obtained single ion limiting molar conductivities in PC agreed with the literature values within 0.5 $\text{S cm}^2 \text{ mol}^{-1}$ in error except for BF_4^- and AsF_6^- as shown in Table 10. As for GBL, there is no reliable data, and the values presented in Table 10 can be regarded as the first reliable set of the single ion limiting molar conductivities in GBL.

It became evident that mobilities of the anions in both solvents decrease in the following order:



In the previous chapter, the author has shown that the single ion limiting molar conductivities of quaternary ammonium ions can be estimated from their formula weight, because ionic mobility correlates linearly with the reciprocal of square root of formula weight [46]. The revised values for asymmetric quaternary ammonium ions between tetramethyl- and tetraethylammonium ion are presented in Table 10. However, a similar relationship was not observed for the anions due to their large difference in structure.

Table 10. Single ion limiting molar conductivities in PC and GBL at 25°C.

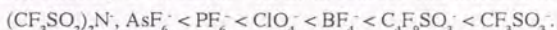
Ion	PC		GBL	
	λ_0	Literature	λ_0	Literature
Li^+	8.43	8.32 (46), 7.86 (35)	13.99	12.95 (28), 15.30 (31)
Me_4N^+	14.50	14.17 (46)	21.52	25.07 (28)
Me_3EtN^+	14.16		20.77	
$\text{Me}_2\text{Et}_2\text{N}^+$	13.90		20.18	
MeEt_3N^+	13.68		19.70	
Et_4N^+	13.50	13.19 (46)	19.32	20.43 (28)
Bu_4N^+	9.09	9.00 (46)	14.03	11.75 (28)
ClO_4^-	18.93	18.43 (46), 18.89 (35)	28.45	26.23 (28), 27.20 (31)
BF_4^-	20.43	19.59 (32)	30.77	
PF_6^-	17.86	17.46 (47)	26.70	
AsF_6^-	17.58	14.67 (36), 19.23 (30)	25.92	20.16 (28), 31.06 (31)
CF_3SO_3^-	16.89	16.90 (48)	24.93	
$(\text{CF}_3\text{SO}_2)_2\text{N}^-$	14.40	14.90 (36)	20.55	
$\text{C}_4\text{F}_9\text{SO}_3^-$	13.03		18.66	
BPh_4^-	8.52	8.10 (46)	11.67	11.52 (28)

λ_0 in $\text{S cm}^2 \text{ mol}^{-1}$.

Association constants

Derived association constants given in Table 9 should be used only for the comparison of each salt and solvent in this work, because it is well known that different expressions of the coefficients in the conductance equation give different K_A , and this effect is larger with smaller association constants ($K_A < 20 \text{ dm}^3 \text{ mol}^{-1}$) [45]. Even when the same expression was used, different ion size parameter R generated fairly different K_A particularly for GBL solutions (See Chap. 6).

Association constants in GBL were larger than those in PC due to the difference of relative permittivities. The ratios of the logarithm of association constants in GBL to those in PC [$\log K_A(\text{GBL}) / \log K_A(\text{PC})$] are also given in Table 9. They were close to the ratio of reciprocal of relative permittivity of GBL to that of PC, [$\epsilon_r^{-1}(\text{GBL}) / \epsilon_r^{-1}(\text{PC})$] = 1.6. It became evident that the association tendency of the anions with Li^+ in both solvents increases in the following order:



However, association with Et_4N^+ was levelled by electrostatic shielding effect of alkyl groups on nitrogen. The association constants for $(\text{CF}_3\text{SO}_2)_2\text{N}^-$ and PF_6^- were still smaller than those for other anions.

Calculation of ion size and solvent size

The radii of ions and solvents give very important information for interpreting the derived parameters from conductivity analysis. However, incorrect or inconsistent data have been used frequently without precaution. The author has systematically determined ion size and solvent size by computer-aided molecular modeling.

There is difficulty in selecting a representative value for molecular size, when the molecule has a shape far from sphere. Therefore, the author has adopted the radius defined by the following equation:

$$r = (3V / 4\pi)^{1/3} \quad (2)$$

, where V is the van der Waals volume.

For the calculation of the van der Waals volume, the van der Waals radii of atoms presented by Bondi [49] were used. These are as follows: H; 0.120, B; 0.190, C; 0.170, N; 0.155, O; 0.152, F; 0.147, Cl; 0.175, P; 0.180, S; 0.180, As; 0.185 nm. Since the van der Waals radius of boron was not given by Bondi, it was estimated from Table I in Ref. 49.

The coordinates of atoms in the molecule were obtained by two methods, crystallographic data (X-ray or neutron diffraction) and MM2 calculation.

The Cartesian coordinates of each atom were generated from the structures of Me_4NI [50] for Me_4N^+ , Et_4NI_3 [51] for Et_4N^+ , Bu_4NI_3 [52] for Bu_4N^+ , Me_4NClO_4 [53] for ClO_4^- , Me_4NBF_4 [54] for BF_4^- , Me_4NPF_6 [55] for PF_6^- , $(\text{ClCH}_2)_2\text{SAsF}_6$ [56] for AsF_6^- , $\text{H}_3\text{OCF}_3\text{SO}_3$ [57] for CF_3SO_3^- and Me_4NBPh_4 [58] for BPh_4^- . The coordinates of $(\text{CF}_3\text{SO}_2)_2\text{N}^-$ were made by replacing H atoms in $\text{H}_3\text{O}(\text{CH}_3\text{SO}_2)_2\text{N}$ [59] by F atoms with keeping average C-F distance 0.1305 nm observed in $\text{H}_3\text{OCF}_3\text{SO}_3$.

MM2 calculation was carried out by optimizing an initial two-dimensional structure. All unknown bending and torsional parameters were supplemented by the method described by

Yoshida [60]. Complete tetrahedral or octahedral models were used without calculation for ClO_4^- , BF_4^- , PF_6^- and AsF_6^- . The space-filling models are depicted in Fig. 3 and the van der Waals volumes V and the derived van der Waals radii r are given in Table 11.

All the molecules were oriented such that their principal axes were coincident with external X, Y, Z coordinate axes, and the longest axis and the shortest axis were fit to external X and Z coordinate axes, respectively. The principal axes were determined by the computation of the moments of inertia I given by the following equation:

$$I = \sum m_i l_i^2 \quad (3)$$

where m and l are the mass of atom and the distance from an axis, respectively. Notations a, b and c in Table 11 are the X, Y, Z lengths of a molecule when it is fit into the smallest box and c/a becomes an easy index of deformation from spherical shape.

The ionic radii obtained by MM2 calculation were very close to those obtained by crystallographic data within 0.003 nm in error except for radii of tetraalkylammonium ions, because C-H distance can be generally underestimated by X-ray crystallography. The author has decided to use values obtained by MM2 calculation summarized in Table 12, because some distortion is observed for the models from crystallographic data, and the models from MM2 calculation are thought to be closer to the real state in solution.

The obtained ionic radii for tetraalkylammonium ion agreed with the values obtained by a similar method [61, 62] and by the measurement of partial molar volume [63], which are listed in

Table 11. Geometric parameters obtained from crystallographic data and MM2 calculations.

Ion	From crystallographic data						From MM2 calculation					
	V	r	a	b	c	c/a	V	r	a	b	c	c/a
Li^+	-	0.076	-	-	-	-	-	-	-	-	-	-
Me_4N^+	0.086	0.274	0.519	0.519	0.519	1.00	0.095	0.283	0.663	0.646	0.628	0.95
Me_3EtN^+	-	-	-	-	-	-	0.111	0.298	0.800	0.673	0.566	0.71
$\text{Me}_2\text{Et}_2\text{N}^+$	-	-	-	-	-	-	0.129	0.313	0.921	0.673	0.556	0.60
MeEt_3N^+	-	-	-	-	-	-	0.146	0.327	0.921	0.801	0.577	0.63
Et_4N^+	0.159	0.336	0.746	0.746	0.736	0.99	0.170	0.343	0.799	0.787	0.595	0.74
Pr_4N^+	-	-	-	-	-	-	0.231	0.381	1.080	1.003	0.488	0.45
Bu_4N^+	0.290	0.411	1.138	1.097	0.637	0.56	0.299	0.415	1.344	1.171	0.770	0.57
ClO_4^-	0.055	0.236	0.547	0.528	0.524	0.96	0.056	0.237	0.543	0.538	0.508	0.93
BF_4^-	0.049	0.227	0.521	0.492	0.461	0.89	0.051	0.229	0.521	0.491	0.479	0.92
PF_6^-	0.069	0.254	0.612	0.516	0.516	0.84	0.069	0.254	0.610	0.610	0.610	1.00
AsF_6^-	0.073	0.259	0.632	0.539	0.539	0.85	0.073	0.260	0.634	0.634	0.634	1.00
CF_3SO_3^-	0.080	0.267	0.565	0.560	0.547	0.97	0.082	0.270	0.625	0.551	0.518	0.83
$(\text{CF}_3\text{SO}_2)_2\text{N}^-$	0.146	0.326	0.980	0.629	0.543	0.55	0.144	0.325	0.994	0.581	0.558	0.56
$\text{C}_4\text{F}_9\text{SO}_3^-$	-	-	-	-	-	-	0.163	0.339	1.082	0.610	0.573	0.53
BPh_4^-	0.310	0.420	1.091	1.035	0.959	0.88	0.309	0.419	1.068	1.017	0.992	0.93
PC	-	-	-	-	-	-	0.088	0.276	0.781	0.641	0.430	0.55
GBL	-	-	-	-	-	-	0.081	0.268	0.680	0.552	0.422	0.62

V in nm^3 , r , a, b and c in nm.

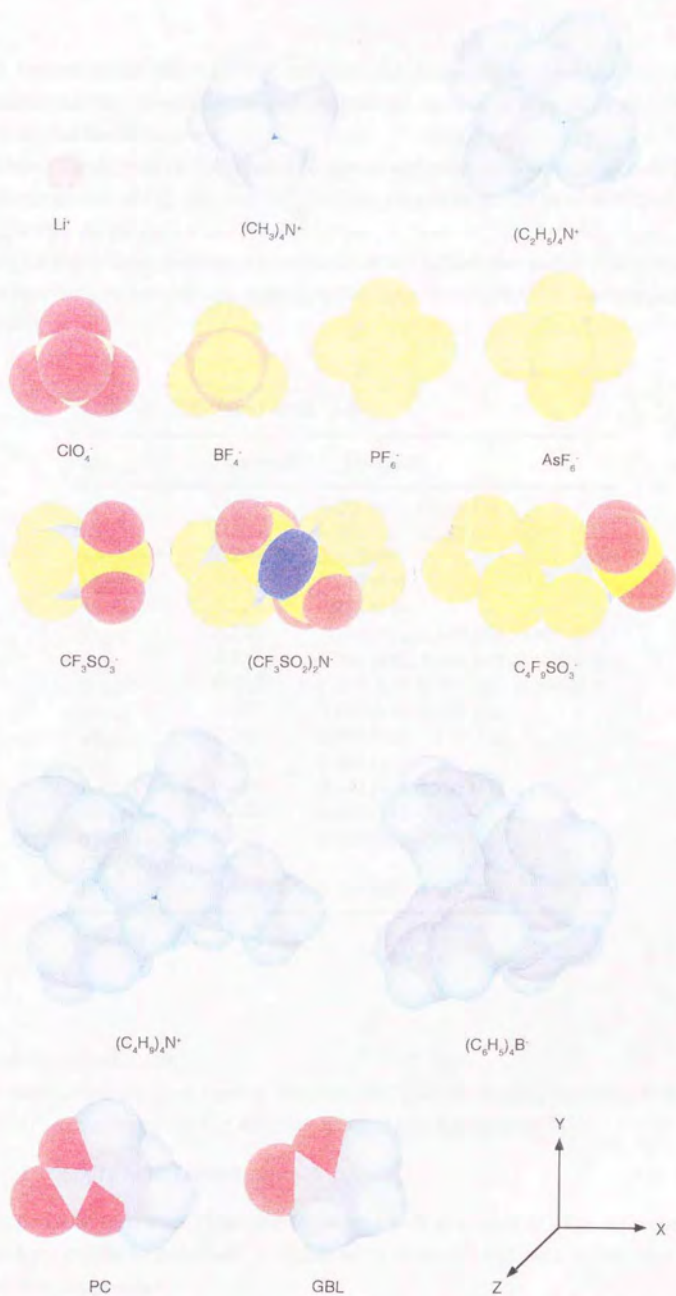


Fig. 3. Space-filling models of ions and solvents constructed by MM2 calculation.

Table 12. The traditional values given by Robinson and Stokes [62] are systematically larger than our values, because they considered the distance from the center of N atom, along the line of the C-C bond, to the surface of H atom.

The obtained ionic radii of ClO_4^- and BF_4^- agreed well with thermochemical radii [64]. It is evident that ionic radii of PF_6^- [65] and AsF_6^- [66] are overestimated and those of CF_3SO_3^- [30] and $(\text{CF}_3\text{SO}_2)_2\text{N}^-$ [35] are wrong.

Although the most frequently used ionic radius of Li^+ is 0.060 nm [67], it was estimated to be 0.076 nm by averaging the effective ionic radii for different coordination numbers presented by Shannon [68].

Table 12. Estimated ionic radii.

Ion	This work	Literature
Li^+	0.076	0.060 (67), 0.078 (3)
Me_4N^+	0.283	0.283 (61), 0.285 (63), 0.347 (62)
Me_3EtN^+	0.298	0.305 (69)
$\text{Me}_2\text{Et}_2\text{N}^+$	0.313	0.319 (69)
MeEt_3N^+	0.327	0.332 (69)
Et_4N^+	0.343	0.339 (61), 0.348 (63), 0.400 (62)
Pr_4N^+	0.381	0.381 (61), 0.398 (63), 0.452 (62)
Bu_4N^+	0.415	0.415 (61), 0.437 (63), 0.494 (62)
ClO_4^-	0.237	0.240 (64), 0.283 (31)
BF_4^-	0.229	0.232 (64), 0.278 (31)
PF_6^-	0.254	0.295 (65)
AsF_6^-	0.260	0.384 (66), 0.326 (31)
CF_3SO_3^-	0.270	0.602 (31)
$(\text{CF}_3\text{SO}_2)_2\text{N}^-$	0.325	0.450 (36)
$\text{C}_4\text{F}_9\text{SO}_3^-$	0.339	
BPh_4^-	0.419	0.480 (62), 0.535 (44)

r in nm.

Applicability of Stokes law

Stokes showed that the force f acting on a spherical particle of radius r moving with uniform velocity of v in a continuous fluid of viscosity η is given by the equation [62]:

$$f = 4\pi\eta rv + 2\pi\eta rv = x\pi\eta rv \quad (4)$$

where the first term represents a force due to pressure built up in front of it and the second term is a frictional force parallel to its surface. If the boundary between the particle and the fluid is slippy, the second term disappears.

However, this Stokes equation must be modified by using a numerical factor x less than 6 in

equation 4, when applied to very small molecules ($r < 0.5$ nm) [62, 70].

The author has attempted to determine an empirical correction factor, because it has practical utility. Walden products $\lambda_o \eta$ of each ion are plotted against the reciprocal of ionic radii r in Fig. 3.

The theoretical behavior calculated from Stokes law is given by the bottom line for perfect stick ($x = 6$) and by the top line for perfect slip ($x = 4$). All ions except Li^+ , Me_4N^+ , Bu_4N^+ and BPh_4^- approached the behavior for perfect slip and average factor was 4.3. This result suggests that ionic mobilities of the most ions discussed here are determined only by ion size. A slightly higher factor for Me_4N^+ ($x = 4.7$) indicates the existence of weak solvation [47]. Higher factors for Bu_4N^+ ($x = 5.0$) and BPh_4^- ($x = 5.7$) are well understood, since larger ions approach the behavior for perfect stick [62].

Assuming the correction factor for solvated Li^+ is 5.7, the solvation number N_s was estimated by the following equation [62]:

$$N_s = 4\pi (r_s^3 - r_c^3) / 3V \quad (5)$$

, where r_s , r_c and V are Stokes radius of solvated Li^+ , crystallographic radius of Li^+ and the molecular volume of solvent, respectively. The solvation numbers were 3.2 for PC and 2.3 for GBL.

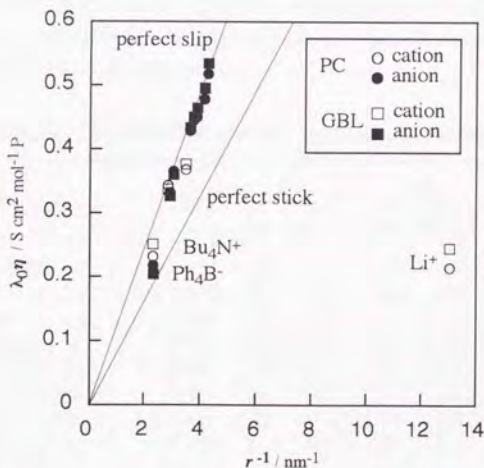


Fig. 4. Walden products as a function of the reciprocal of ionic radii.

Applicability of Bjerrum theory

Within the framework of Justice treatment ($R = q$), the association constant is strictly defined for electrostatic interactions by the Bjerrum equation [45]:

$$K_B = 4\pi N \int_a^q \exp(-e^2/\epsilon_r kT R) R^2 dR \quad (6)$$

, where N is Avogadro number, a represents the contact distance for two spherical ions and q is some critical distance at which ion pairing no longer is regarded to exist. For a contact ion pair a is simply the sum of the ionic radii ($r_+ + r_- = a_B$) and for a solvent-separated ion pair a is the sum of the ionic radii and the diameter of the solvent ($r_+ + r_- + 2r_s$).

Theoretical association constants K_B were calculated from equation 6 using the contact distance a_B . The results are given in Table 13, where the ratios of the theoretical association constant to the observed one are given. All observed association constants in PC were larger than calculated ones, which indicates contact ion pairs are formed in PC. On the other hand, LiClO_4 , LiPF_6 , LiAsF_6 and $\text{Li}(\text{CF}_3\text{SO}_2)_2\text{N}$ in GBL showed smaller association constants. Salomon *et al.* have obtained the similar results, and they concluded that alkali metal salts form solvent-separated ion pairs in GBL, even though they used a too small diameter (0.264 nm) for GBL [28]. If the solvent-separated ion pairs are formed, all lithium salts should be completely dissociated by equation 6.

The author considers that this kind of argument is difficult for slightly associated electrolytes, because the present conductance theories do not have completeness to afford an exact association constant (ambiguity of the coefficients in the conductance equation, inconsistency of ion size parameter and validity of Bjerrum theory itself).

Table 13. Contact distances and calculated association constants.

Salt	a_B	PC		GBL	
		K_B	K_B/K_A	K_B	K_B/K_A
LiClO_4	0.313	1.2	0.4	11.5	1.4
LiBF_4	0.305	1.3	0.2	11.9	0.7
LiPF_6	0.330	1.0	0.5	10.7	1.9
LiAsF_6	0.336	1.0	0.9	10.4	1.8
LiCF_3SO_3	0.346	0.9	0.1	9.9	0.4
$\text{Li}(\text{CF}_3\text{SO}_2)_2\text{N}$	0.401	0.3	0.2	7.5	2.0
$\text{LiC}_4\text{F}_9\text{SO}_3$	0.415	0.2	0	7.0	0.4
Et_4NClO_4	0.580	0	0	2.2	0.2
Et_4NBF_4	0.572	0	0	2.3	0.2
Et_4NPF_6	0.597	0	0	1.8	0.2
$\text{Et}_4\text{NCF}_3\text{SO}_3$	0.613	0	0	1.4	0.2
$\text{Me}_4\text{N}(\text{CF}_3\text{SO}_2)_2\text{N}$	0.608	0	0	1.5	0.3
$\text{Et}_4\text{N}(\text{CF}_3\text{SO}_2)_2\text{N}$	0.668	0	0	0.4	0.1
Bu_4NClO_4	0.652	0	0	0.7	0.1
Bu_4NBPh_4	0.834	0	0	0	0

a_B in nm, K_B in $\text{dm}^3 \text{mol}^{-1}$.

4.4. Conductometric Analysis of Diluted Solutions (2)

Our previous study on conductometric analysis of lithium salts including LiClO_4 , LiBF_4 , LiPF_6 , LiAsF_6 , LiCF_3SO_3 , $\text{Li}(\text{CF}_3\text{SO}_2)_2\text{N}$ and $\text{LiC}_4\text{F}_9\text{SO}_3$ in propylene carbonate (PC) and γ -butyrolactone (GBL) is now extended into mixtures of PC with either 1,2-dimethoxyethane (DME) or ethyl methyl carbonate (EMC).

Mixed solvent systems such as $\text{LiClO}_4/\text{PC}/\text{DME}$ and $\text{LiBF}_4/\text{GBL}/\text{DME}$ have a long history of use as nonaqueous electrolytes in the primary Li/MnO_2 and $\text{Li}/(\text{CF}_x)_n$ batteries, because the addition of the ether increases the electrolytic conductivity of the electrolytes due to its low viscosity [1, 2]. However, the ether solvents have been replaced with linear ester and linear carbonates, e.g. methyl formate (MF), methyl acetate (MA), dimethyl carbonate (DMC) and diethyl carbonate (DEC), because the 4 V class rechargeable lithium (ion) battery using a Li_xCoO_2 cathode requires much more stable solvents towards oxidation [71 - 73]. Properties of the ethylene carbonate (EC)-based electrolytes [74 - 77] and PC-based electrolytes [77, 78] containing these linear solvents have already been investigated.

Conductometric analysis on lithium salts in MF [36, 79], MA [80] and DMC [81] in the dilute range has already been reported by Salomon *et al.*, however, there is no report on the mixed solvents with these solvents. EMC, which shows intermediate properties between DMC and DEC, was recently introduced as a cosolvent in the rechargeable lithium ion battery [76]. In order to compare EMC with DME as a cosolvent, conductometric analysis on lithium salts in equimolar mixtures of PC with either DME or EMC has been carried out.

4.4.1. Experimental

Materials

LiClO_4 (Japan Carlit Co.), LiBF_4 , LiPF_6 , LiCF_3SO_3 (Morita Chemical Industries), and $\text{Li}(\text{CF}_3\text{SO}_2)_2\text{N}$ (3M) were purified by recrystallization, and were then vacuum dried at 100°C . Propylene carbonate, 1,2-dimethoxyethane and ethyl methyl carbonate (Mitsubishi Petrochemical Co., Battery-grade F-PC, F-DME and F-EMC) were used without further purification.

Electrolyte preparation

Each lithium salt was dissolved in equimolar mixtures of PC/DME or PC/EMC, so as to make 1 mol dm^{-3} solutions. Water content in these mother solutions (20 - 100 ppm) was measured by a moisture meter (Mitsubishi Kasei Co., CA-06) and concentration of the solutions was calibrated. The mother solutions were then diluted to about $10^{-2} \text{ mol dm}^{-3}$ to make stock solutions.

Measurements of physical properties of the solvents

Density of the (mixed) solvents was measured at $25 \pm 0.1^\circ\text{C}$ by a digital density meter (PAAR, DMA 45). Viscosity was determined using a viscosity meter (Tokyo Keiki Co., Visconic ED). Relative permittivity was measured by an LCR meter equipped with a capacitor cell (Ando Electric Co., AG-4311).

Conductivity measurements

The stock solutions were successively diluted and molar concentrations C (mol dm^{-3}) were calculated from the concentrations m' (mol kg^{-1} -solution) and the densities d (g cm^{-3}) of each solution by $C = m'd$. Densities were calculated from $d = d_o + Dm'$, where d_o is the solvent's density

and D is a characteristic constant of the solution.

Electrolytic conductivity of the mother solutions, their diluted solutions and the (mixed) solvents was measured at $25 \pm 0.1^\circ\text{C}$ by a conductivity meter (Toa Electronics, CM-60S/CGT-511B), a bridge (Toa Electronics, CM-25E/CG-2001PL) and an LCR meter (Ando Electric Co., AG-4311) equipped with the same conductivity cell (CG-2001PL), respectively.

Transport number measurements

The transport numbers of Li^+ and PF_6^- ions in PC/EMC were determined through measuring the electromotive force of the concentration cell with a liquid junction [82]:

$\text{Li} \mid \text{LiPF}_6 (x \text{ mol dm}^{-3}) \text{ in PC/EMC} \mid \text{LiPF}_6 (y \text{ mol dm}^{-3}) \text{ in PC/EMC} \mid \text{Li}$

, where three solutions ($x = 0.0125$ and 0.00625 , $y = 0.025 \text{ mol dm}^{-3}$) were used.

Calculation of solvent size

The van der Waals volumes of the solvents were calculated from the molecular model constructed by a molecular modeling system CHEMLAB-II (Molecular Design Co.) on a VAX8350 (Digital Equipment Corp.).

4.4.2. Results and Discussion

Relevant properties of PC, DME, EMC and their equimolar mixtures utilized in this study are summarized in Table 14, where d_0 , η , ϵ_r , κ and q are density, viscosity, relative permittivity, electrolytic conductivity and Bjerrum critical distance, respectively.

Molar conductivities

Molar conductivities Λ were calculated from experimental electrolytic conductivities σ after subtracting the solvent's electrolytic conductivity κ . Molar conductivities over the concentration range of 10^{-2} to $10^{-3} \text{ mol dm}^{-3}$ in PC/DME and PC/EMC are listed in Table 15.

Analysis of conductivity data

The data were analyzed by means of the Fernández-Prini expansion of the Fuoss-Hsia equation (See Chap. 6).

Derived parameters are summarized in Table 16 with the standard error of estimate σ_λ . The standard errors of estimate were less than 0.15 and standard deviations in Λ_0 and K_λ were less than 0.15 and 1.5, respectively.

Limiting molar conductivities

Ratios of the limiting molar conductivities of lithium salts in PC/DME to those in PC resembled the value deduced from solvent viscosities, while the ratios of those in PC/EMC to PC were lower than expectation as shown in Table 17. The ratios of those in PC/EMC to PC/DME ranged from 0.69 to 0.71 in contrast to 0.85, which is the ratio of the viscosity of PC/DME to that of PC/EMC. The lower limiting molar conductivities for PC/EMC suggest the existence of a stronger solute-solvent interaction than in PC/DME.

The limiting molar conductivities were plotted against the reciprocal of solvent's viscosities in Fig. 5. It is evident that the mobility order was not altered by the addition of cosolvents.

Single ion limiting molar conductivities

The single ion limiting molar conductivities were calculated by the following equations:

$$\lambda_0^+ (\text{Li}^+) = t^+ \Lambda_0 (\text{LiX}), \lambda_0^- (\text{X}^-) = t^- \Lambda_0 (\text{LiX}) \quad (7)$$

, where t^+ and t^- are the transport numbers of Li^+ and X^- ions, respectively.

The transport number t^+ (LiPF_6 in PC/EMC) was calculated to be 0.41 by using following equation [82]:

$$\Delta E = 2RT/F(1-t^+) \ln(a_x/a_y) \quad (7)$$

, where ΔE , R , F and a are the electromotive force, gas constant, Faraday constant and activity. It was assumed that the activity coefficients are the same for both x and y solutions. A reported value t^+ (LiClO_4 in PC/DME) = 0.43 [26] was used for PC/DME solutions. The resulting sets of the single ion limiting molar conductivities are given in Table 18.

Fig. 6 shows the relationship between Walden product and ionic radius. Every anion tends to have a lower Walden product (*ie.* larger Stokes radius) in PC/EMC than that in PC. This was also true for PC/DME as previously reported in PC/DME [26] and PC/dimethoxymethane [27].

Walden product of Li^+ was not enhanced by the addition of EMC as observed in the case of DME. It seems that EMC has no specific solvation with Li^+ , because a specific solvation of Li^+ with DME caused the conductivity enhancement [26, 29]. This is reasonable from the fact that EMC has the same functional group with PC.

As a measure of the Li^+ -solvent interaction, the solvation number N_s was estimated by equation 5. The molecular volumes V were estimated by MM2 calculation, being considered to be 0.098 nm^3 for EMC and 0.097 nm^3 for DME. The solvation numbers were 2.2 for EMC and 1.0 for DME, assuming these solvents are preferentially solvated with Li^+ .

Association constants

Ratios of the logarithm of the association constants of lithium salts among different solvents are listed in Table 19. The ratios of PC/DME to PC and PC/EMC to PC became larger than the values expected from solvent's relative permittivities, as the strength of the conjugated acids of anions increased. The ratio of PC/EMC to PC/DME was close to that expected from solvent's relative permittivities. The association constants were plotted against the reciprocal of the solvent's relative permittivities in Fig. 7. LiPF_6 and $\text{Li}(\text{CF}_3\text{SO}_2)_2\text{N}$ showed relatively good dissociating ability in PC/EMC.

Fig. 8 shows the relationship between association constant and contact distance a_B , which is simply the sum of the ionic radii of the anion and cation. Theoretical association constants K_B in equation 6 are given by the dotted lines, when \bar{a} is assumed to be a_B .

It seems that LiPF_6 and $\text{Li}(\text{CF}_3\text{SO}_2)_2\text{N}$ form solvent-separated ion pairs in PC/EMC, because K_A is fairly lower than K_B .

Table 14. Physical properties of the solvents at 25°C.

Solvent	$d_0 / \text{g cm}^{-3}$	η / cP	$\epsilon_r / -$	$\kappa / \text{S cm}^{-1}$	q / nm
PC	1.1998	2.51	64.9	0.9×10^{-7}	0.432
DME	0.8612	0.47	7.2	$< 5 \times 10^{-9}$	3.892
EMC	1.0070	0.65	2.4	6×10^{-9}	11.675
PC/DME	1.0229	1.06	35.5	2.5×10^{-7}	0.789
PC/EMC	1.0994	1.25	27.4	1.1×10^{-7}	1.023

Table 15. Molar conductivities of Li salts in PC/DME and PC/EMC in the dilute range at 25°C.

PC/DME		PC/EMC	
$10^3 C$	Λ	$10^3 C$	Λ
$/ \text{mol dm}^{-3}$	$/ \text{S cm}^2 \text{mol}^{-1}$		
LiBF ₄		LiBF ₄	
11.4372	47.804	12.2242	27.346
8.5740	49.889	9.1656	29.293
5.7140	52.529	6.1081	31.825
2.8564	56.451	3.0546	35.615
2.0042	58.203	2.1416	37.444
1.1429	60.240	1.2241	39.819
LiClO ₄		LiClO ₄	
11.3899	51.173	12.2354	32.152
8.5663	52.537	9.1724	33.458
5.7084	54.525	6.1158	35.284
2.8556	57.379	3.0571	38.171
2.0016	58.628	2.1416	39.102
1.1422	60.324	1.2204	40.881
LiPF ₆		LiPF ₆	
11.7191	51.604	12.8101	34.144
8.7841	52.794	9.6045	35.232
5.8547	54.699	6.4000	36.624
2.9257	57.326	3.1995	38.846
2.0526	58.682	2.2439	39.815
1.1722	60.057	1.2808	41.137
LiCF ₃ SO ₃		LiCF ₃ SO ₃	
11.3827	42.850	12.3262	20.660
8.5329	45.207	9.2405	22.444
5.6864	48.212	6.1601	25.079
2.8426	52.645	3.0787	29.653
1.9935	54.453	2.1585	31.754
1.1416	57.067	1.2352	35.007
Li(CF ₃ SO ₂) ₂ N		Li(CF ₃ SO ₂) ₂ N	
11.4257	48.159	12.2583	31.260
8.5623	49.432	9.1886	32.245
5.7067	51.194	6.1135	33.580
2.8534	53.674	3.0597	35.556
2.0001	54.674	2.1463	36.430
1.1431	56.161	1.2243	37.606

Table 16. Derived parameters for PC/DME and PC/EMC electrolytes at 25°C.

Salt	PC ^a			PC/DME			PC/EMC		
	Λ_0	K_A	σ_Λ	Λ_0	K_A	σ_Λ	Λ_0	K_A	σ_Λ
LiBF ₄	28.83	8.4	0.047	66.11	40.1	0.058	47.20	119.0	0.085
LiClO ₄	27.35	2.8	0.063	65.02	20.0	0.110	45.97	47.7	0.130
LiPF ₆	26.31	2.1	0.019	64.73	16.7	0.140	45.63	26.9	0.110
LiCF ₃ SO ₃	25.33	16.1	0.088	63.57	59.4	0.075	45.39	266.5	0.057
Li(CF ₃ SO ₂) ₂ N	22.80	1.5	0.036	60.54	16.0	0.049	41.78	25.3	0.078

Λ_0 in S cm² mol⁻¹, K_A in dm³ mol⁻¹. ^a Taken from Table 8.

Table 17. Ratios of limiting molar conductivities among different solvents.

Salt	$\frac{\Lambda_0(\text{PC/DME})}{\Lambda_0(\text{PC})}$	$\frac{\Lambda_0(\text{PC/EMC})}{\Lambda_0(\text{PC})}$	$\frac{\Lambda_0(\text{PC/EMC})}{\Lambda_0(\text{PC/DME})}$
	LiBF ₄	2.29	1.64
LiClO ₄	2.38	1.68	0.71
LiPF ₆	2.46	1.73	0.70
LiCF ₃ SO ₃	2.51	1.79	0.71
Li(CF ₃ SO ₂) ₂ N	2.66	1.83	0.69

Solvent index	$\frac{\eta(\text{PC})}{\eta(\text{PC/DME})}$	$\frac{\eta(\text{PC})}{\eta(\text{PC/EMC})}$	$\frac{\eta(\text{PC/DME})}{\eta(\text{PC/EMC})}$
	2.37	2.01	0.85

Table 18. Single ion limiting molar conductivities at 25°C.

Ion	PC ^a	PC/DME	PC/EMC
Li ⁺	8.43	27.96	18.71
BF ₄ ⁻	20.43	38.15	28.49
ClO ₄ ⁻	18.93	37.06	27.26
PF ₆ ⁻	17.86	36.77	26.92
CF ₃ SO ₃ ⁻	16.89	35.61	26.68
(CF ₃ SO ₂) ₂ N ⁻	14.40	32.58	23.07

in S cm² mol⁻¹. ^a Taken from Ref. 8.

Table 19. Ratios of association constants among different solvents.

Salt	$\frac{\log K_A(\text{PC/DME})}{\log K_A(\text{PC})}$	$\frac{\log K_A(\text{PC/EMC})}{\log K_A(\text{PC})}$	$\frac{\log K_A(\text{PC/EMC})}{\log K_A(\text{PC/DME})}$
LiBF ₄	1.7	2.2	1.3
LiClO ₄	2.9	3.8	1.3
LiPF ₆	3.8	4.4	1.2
LiCF ₃ SO ₃	1.5	2.0	1.4
Li(CF ₃ SO ₂) ₂ N	6.8	8.0	1.2

Solvent index	$\frac{\epsilon_r(\text{PC})}{\epsilon_r(\text{PC/DME})}$	$\frac{\epsilon_r(\text{PC})}{\epsilon_r(\text{PC/EMC})}$	$\frac{\epsilon_r(\text{PC/DME})}{\epsilon_r(\text{PC/EMC})}$
	1.8	2.4	1.3

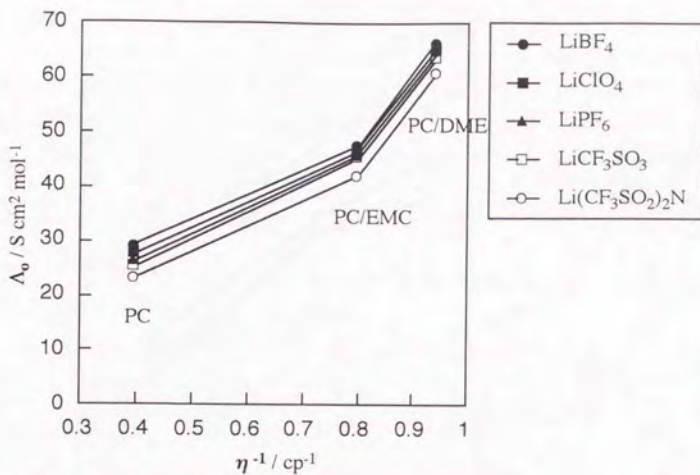


Fig. 5. Relationship between limiting molar conductivity and the reciprocal of solvent's viscosity.

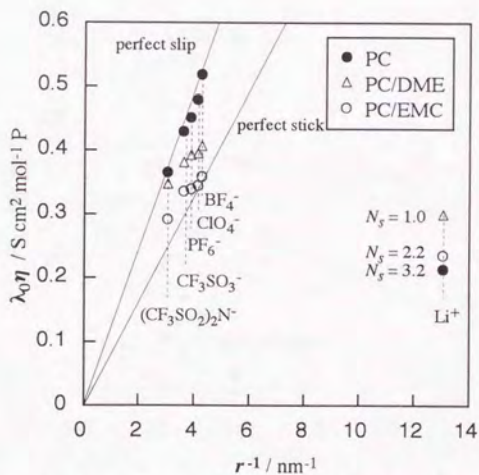


Fig. 6. Relationship between Walden product and the reciprocal of ionic radius.

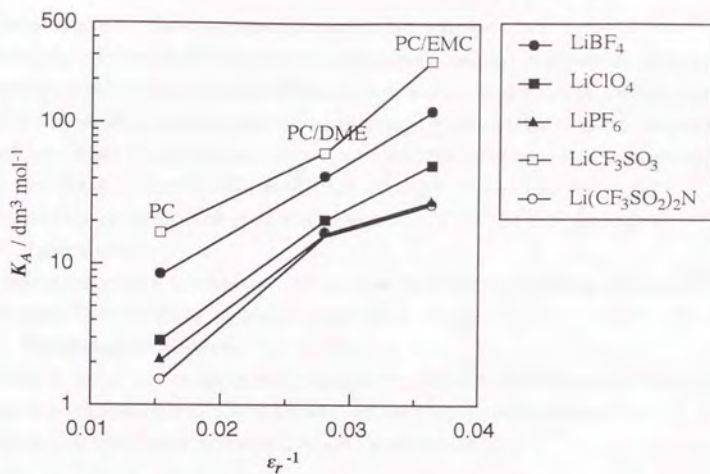


Fig. 7. Relationship between association constant and the reciprocal of solvent's relative permittivity.

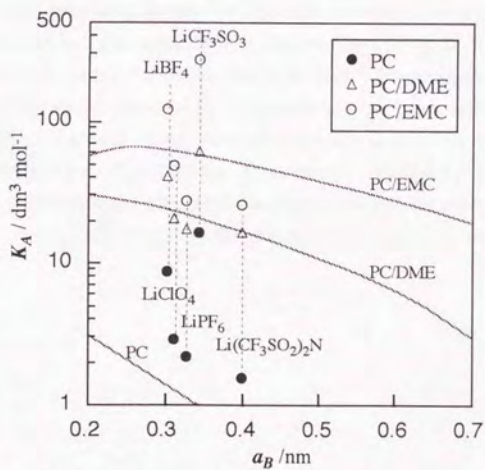


Fig. 8. Relationship between association constant and contact distance.

4.5. Correlation between Concentrated and Diluted Solutions

There is a widespread belief that the conductometric analysis in the dilute range is vain to understand the conductivities of practical electrolytes, because even the most advanced theory can be applied only upto the concentration of 0.1 mol dm^{-3} . However, the author considers that less effort has been made to correlate between two areas rather than to blame the incompleteness of the conductance theory. Therefore, the author has attempted to correlate the conductivity data of concentrated solutions with those of diluted solutions.

4.5.1. Experimental

The multiple regression analysis was carried out by the StatView II software (Abacus Concepts) on a Macintosh Quadra 840AV (Apple computer, Inc.).

4.5.2. Results and Discussion

Although Λ_0 and K_A are not intrinsically independent variables, multiple regression analysis was attempted to predict molar conductivity Λ_c at 1 mol dm^{-3} for practical purposes.

The regression equation is represented by the following equation:

$$\Lambda_c = C_A \Lambda_0 + C_K K_A \quad (7)$$

where C_A and C_K are regression coefficients.

The results are summarized in Table 20. Standardized regression coefficients and probability values are also listed for comparing the relative importance between the regression coefficients. Good fitting result was obtained for each solvent system as shown in Fig. 9. For lithium salts, K_A is more important than Λ_0 in helping to predict the Λ_c at high concentrations, whereas K_A is not important for tetraethylammonium salts. This information completely agrees with the understanding that lithium ion tends to associate and quaternary ammonium ion tends to dissociate by electrostatic shielding effect of alkyl groups. It became evident that the dissociating ability of lithium salts must be improved to get a highly conductive electrolyte for lithium batteries, because K_A is more important than Λ_0 in helping to predict the Λ at high concentrations.

Table 20. Results of multiple regression analysis.

Electrolyte		γ^2 *	Coefficient		Std. Coeff.		P-Value	
			Λ_o	K_A	Λ_o	K_A	Λ_o	K_A
Li salts	PC	0.991	0.232	-0.294	0.297	-0.885	0.0000	0.0003
	GBL	0.995	0.321	-0.361	0.410	-0.872	0.0000	0.0002
	PC/DME	0.997	0.280	-0.198	0.159	-1.004	0.0002	0.0037
	PC/EMC	0.956	0.173	-0.026	0.123	-0.927	0.0051	0.0465
Et ₄ N salts	PC	0.998	0.385	-0.169	0.961	-0.100	0.0096	0.8470
	GBL	0.999	0.392	-0.260	1.108	-0.342	0.0019	0.2863

* the coefficient of determination.

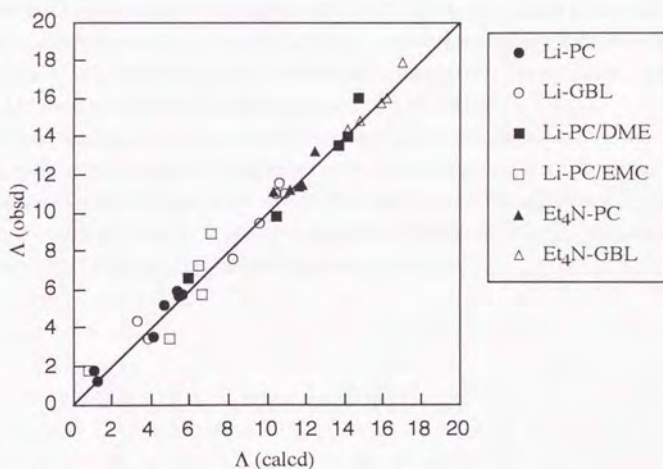


Fig. 9. Fitting results of multiple regression analysis.

4.6. Summary

The conductivities of popular lithium salts have been measured in propylene carbonate and γ -butyrolactone, and equimolar mixtures of propylene carbonate with either 1,2-dimethoxyethane or ethyl methyl carbonate at a practical concentration (1 mol dm⁻³) and a diluted range.

The limiting molar conductivities and the ionic association constants were calculated by the expanded Fuoss-Hsia equation. The mobility of anions in these solvents decreased in the following order: BF₄⁻ > ClO₄⁻ > PF₆⁻ > AsF₆⁻ > CF₃SO₃⁻ > (CF₃SO₂)₂N⁻ > C₄F₉SO₃⁻ > BPh₄⁻.

The association constants increased in the following order: Li(CF₃SO₂)₂N, LiAsF₆ < LiPF₆ < LiClO₄ < LiBF₄ < LiC₄F₉SO₃ < LiCF₃SO₃.

The results in pure solvents were correlated with ionic radii obtained by MM2 calculation. All anions except BPh₄⁻ approached the behavior for perfect slip and average factor was 4.3, which suggests that ionic mobilities are determined only by ion size. The solvation numbers of Li⁺ were 3.2 for PC and 2.3 for GBL. The comparison between experimental and theoretical association constants indicated contact ion pairs are formed in PC, and solvent-separated ion pairs might be formed in GBL.

The comparison between 1,2-dimethoxyethane and ethyl methyl ketone as a cosolvent revealed that ethyl methyl ketone cannot increase electrolytic conductivity as much as 1,2-dimethoxyethane does, even though ethyl methyl ketone is considered to be a low viscosity solvent useful for 4 V class rechargeable lithium batteries. Only highly dissociative salts; LiPF₆, LiAsF₆ and Li(CF₃SO₂)₂N seem to be useful from the viewpoint of conductivity.

The multiple regression analysis was attempted to predict molar conductivities at a higher concentration from the conductivity parameters obtained from the analysis of diluted solutions and good fitting result was obtained. It became evident that the dissociating ability of lithium salts must be improved to get a highly conductive electrolyte for lithium batteries, because K_A is more important than Λ_0 in helping to predict Λ at high concentrations.

4.7. References

1. H. V. Venkatasetty, Editor, *Lithium Battery Technology*, Wiley-Interscience, New York (1984).
2. J. P. Gabano, Editor, *Lithium Batteries*, Academic Press, New York (1983).
3. J. Barthel, H. J. Gores, G. Schmeer and R. Wachter, *Topics in Current Chemistry*, **111**, 33 (1983).
4. S. B. Brummer, V. R. Koch and R. D. Rauch, in *Materials for Advanced Batteries*, D. W. Murphy and B. C. H. Steele, Editors, Plenum Press, New York (1980).
5. G. J. Janz and R. P. T. Tomkins, Editors, *Nonaqueous Electrolyte Handbook*, Academic Press, New York, Vol. I (1972), Vol. II (1973).
6. R. Jasinski, in *Advances in Electrochemistry and Electrochemical Engineering*, C.W. Tobias, Editor, Wiley, New York, Vol. 8 (1971).
7. J. Barthel, H. J. Gores and G. Schmeer, *Ber. Bunsenges. Phys. Chem.*, **83**, 911 (1979).
8. H. J. Gores and J. Barthel, *J. Solution Chem.*, **9**, 939 (1980).
9. S. Tobishima and A. Yamaji, *Electrochim. Acta*, **28**, 1067 (1983).
10. Y. Matsuda, *J. Power Sources*, **20**, 19 (1987).
11. J. T. Dudley, D. P. Wilkinson, G. Thomas, R. LeVae, S. Woo, H. Blom, C. Horvath, M. W. Juzkow, B. Denis, P. Juric, P. Aghakian and J. R. Dahn, *J. Power Sources*, **35**, 59 (1991).
12. A. Webber, *J. Electrochem. Soc.*, **138**, 2586 (1991).
13. F. Kita, A. Kawakami, T. Sonoda and H. Kobayashi, in *Proceedings of the Symposium on New Sealed Rechargeable Batteries and Supercapacitors*, B. M. Barnett, E. Dowgiallo, G. Halpert, Y. Matsuda and Z-i. Takehara, Editors, PV 93-23, p. 321, The Electrochemical Society Proceedings Series, Pennington, NJ (1993).
14. Y. Matsuda, M. Morita and K. Kosaka, *J. Electrochem. Soc.*, **130**, 101 (1983).
15. F. Breivogel and M. Eisenberg, *Electrochim. Acta*, **14**, 459 (1969).
16. L. M. Mukherjee and D. P. Boden, *J. Phys. Chem.*, **73**, 3965 (1969).
17. L. M. Mukherjee, D. P. Boden and R. Lindauer, *J. Phys. Chem.*, **74**, 1942 (1970).
18. J. Courtot-Coupez and M. L'Her, *C. R. Acad. Sci. Ser. C*, **271**, 357 (1970).
19. M. L. Jansen and H. L. Yeager, *J. Phys. Chem.*, **77**, 3089 (1973).
20. R. L. Benott, D. Lahaie and G. Boire, *Electrochim. Acta*, **20**, 377 (1975).
21. H. V. Venkatasetty, *J. Electrochem. Soc.*, **122**, 245 (1975).
22. S. Singh, J. S. Jha and R. Gopal, *Indian J. Chem.*, **14A**, 127 (1976).
23. J. Barthel, R. Wachter and H. J. Gores, *Faraday Discuss. Chem. Soc.*, **64**, 285 (1977).
24. N. V. Timofeeva, E. M. Eingel and I. A. Kedrinskii, *Zh. Fiz. Khim.*, **53**, 447 (1979).
25. S. L. Maiofis, B. K. Filanovskii and M. S. Grilikhes, *Zh. Fiz. Khim.*, **53**, 1257 (1979).
26. Y. Matsuda, H. Nakashima, M. Morita and Y. Takasu, *J. Electrochem. Soc.*, **128**, 2552 (1981).
27. M. Salomon and E. Plichta, *Electrochim. Acta*, **28**, 1681 (1983).
28. M. Salomon and E. J. Plichta, *Electrochim. Acta*, **29**, 731 (1984).

29. M. Salomon and E. J. Plichta, *Electrochim. Acta*, **30**, 113 (1985).
30. G. Wawrzyniak and T. Jasifski, *Pol. J. Chem.*, **59**, 1181 (1985).
31. S. Tobishima and T. Okada, *Electrochim. Acta*, **30**, 1715 (1985).
32. P. K. Muhuri and D. K. Hazra, *J. Chem. Soc. Faraday Trans.*, **87**, 3847 (1991).
33. M. Hojo, Y. Miyauchi, A. Tanio and Y. Imai, *J. Chem. Soc. Faraday Trans.*, **87**, 3847 (1991).
34. G. Wawrzyniak, L. Chmurzyński and R. Korewa, *Pol. J. Chem.*, **66**, 175 (1992).
35. A. A. Al-Najar, K. M. H. Alami and A. M. Ebraheem, *J. Chem. Eng. Data*, **37**, 443 (1992).
36. M. Salomon, *J. Solution Chem.*, **22**, 715 (1993).
37. L. Werblan, A. Suzdorf and E. Lin, *Pol. J. Chem.*, **56**, 1071 (1982).
38. A. D'Aprano, D. I. Donato and A. Carrubba, *J. Solution Chem.*, **12**, 209 (1983).
39. A. Balkowska, G. Szymański and L. Werblan, *J. Electroanal. Chem.*, **287**, 229 (1990).
40. A. Balkowska, J. Lensiński, G. Szymański and L. Werblan, *J. Electroanal. Chem.*, **289**, 171 (1990).
41. K. Hasegawa and Y. Arakawa, *J. Power Sources*, **43-44**, 523 (1993).
42. J. Foropoulos, Jr. and D. D. DesMarteau, *Inorg. Chem.*, **23**, 3720 (1977).
43. D. S. Gill and M. B. Sekhri, *J. Chem. Soc. Faraday Trans. 1*, **78**, 119 (1982).
44. R. Zana, J. E. Desnoyers, G. Perron, R. L. Kay and K. Lee, *J. Phys. Chem.*, **86**, 3996 (1982).
45. A. K. Convington and T. Dickinson, Editors, *Physical Chemistry of Organic Solvent Systems*, Plenum Press, London (1973).
46. Y. Kiso and T. Hirokawa, *Chem. Lett.*, 891 (1979).
47. J. F. Reardon, *Electrochim. Acta*, **32**, 1595 (1987).
48. T. Fujinaga and I. Sakamoto, *J. Electroanal. Chem.*, **85**, 185 (1977).
49. A. Bondi, *J. Phys. Chem.*, **68**, 441 (1964).
50. V. G. Herrschaft and H. Hartl, *Acta Cryst.*, **C45**, 1021 (1989).
51. T. Migchelsen and A. Vos, *Acta Cryst.*, **23**, 796 (1967).
52. F. H. Herbststein, M. Kaftory, M. Kapon and W. Saenger, *Z. Krist.*, **154**, 11 (1981).
53. J. D. McCullough, *Acta Cryst.*, **17**, 1067 (1964).
54. G. Giuseppetti, F. Mazzi, C. Tadini, P. Ferloni and S. Torre, *Z. Krist.*, **202**, 81 (1992).
55. A. L. Rohl and D. M. P. Mingos, *J. Chem. Soc. Dalton Trans.*, 3541 (1992).
56. R. Minkwitz, V. Gerhard and H. Preut, *Z. Anorg. Allg. Chem.*, **580**, 115 (1990).
57. J. O. Lundgren, R. Tellgren and I. Olovsson, *Acta Cryst.*, **B34**, 2945 (1978).
58. K. Hoffmann and E. Weiss, *J. Organomet. Chem.*, **67**, 221 (1974).
59. R. Attig and D. Mootz, *Acta Cryst.*, **B31**, 1212 (1975).
60. S. Yoshida, *MM2 Force Field Parameter Data Book*, Martech, Tokyo (1991).
61. J. T. Edward, *J. Chem. Educ.*, **47**, 261 (1970).
62. R. A. Robinson and R. H. Stokes, *Electrolyte Solutions*, 2nd ed. rev., Butterworths, London (1970).

63. B. E. Conway, R. E. Verrall and J. E. DesNoyers, *Trans. Faraday Soc.*, **62**, 2738 (1966).
64. H. D. B. Jenkins and K. P. Thakur, *J. Chem. Educ.*, **56**, 576 (1979).
65. J. Eliassaf, R. M. Fuoss and J. E. Lind, *J. Phys. Chem.*, **67**, 1941 (1963).
66. G. Atkinson and C. J. Hallada, *J. Phys. Chem.*, **64**, 1487 (1960).
67. L. Pauling, *The Nature of the Chemical Bond*, 2nd ed., Cornell University Press, Ithaca, New York (1948).
68. R. D. Shannon, *Acta Cryst.*, **A32**, 751 (1976).
69. by MNDO calculation, See M. Ue, T. Sato and M. Takeda, *Denki Kagaku*, **61**, 1080 (1993).
70. N. Matsuura, K. Umemoto and Y. Takeda, *Bull. Chem. Soc. Jpn.*, **48**, 2253 (1975).
71. E. Plichta, M. Salomon, S. Slane, M. Uchiyama, D. Chua, W. B. Ebner, and H. W. Lin, *J. Power Sources*, **21**, 25 (1987).
72. E. Plichta, S. Slane, M. Uchiyama, M. Salomon, D. Chua, W. B. Ebner and H. W. Lin, *J. Electrochem. Soc.*, **136**, 1865 (1989).
73. M. Salomon, *J. Power Sources*, **26**, 9 (1989).
74. S. Tobishima, M. Arakawa, T. Hirai and J. Yamaki, *J. Power Sources*, **26**, 449 (1989).
75. S. Tobishima, M. Arakawa and J. Yamaki, *Electrochim. Acta*, **35**, 383 (1990).
76. M. Terasaki, H. Yoshida, H. Tukamoto, M. Mizutani and M. Yamachi, *Denki Kagaku*, **61**, 1417 (1993).
77. M. Ishikawa, M. Morita, M. Asao and Y. Matsuda, *J. Electrochem. Soc.*, **141**, 1105 (1994).
78. Y. Sasaki, S. Goto and M. Handa, *Denki Kagaku*, **61**, 1419 (1993).
79. E. Plichta, M. Salomon, S. Slane and M. Uchiyama, *J. Solution Chem.*, **16**, 225 (1987).
80. M. Salomon, M. Uchiyama, M. Xu and S. Petrucci, *J. Phys. Chem.*, **93**, 4375 (1989).
81. M. Delsignore, H. Farber and S. Petrucci, *J. Phys. Chem.*, **89**, 4968 (1985).
82. J. P. Hoare and C. R. Wiese, *J. Electrochem. Soc.*, **121**, 83 (1974).

5. Solid Organic Electrolytes for Rechargeable Lithium Cells

5.1. Introduction

Electrochemical devices employing liquid electrolytes suffer from a safety problem caused by the leakage of the liquid electrolytes. Organic electrolytes based on organic polymers appear to have some attractive features compared with liquid counterparts. The macromolecule itself acts as an immobile solvent for a salt which becomes partially dissociated in the matrix, leading to ionic conductivity. No solvent is required for the conduction process. Wright *et al.* first described the solvent free complexes formed between polyethylene oxide (PEO) and alkali metal salts [1]. It was only in 1978 that Armand highlighted the significance of PEO as a medium capable of dissolving salts to form novel class of ionic conductor [2]. Since then, considerable effort has gone into the development of solid polymer electrolytes (SPE), which make possible ultra-thin film batteries with high energy density and enhanced safety due to the absence of liquid electrolyte.

Solid polymer electrolytes are easily prepared by dissolving PEO and an appropriate salt in a volatile solvent such acetonitrile and casting the solution. Extensive reviews discussing the formation, structure, morphology and ion transport of SPE were published [3 - 5].

5.2. Quasi-Solid Organic Electrolytes

Solid polymer electrolytes such as complexes of polyethylene oxide with lithium salts cannot reach useful conductivity (ca. 10^{-3} S cm^{-1}) at ambient temperature. Their low conductivity considerably limits their usage in solid-state lithium batteries [3].

A promising approach to enhance the conductivity of solid polymer electrolytes is the addition of organic solvents as a plasticizer [6 - 12]. An alternative approach is the addition of gelling agents to immobilize liquid electrolytes in order to produce quasi-solid electrolytes [13 - 15]. Both approaches aim to obtain solid electrolytes with high conductivity and high dimensional stability.

1,3:2,4-Dibenzylidenesorbitol (DBS) is a non polymeric gelling agent used in lithium cells [16]. We have found that the introduction of ester groups in DBS can remarkably increase its gel-forming ability. Quasi-solid organic electrolytes containing this new gelling are proposed as an electrolyte for thin film lithium cells.

5.2.1. Experimental

Preparation

The gelling agents of DBS derivatives were prepared by a method described elsewhere [17].

1,3-(p-methoxycarbonylbenzylidene)-2,4-benzylidenesorbitol

Into a 200 ml flask were introduced 36.4 g (200 mmol) of D-sorbitol, 21.2 g (200 mmol) of benzaldehyde, 24.0 g of water and 2.3 g (12 mmol) of p-toluenesulfonic acid monohydrate. The resulting mixture was stirred at 35°C for 6 hours under a nitrogen atmosphere. After being cooled, the white creamy mixture was neutralized with 100ml of 0.125 mol dm^{-3} aqueous sodium hydroxide solution (12.5 mmol) and then filtered to obtain a white solid, which was washed with water and ether, and vacuum dried to give 46.4 g of 2,4-benzylidenesorbitol in a yield of 85.9 %.

46.4 g (170 mmol) of 2,4-benzylidenesorbitol, 27.9 g (170 mmol) of methyl p-formylbenzoate, 800 ml of benzene and 0.32 g (1.7 mmol) of p-toluenesulfonic acid monohydrate were introduced into a 2 l flask equipped with a Dean-Stark type fractionating column and a powerful stirrer. The resulting mixture was stirred and refluxed under nitrogen atmosphere for 6 hours. During the reaction, the water distilled out in the fractionating column was removed occasionally. After being cooled, the white gelatinous mixture was neutralized with 300ml of 0.006 mol dm^{-3} aqueous sodium hydroxide solution (1.8 mmol). The mixture was stirred thoroughly and then filtered to obtain a white solid. This white solid was washed with hot water and hot ethanol and vacuum dried to give 65.8 g of the product. The yield was 92.0 %. mp: 204.0 - 208.5°C.

¹H-n.m.r. (in DMSO-d₆) in ppm: 7.98 (2H, d), 7.61 (2H, d), 7.44 - 7.48 (2H, m), 7.35 - 7.39 (3H, m), 5.76 (1H, s, CH₂-OH), 5.67 (1H, s, CH-OH), 4.81 (1H, d), 4.77 (1H, t), 3.45 - 4.36 (8H, m, -C₆H₄-), 3.86 (3H, s, CO₂-CH₃).

mass spectrum in m/e (relative intensity): 416 (4.0, M⁺), 385 (3.5), 355 (6.8), 267 (6.8), 207 (14), 149 (78), 105 (100), 91 (76), 77 (35).

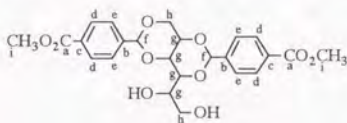
1,3:2,4-bis(p-methoxycarbonylbenzylidene)sorbitol

Into a 1 l flask equipped with a Dean-Stark type fractionating column and a powerful stirrer were introduced 13.7 g (75 mmol) of D-sorbitol, 24.6 g (150 mmol) of methyl p-formylbenzoate,

400 ml of benzene and 0.29 g (1.5 mmol) of p-toluenesulfonic acid monohydrate. The resulting mixture was stirred and refluxed under nitrogen atmosphere for 4 hours. After being cooled, the white gelatinous mixture was neutralized with an aqueous sodium hydroxide solution, and the benzene was removed under reduced pressure. Subsequently, water was added to the reaction mixture, which was then stirred thoroughly and then filtered to obtain a white solid. This white solid was washed with ethanol and vacuum dried to give 32.6 g of the product. The yield was 91.6%. mp: 223.5 - 226°C

¹H-n.m.r. (in DMSO-d₆) in ppm: 7.95 (4H, d), 7.55 (4H, d), 4.75 (1H, d), 4.35 (1H, t), 3.40 - 4.25 (8H, m, -C₆H₄-), 3.85 (6H, s, CO₂-CH₃).

¹³C-n.m.r. (in DMSO-d₆) in ppm: 165.9 (a), 143.3, 143.0 (b), 129.8, 129.7 (c), 128.9, 128.8 (d), 126.4 (e), 98.5, 98.4 (f), 77.6, 70.1, 68.5, 67.6 (g), 69.3, 62.5 (h), 52.0 (i).



mass spectrum in m/e (relative intensity): 474 (6.8, M⁺), 473 (6.8), 443 (15), 382 (6.8), 250 (27), 207 (54), 165 (97), 163 (100), 149 (62), 133 (51), 105 (45), 77 (22), 59 (22).

Quasi-solid electrolyte

A DBS derivative was dissolved in an electrolyte solution at 100-130°C and cooled to room temperature to yield a gelled electrolyte. A polymer matrix was prepared by adding 7.2 wt% of methoxy poly(ethylene glycol) methacrylate (n=23), 3.6 wt% of poly(ethylene glycol) dimethacrylate (n=23) and 0.03 wt% of tert-butyl peroxy-2-ethylhexanoate into an electrolyte solution (with or without a DBS derivative), followed by radical copolymerization at 70°C for 15 hours under nitrogen atmosphere.

Measurements

The conductivity of the electrolytes was measured by a conductivity meter (Toa Electronics, CM-60S). The mechanical strength of the gelled electrolytes was measured by a rheometer (Fudoh, NRM-2002J) and was expressed as the stress when the gel's destruction occurred.

5.2.2. Results and Discussion

The gelling agents used in this work have the chemical structure shown in Fig. 1.

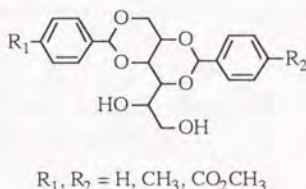


Fig. 1. Chemical structure of DBS derivatives.

As a preliminary test, the gel-forming ability of each compound was investigated using three organic solvents; N,N-dimethylformamide (DMF), γ -butyrolactone (γ -BL) and propylene carbonate (PC).

Table 1 shows the least required amount of each compound to form an immobilized gel (wt% vs. solvent). The substitution of a methoxycarbonyl group markedly decreased the required amount of the gelling agent and the disubstituent; 1,3:2,4-bis(p-methoxycarbonylbenzylidene)sorbitol (2pMC-DBS) showed the strongest gel-forming ability. The mechanical strength of the gel increased with the concentration of 2pMC-DBS as shown in Fig. 2

Table 1. Required amount of DBS derivatives to immobilize organic solvents.

R ₁	H	Me	CO ₂ Me	CO ₂ Me	CO ₂ Me
R ₂	H	Me	H	Me	CO ₂ Me
DMF	30	5	3	2.5	1
GBL	10	3	1.5	1.5	1
PC	2	1.5	1	1	1

in wt% vs. solvent

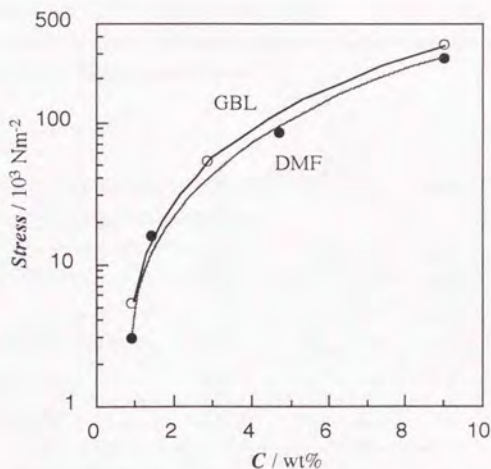


Fig. 2. Dependence of mechanical strength of gels on concentration of 2pMC-DBS.

Traditional liquid electrolytes which are used in commercial lithium cells were immobilized with DBS and 2pMC-DBS. Table 2 lists the required amount of the gelling agent to immobilize liquid electrolytes and the conductivity of resultant gelled electrolytes, which was measured at 25°C after standing several days at room temperature. As little as 1 to 1.5 wt% of 2pMC-DBS afforded gelled electrolytes whose mechanical strength is of the magnitude of 10^3 N m^{-2} . The strong gel-forming ability of 2pMC-DBS resulted in only about 5% decrease in conductivity from the liquid counterpart.

Since the existence of hydroxy groups in DBS derivatives is expected to be unfavorable for the application of lithium batteries, their reactivity was examined by direct contact with lithium metal and cyclic voltammetry. PC/LiClO₄/2pMC-DBS gelled electrolyte maintained a clear surface of the lithium metal and no remarkable peak was observed in the range of the electrochemical window of the liquid electrolyte itself as shown in Fig. 3.

These new gelled electrolytes are very attractive from the viewpoint of high conductivity, however they are too brittle to make a film. To circumvent this problem, a polymer matrix; poly(ethylene oxide)-grafted poly(methacrylate) (PEGPM; Fig. 4) was incorporated in the gelled electrolyte. We have found a remarkable enhancement of mechanical strength of the composite gelled electrolyte without a significant decrease in conductivity.

For example, a solid electrolyte comprising 81.0 wt%-PC, 7.5 wt%-LiClO₄, 10.6 wt%-PEGPM and 0.9 wt%-2pMC-DBS showed $2.7 \times 10^4 \text{ N m}^{-2}$ in mechanical strength and $4.6 \times 10^{-3} \text{ S cm}^{-1}$ in conductivity, whereas the polymer electrolyte without 2pMC-DBS showed $1.3 \times 10^3 \text{ N m}^{-2}$ in mechanical strength and $4.7 \times 10^{-3} \text{ S cm}^{-1}$ in conductivity.

Optimizations of these composite solid electrolytes is now in progress to make a thin film with high dimensional stability and high conductivity.

Table 2. Required amount of DBS derivatives to immobilize liquid electrolytes and conductivity of gelled electrolytes.

DBS derivative	None	DBS		2pMC-DBS	
	σ	C	σ	C	σ
LiClO ₄ / PC+DME	13.6	5	10.7	1.5	12.5
LiBF ₄ / GBL	7.5	15	4.5	1	7.2
LiClO ₄ / PC	5.6	4	4.6	1	5.3

Electrolyte concentration: 1 mol dm^{-3} ,
C in wt% vs. electrolyte, σ in mS cm^{-1} at 25°C.

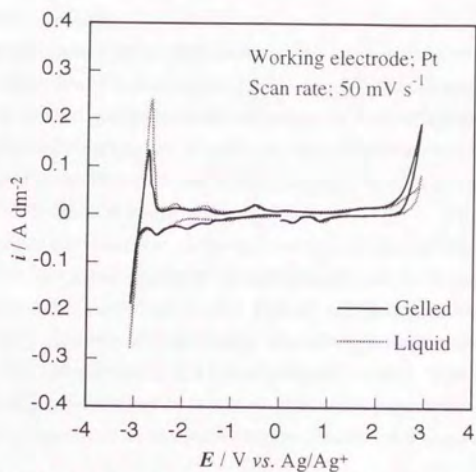


Fig. 3. Cyclic voltammetry of liquid and gelled electrolytes of $1 \text{ mol dm}^{-3} \text{ LiClO}_4/\text{PC}$.

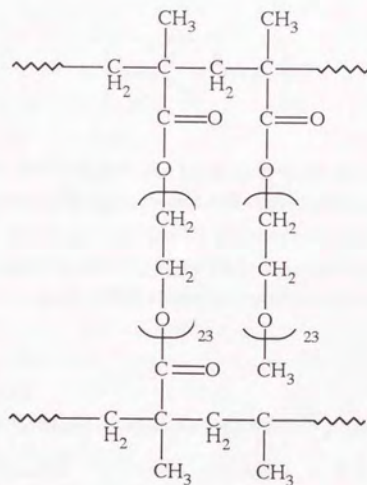


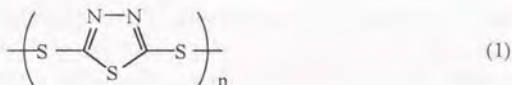
Fig. 4. Chemical structure of poly(ethylene oxide)-grafted poly(methacrylate) (PEGPM).

5.3. Solid Polymer Electrolytes

All-solid-state rechargeable lithium cells based on solid polymer electrolytes represented by a complex formed between a polyethylene oxide (PEO) and a lithium salt have proposed by Armand [2 - 5]. Subsequently, several groups have shown interest in developing the practical batteries for consumer electronics, load-levelling and electric vehicle applications based on this concept [18 - 21]. However, successful results are limited to high-temperature cells due to the low conductivity of polymer electrolytes at ambient temperature.

The cathode materials tested in these advanced batteries can be classified into three categories. The first one includes inorganic intercalation compounds such as titanium disulfide [19, 20], molybdenum dioxide [19], vanadium oxides [18, 21 - 25], titanium dioxide [25, 26] and manganese dioxide [27]. The second one consists of electronically conducting polymers such as polyacetylene [28, 29], polypyrrole [30, 31] and polyaniline [32]. The last one is a group of polymeric organodisulfides, which has been named solid redox polymerization electrodes (SRPE) due to the reversible polymerization-depolymerization reaction that occurs on charge-discharge process [33 - 38].

Among polymeric organodisulfides, a polymer prepared from 2,5-dimercapto-1,3,4-thiadiazole (noted as X1) is a promising active material from the point of good reversibility, high open circuit voltage and high energy density based on the simple delocalized structure [34, 35].

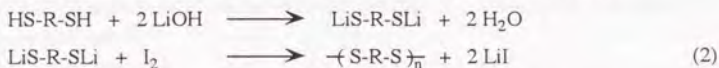


We will report initial results on how the loading level of an active material in a cathode composite influences the available capacity of a PEO-based thin film rechargeable lithium cell operated at 95°C. As an active material, the X1 polymer was evaluated in comparison with a reliable inorganic sulfide counterpart, TiS_2 . Two kinds of supporting electrolyte salts, LiCF_3SO_3 and $\text{Li}(\text{CF}_3\text{SO}_2)_2\text{N}$ [39], were used in PEO electrolytes and their performance in the cell was also examined.

5.3.1. Experimental

Preparation of polymer X1

The general preparative method is illustrated by the following reaction [34, 35].



2,5-Dimercapto-1,3,4-thiadiazole (Aceto Chemical) was recrystallized twice from acetone to give a white powder.

ir: 3400 (broad), 1500, 1450 cm^{-1} . mp: 161 °C.

4.508 g (30 mmol) of the recrystallized monomer and 2.518 g (60 mmol) of $\text{LiOH} \cdot \text{H}_2\text{O}$ (Aldrich) were dissolved in 50 ml of water, respectively. When one equivalent of LiOH solution

was added to the monomer solution, the color of the mixture turned slightly yellow and the addition of another equivalent of LiOH solution changed it to a colorless solution. The solution was evaporated to dryness and the resultant white powder was washed with hexane and dried *in vacuo* at 120°C for 24 hours. The yield was 6.62 g, which indicated the incorporation of about three water molecules per dithiolate salt.

ir: 3250 cm^{-1} (broad).

Calcd. for $\text{C}_2\text{N}_2\text{S}_3\text{Li}_2 \cdot 3\text{H}_2\text{O}$: C; 11.11, H; 2.80, N; 12.96.

Found: C; 12.13, H; 2.51, N; 13.53.

The polymer X1 was prepared without the isolation of the lithium salt. Into the solution of lithium dithiolate (30 mmol), 7.614 g (30 mmol) of iodine (J. T. Baker) was added and heated at 75°C for 2 hours to give a slightly yellow precipitate. The precipitate was washed with boiling water, hot acetone, methanol, hexane and ether successively and dried *in vacuo* at 120°C for 24 hours to give 3.74 g (84 % in yield) of the polymer, which was ground into a fine powder.

ir: 1500, 1475, 1450 cm^{-1} . Decomp. temp.: 188°C.

Calcd. for $(\text{C}_2\text{N}_2\text{S}_3)_n$: C; 16.21, N; 18.90, S; 64.90.

Found: C; 16.13, N; 18.60, S; 65.00.

Impurities: Li; 57 ppm, Na; 27 ppm.

Preparation of cathode and electrolyte films

Cathode films were prepared from polymer X1 powder or TiS_2 powder (Cerac), Shawinigan acetylene black powder (Chevron Chemical), Brij 35 (Aldrich) as a dispersant and PEO (5×10^6 in average molecular weight, Aldrich). Electrolyte films were prepared from LiCF_3SO_3 (3M) or $\text{Li}(\text{CF}_3\text{SO}_2)_2\text{N}$ (3M) and the same PEO. All materials were dried under vacuum at 50°C for several days and stored under helium atmosphere.

When the loading level of active materials was changed, the amount ratios of acetylene black and Brij 35 to the active material were kept constant as shown in Table 3. The ratio of Li^+ ion to an ethylene oxide monomer unit in the polymer electrolytes was adjusted to 1 : 8 as shown in Table 4.

A viscous slurry mixture was obtained in acetonitrile (HPLC grade, Aldrich) by vigorous stirring with a high-speed homogenizer. Appropriate amounts of the homogenized mixtures depending on the desired film thickness were cast into glass rings (41.8 mm in diameter) placed on a clean Teflon surface and the solvent was allowed to evaporate in air overnight. The thin cathode film (30 - 120 μm in thickness) and the thin electrolyte film (35 - 45 μm in thickness) were peeled off and were cut into disks (16.0 and 25.0 mm in diameter, respectively) and dried under vacuum at 50°C for several days and stored under helium atmosphere. These films were subjected to vacuum drying prior to use.

Estimation of film thickness

Thickness t of the films was estimated using apparent densities d of the films, which were calculated based on physical mixing of each component. Densities of Li, PEO, polymer X1, TiS_2 , acetylene black, Brij 35, LiCF_3SO_3 and $\text{Li}(\text{CF}_3\text{SO}_2)_2\text{N}$ were 0.53, 1.21, 1.60, 3.22, 2.26, 0.95, 1.90 and 1.91, respectively. Estimated thickness of the films agreed with the measured values within 10 % in error.

Table 3. Formulation of cathode mixtures.

Material	Loading level	
	30 wt %	45 wt %
PEO (MW = 5×10^6)	600 mg	400 mg
Polymer XI or TiS_2	300 mg	450 mg
Acetylene black	70 mg	105 mg
Brij 35	30 mg	45 mg
CH_3CN	22 ml	15 ml

Table 4. Formulation of electrolyte mixtures.

Material	A	B
PEO (MW = 5×10^6)	693 mg	551 mg
LiCF_3SO_3	307 mg	-
$\text{Li}(\text{CF}_3\text{SO}_2)_2\text{N}$	-	449 mg
CH_3CN	40 ml	30 ml

Assembly and evaluation of test cells

Battery-grade lithium foil (25 μm in thickness, Lithco) was cut into disks (18.4 mm in diameter) and test cells were assembled using exterior cases of 2016 coin cells as shown in Fig. 5. A screw clamp was used to apply slight pressure on the assembled cell. The cell was maintained in a furnace thermostatted at $95 \pm 2^\circ\text{C}$. All the above procedures were carried out inside a helium glove box equipped with a moisture removing apparatus (Vacuum Atmospheres) as shown in Fig. 6.

Discharge-charge characteristics were examined with a galvanostat (Princeton Applied Research, model 371) controlled by a personal computer (IBM, PC/AT) equipped with a D/A board and developed software [40]. Test cells were discharged/charged at 0.5/0.1 mA cm^{-2} between 3.1 and 2.0 V (1.5 V for TiS_2). Open circuit voltages of the cell were monitored periodically in order to know the polarization. Cell impedances were also measured before and after discharge by a pulse technique. Because large cell impedance ($> 70 \Omega \text{ cm}^{-2}$) occasionally resulted from poor contact between cell components and these cells generally showed poor discharge behavior.

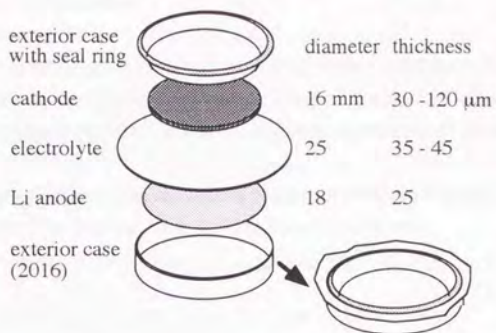


Fig. 5. A schematic view of a test cell.

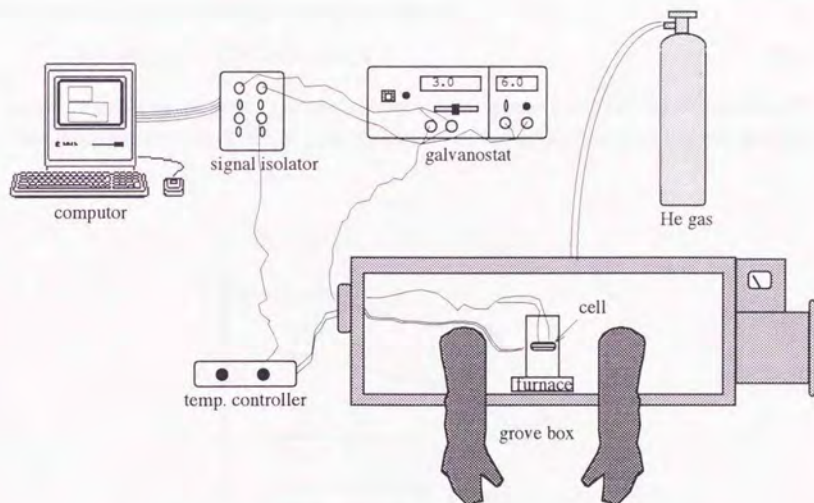


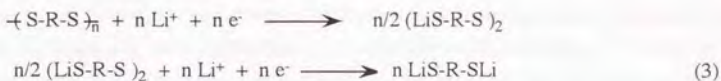
Fig. 6. An evaluation apparatus for lithium cells.

5.3.2. Results and Discussion

Discharge-charge profile

Representative discharge-charge curves both for Li/X1 and Li/TiS₂ cells using a PEO-LiCF₃SO₃ electrolyte are shown in Fig. 7, where cell voltage *E* was plotted against capacity *Q*. Since all cells were constructed cathode-limited, theoretical capacities were derived by weighing the cathode films.

The polymer X1 cathode always shows two plateaus, which come from the different electrode potentials of the reactions, polymer to dimer and dimer to monomer:



This observation was also confirmed in the solution containing the monomer by cyclic voltammetry [41, 42].

Although the TiS₂ cathode initially shows a high open circuit voltage around 3.0 V, the potential falls rapidly upon discharge. It decreases constantly with time, because the electrode potential of the cathode decreases as the following reaction proceeds:



The discharge-charge curve fairly agrees with the curves reported for Li/p(EO)₈LiClO₄/TiS₂ [19], although it was reported that LiCF₃SO₃ was inferior to LiClO₄ in Li/PEO-LiX/TiS₂ cells [19, 34].

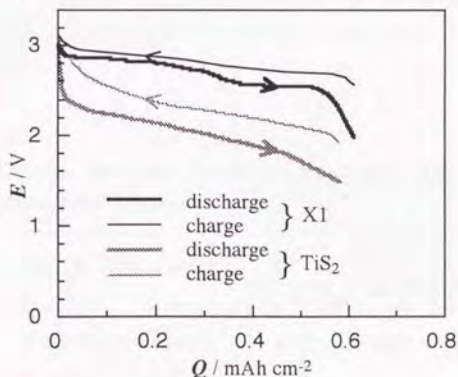


Fig. 7. Typical discharge-charge curves for Li/p(EO)₈LiCF₃SO₃/X1 and Li/p(EO)₈LiCF₃SO₃/TiS₂ cells at 95°C.

theoretical capacity: 0.75 mAh cm⁻² (30wt % loading).
discharge rate: 0.5 mA cm⁻², charge rate: 0.1 mA cm⁻².

Cathode utilization

The capacity of the test cell was varied from 0.6 to 2.3 mAh cm⁻² by changing the amount of an active material in the cathode in two ways, by changing thickness of the cathode film and changing a mixing ratio of an active material in the cathode composites (loading level). The first discharge curves of the test cells using a p(EO)₈LiCF₃SO₃ or a p(EO)₈Li(CF₃SO₂)₂N electrolyte were shown in Fig. 8 for Li/X1 and Fig. 9 for Li/TiS₂ cells, respectively. Horizontal axes of all figures are represented by the cathode utilization U , which indicates the ratio of available capacity Q to theoretical capacity Q_t .

Theoretical capacity of each cell is given in the figures and the corresponding film thickness to the theoretical capacity can be estimated from the conversion coefficients t/Q_t given in Table 5.

The following three factors on the cathode utilization can be discussed from these results both for Li/X1 and Li/TiS₂ cells.

- i. Thickness of a cathode film
- ii. Loading level of an active material in a cathode film
- iii. Kind of a supporting salt (LiX) in a PEO-based electrolyte

The values of cathode utilization obtained in each cell were plotted against the thickness of the cathode films in Fig. 11 for Li/X1 and Fig. 12 for Li/TiS₂.

(a) Li/X1 cell

The cathode utilization generally became lower as the thickness of the cathode film and the loading level of X1 in the cathode increased as shown in Fig. 8a vs. 8b and Fig. 8c vs. 8d. It is believed that this is because of the inadequate transport of Li⁺ in the cathode composite.

However, the utilization of Li(CF₃SO₂)₂N as a supporting salt in the polymer electrolyte markedly enhanced the cathode utilization as shown in Fig. 8a vs. 8c and Fig. 8b vs. 8d. Particularly, Li/p(EO)₈Li(CF₃SO₂)₂N/X1 (30 wt %) cell showed no decline of the cathode utilization as shown in Fig. 11.

Table 5. Estimated density and thickness of the cathode composites.

Cathode composite	d / g cm ⁻³	t/Q_t / μm/mAh cm ⁻²
30 wt % polymer X1	1.34	68.8
45 wt % polymer X1	1.42	43.3
30 wt % TiS ₂	1.53	91.1
45 wt % TiS ₂	1.77	52.4

It is known that the conductivity of $p(\text{EO})_8\text{LiClO}_4$ at 95°C ($10^{-3} \text{ S cm}^{-1}$) is about ten times higher than that of $p(\text{EO})_8\text{LiCF}_3\text{SO}_3$, although $p(\text{EO})_8\text{LiClO}_4$ has a higher glass temperature than $p(\text{EO})_8\text{LiCF}_3\text{SO}_3$ [3, 43]. The conductivity of $p(\text{EO})_8\text{Li}(\text{CF}_3\text{SO}_2)_2\text{N}$ at 95°C is almost the same as that of $p(\text{EO})_8\text{LiClO}_4$ and the $p(\text{EO})_8\text{Li}(\text{CF}_3\text{SO}_2)_2\text{N}$ film has a similar elastic character (softness and stickiness) with the $p(\text{EO})_8\text{LiClO}_4$ film [39, 43].

The enhancement in the cathode utilization caused by $\text{Li}(\text{CF}_3\text{SO}_2)_2\text{N}$ is explained by this conductivity enhancement of the polymer electrolyte, itself.

However, the improvement of the contact between the electrolyte and the cathode by the elastic character of the $p(\text{EO})_8\text{Li}(\text{CF}_3\text{SO}_2)_2\text{N}$ film should be considered, because the addition of a small amount of $\text{Li}(\text{CF}_3\text{SO}_2)_2\text{N}$ in the cathode increased the cathode utilization of a $\text{Li}/p(\text{EO})_8\text{LiCF}_3\text{SO}_3/\text{X1}$ cell as shown in Fig. 10.

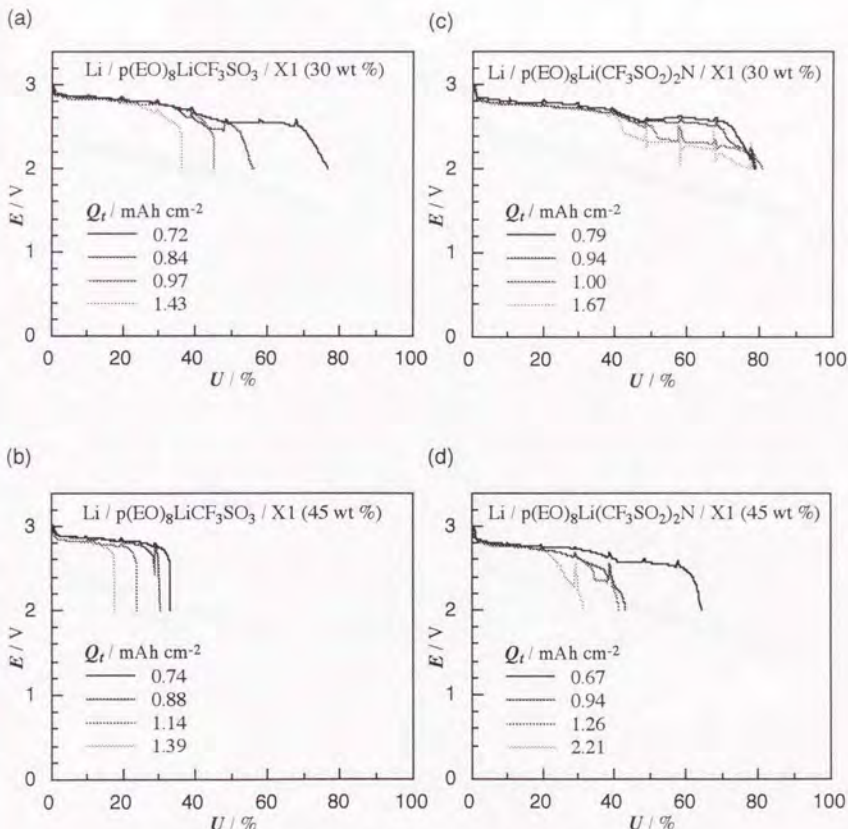


Fig. 8. Discharge curves at 0.5 mA cm^{-2} for $\text{Li}/\text{X1}$ cells at 95°C .

(b) Li/TiS_2 cell

Similar tendencies have been observed for Li/TiS_2 cell as far as the cathode utilization is concerned. However, only $\text{Li}/\text{p}(\text{EO})_8\text{LiCF}_3\text{SO}_3/\text{TiS}_2$ (45 wt %) cell showed a decline of the cathode utilization as shown in Fig. 12.

Since the density of TiS_2 is twice that of X1, smaller volume occupied by TiS_2 in the cathode film resulted in the better cathode utilization than X1 at the same loading levels based on weight. However, the cathode utilization of Li/TiS_2 cells became almost the same as $\text{Li}/\text{X1}$ cell, if loading level on a volume basis was taken into account. Loading levels of 30 wt % X1 and 45 wt % TiS_2 are equivalent to 25 vol % for both X1 and TiS_2 . Furthermore, the cathode utilization of 60 wt % (35 vol %) loading of TiS_2 declined as shown in Fig. 9d and it coincided with that of 45 wt % (40 vol %) loading of X1. This observation indicates Li^+ transport in the cathode composite may be impeded by the existing volume of active materials.

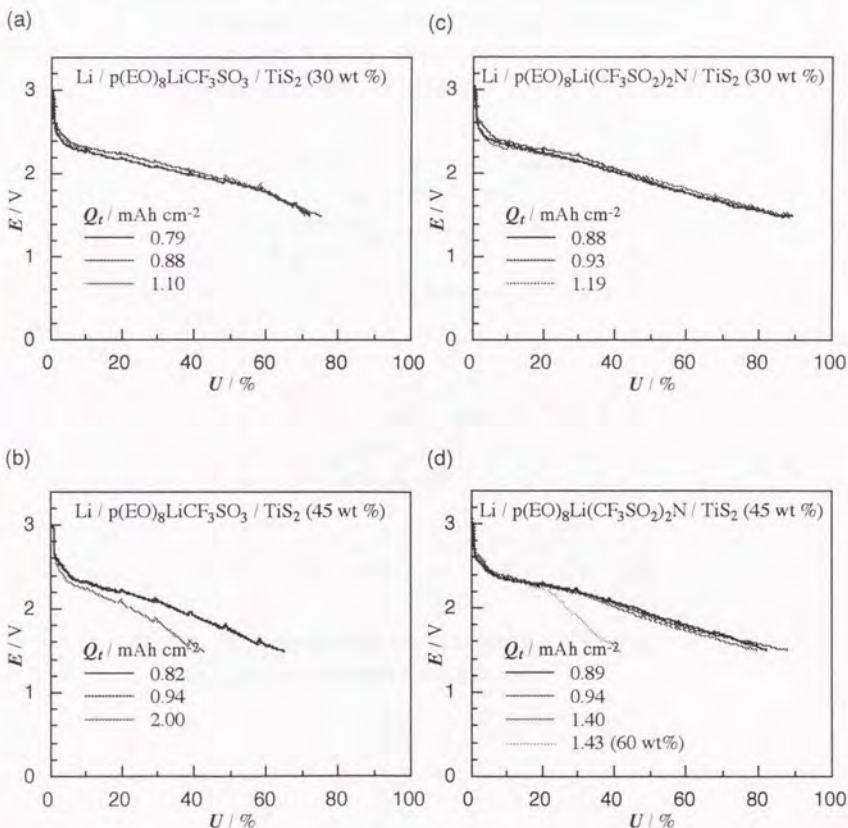


Fig. 9. Discharge curves at 0.5 mA cm^{-2} for Li/TiS_2 cells at 95°C .

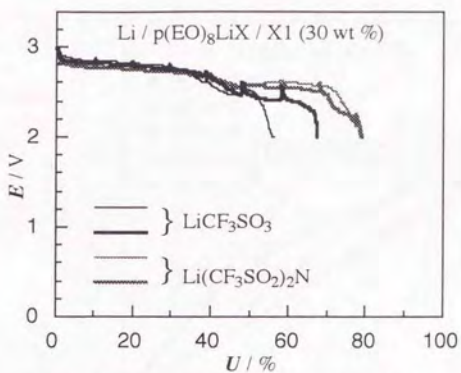


Fig. 10. Addition effect of $\text{Li}(\text{CF}_3\text{SO}_2)_2\text{N}$ ($\text{Li}/\text{EO}=1/16$) in the cathode of $\text{Li}/\text{p}(\text{EO})_8\text{LiX}/\text{X1}$ (30 wt%) cells. discharge rate: 0.5 mA cm^{-2} at 95°C . bold lines: $\text{Li}(\text{CF}_3\text{SO}_2)_2\text{N}$ added.

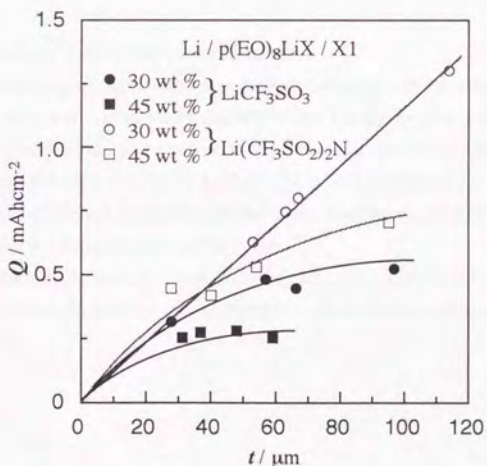


Fig. 11. Available capacity of $\text{Li}/\text{p}(\text{EO})_8\text{LiX}/\text{X1}$ cells as a function of cathode film thickness.

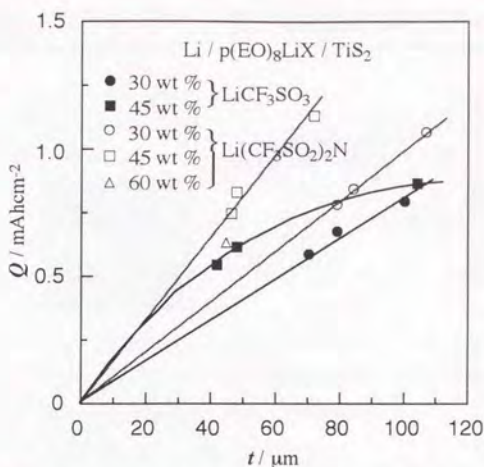


Fig. 12. Available capacity of Li/p(EO)₈LiX/TiS₂ cells as a function of cathode film thickness.

Calculation of energy density and power density

On the basis of the experimental results, energy densities W and sustained power densities P of Li/X1 and Li/TiS₂ cells were calculated volumetrically (ρ) and gravimetrically (ρ_g) as shown in Fig. 13. The cell capacity was fixed to 1 mAh cm⁻² at 0.5 mA cm⁻² discharge rate, which is comparable with reported values (0.4 [18], 0.97 [19], 1.45 [20], 1.5 [21] mAh cm⁻²).

Current collectors were neglected and cathode utilization was assumed to be 75%. An average cell voltage E_m was used instead of an initial value E_0 .

In spite of a lower loading level on a weight basis, the Li/X1 cell affords higher energy and power density than the Li/TiS₂ cell, because of a higher cell voltage and a lower equivalent weight (74 for X1 and 112 for TiS₂).

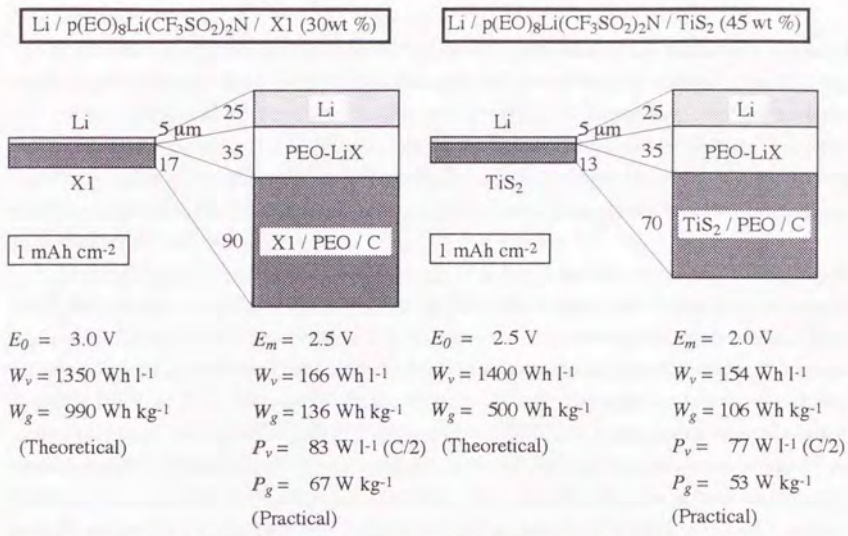


Fig. 13. Estimation of energy density and sustained power density for thin film rechargeable lithium cells.

5.4. Summary

The introduction of ester groups in 1,3:2,4-dibenzylidenesorbitol (DBS) remarkably increased its gel-forming ability. Quasi-solid organic electrolytes immobilized by a small amount of this new non polymeric gelling agent showed high conductivities. Although they were too brittle to make a film, incorporation of a polymer matrix; poly(ethylene oxide)-grafted poly(methacrylate) enabled to make a thin film with an enhanced mechanical strength and without a significant decrease in conductivity. The application of the quasi-solid organic electrolytes was proposed as an electrolyte for thin film lithium cells.

Next, solid polymer electrolytes consisting of a polyethylene oxide and LiCF_3SO_3 or $\text{Li}(\text{CF}_3\text{SO}_2)_2\text{N}$ were applied to all-solid-state rechargeable lithium cells based on a polymeric organodisulfide cathode prepared from 2,5-dimercapto-1,3,4-thiadiazole or titanium disulfide cathode. Cathode utilization of the polymeric organodisulfide was compared with that of titanium disulfide at 95°C . The cathode utilization of the polymeric organodisulfide was remarkably enhanced by the use of $\text{Li}(\text{CF}_3\text{SO}_2)_2\text{N}$ instead of LiCF_3SO_3 in a polyethylene oxide-based electrolyte and achieved up to 80% (1.3 mAh cm^{-2}) at a 0.5 mA cm^{-2} discharge rate, where 30 wt % of the active material was loaded in the cathode. The cathode utilization of titanium disulfide was almost the same as the polymeric organodisulfide at equivalent loading levels on a volume basis.

5.5. References

1. D. E. Fenton, J. M. Parker and P. V. Wright, *Polymer*, **14**, 589 (1973).
2. M. Armand, J. M. Chabagno and M. Duclot, in *Fast Ion Transport in Solids*, P. Vashishta, J. N. Mundy and G. K. Shenoy, Editors., North-Holland, New York (1979).
3. J. R. MacCallum and C. A. Vincent, Editors, *Polymer Electrolyte Review*, Elsevier Applied Science, London, Vol. 1 (1987), Vol. 2 (1989).
4. M. Gauthier, M. Armand and D. Muller, *Electroresponsive Molecular and Polymeric Systems Vol. 1.*, T. A. Skotheim, Editor, Marcel Dekker, New York (1988).
5. *Solid State Batteries*, NATO ASI series, C. A. C. Sequeira and A. Hooper, Editors, Martinus Nijhoff Publishers, Dordrecht (1985).
6. M. Watanabe, M. Kanba, K. Nagaoka and I. Shinohara, *J. Polymer Sci.*, **21**, 939 (1983).
7. S. Ikeda, M. Kida, K. Nomura and K. Ito, *Denki Kagaku*, **58**, 569 (1990).
8. K. M. Abraham and M. Alamgir, *J. Electrochem. Soc.*, **137**, 1657 (1990).
9. M. Morita, T. Fukumasa, M. Motoda, H. Tsutsumi, Y. Matsuda, T. Takahashi and H. Ashitaka, *J. Electrochem. Soc.*, **137**, 3401 (1990).
10. H. Hong, C. Liqun, H. Xuefie and X. Rongjian, *Electrochim. Acta*, **37**, 1671 (1992).
11. M. Alamgir and K. M. Abraham, *J. Electrochem. Soc.*, **140**, L96 (1993).
12. C. W. Walker, Jr. and M. Salomon, *J. Electrochem. Soc.*, **140**, 3409 (1993).
13. G. Feuillade and Ph. Perche, *J. Appl. Electrochem.*, **5**, 63 (1975).
14. T. Iijima, Y. Toyoguchi and N. Eda, *Denki Kagaku*, **53**, 619 (1985).
15. H. P. Fritz and K. Stein, *J. Power Sources*, **37**, 315 (1992).
16. Y. Uetani and K. Hisatomi, *JP 74-70139A* (1974).
17. M. Kaitoh and S. Mori, *USP 4,996,334* (1991).
18. A. Hooper and J. M. North, *Solid State Ionics*, **9-10**, 1161 (1983).
19. M. Gauthier, D. Fauteux, G. Vassort, A. Bélanger, M. Duval, P. Ricoux, J. M. Chabagno, D. Muller, P. Rigaud, M. B. Armand and D. Deroo, *J. Electrochem. Soc.*, **132**, 1333 (1985).
20. K. M. Abraham, M. Alamgir and S. J. Perrotti, *J. Electrochem. Soc.*, **135**, 535 (1988).
21. Y. Nakacho, Y. Tada, A. Inubushi, S. Masuda and M. Taniguchi, *Proc. 29th Bat. Symp. Jpn.*, p 205 (1988).
22. K. West, B. Zachau-Christiansen, M. J. L. Østergård and T. Jacobsen, *J. Power Sources*, **20**, 165 (1987).
23. F. Bonino, M. Ottaviani, B. Scrosati and G. Pistoia, *J. Electrochem. Soc.*, **135**, 12 (1988).
24. M. Z. A. Munshi and B. B. Owens, *Solid State Ionics*, **26**, 41 (1988).
25. M. G. Minett and J. R. Owen, *J. Power Sources*, **32**, 81 (1990).
26. W. J. Macklin and R. J. Neat, *Solid State Ionics*, **53-56**, 694 (1992).
27. W. J. Macklin, R. J. Neat and R. J. Powell, *J. Power Sources*, **34**, 39 (1991).
28. T. Nagatomo, C. Ichikawa and Q. Omoto, *J. Electrochem. Soc.*, **134**, 305 (1987).
29. D. Billaud, S. Lemont and R. Yazami, *Electrochim. Acta*, **37**, 1675 (1992).

30. P. Novák, O. Inganäs and R. Bjorklund, *J. Electrochem. Soc.*, **134**, 1341 (1987).
31. F. Croce, S. Panero, P. Prospero and B. Scrosati, *Solid State Ionics*, **28-30**, 895 (1988).
32. L. S. Yang, Z. Q. Shan and Y. D. Liu, *Solid State Ionics*, **40-41**, 967 (1990).
33. S. J. Visco, M. Liu, M. B. Armand and L. C. De Jonghe, *Mol. Cryst. Liq. Cryst.*, **190**, 185 (1990).
34. M. Liu, S. J. Visco and L. C. De Jonghe, *J. Electrochem. Soc.*, **138**, 1891 (1991).
35. M. M. Doeff, S. J. Visco and L. C. De Jonghe, *J. Electrochem. Soc.*, **139**, 1808 (1992).
36. M. M. Lerner, S. J. Visco, M. Ue, M. M. Doeff and L. C. De Jonghe, *Mat. Res. Soc. Symp. Proc.*, **210**, 81 (1991).
37. M. M. Doeff, M. M. Lerner, S. J. Visco and L. C. De Jonghe, *J. Electrochem. Soc.*, **139**, 2077 (1992).
38. The organosulfur battery technology is proprietary to Poly Plus, Inc., 809 Bancroft Way, Berkeley, California 94710, USA.
39. M. Armand and W. Gorecki and R. Andréani, *Second International Symposium on Polymer Electrolytes*, B. Scrosati, Editor, Elsevier Applied Science, New York (1990).
40. S. J. Visco and M. Liu, *J. Appl. Electrochem.*, **22**, 307 (1992).
41. K. Naoi, M. Menda, H. Ooike and N. Oyama, *J. Electroanal. Chem.*, **318**, 395 (1991).
42. T. Sotomura, H. Uemachi, K. Naoi and N. Oyama, *Electrochim. Acta*, **37**, 1851 (1992).
43. A. Vallée, S. Besner and J. Prud'homme, *Electrochim. Acta*, **37**, 1579 (1992).

6. Appendixes

6.1. Electrical Conductance Theory

Electrical conductance measurements provide several important parameters. The basic quantity of primary interest is the limiting molar conductivity of the electrolyte, Λ_0 . The parameter Λ_0 coupled with transference number data can be used to generate the limiting single ion conductivities or mobilities, λ_0^+ and λ_0^- for the cations and anions, respectively. The second quantity is the association constant, K_A .

Several techniques are available for the analysis of conductivity data and typical theories are briefly outlined here [1-9]. For simplification, all equations are given in c.g.s. units for the 1:1-type electrolyte, where the ion association is represented by the following equation:



The association constant K_A is given in the mass action equation:

$$K_A = (1-\gamma) / C\gamma^2 f_{\pm}^2 \quad (2)$$

, where C , γ and f_{\pm} are the molar concentration, the degree of dissociation and the mean molar activity coefficient, respectively. The activity coefficient for the neutral ion pair is assumed to equal unity.

The mean molar activity coefficient f_{\pm} is calculated by the Debye-Hückel equation:

$$\ln f_{\pm} = -A(\gamma C)^{1/2} / [1 + BR(\gamma C)^{1/2}] \quad (3)$$

, where A and B are the coefficients determined by the relative permittivity of the solvent ϵ_r and absolute temperature T . R is the distance of closest approach in cm.

$$A = \frac{e^2}{2\epsilon_r kT} \left(\frac{8\pi e^2 N}{1000\epsilon_r kT} \right)^{1/2} = 4.202 \times 10^6 (\epsilon_r T)^{-3/2} \quad (4)$$

$$B = \left(\frac{8\pi e^2 N}{1000\epsilon_r kT} \right)^{1/2} = 50.29 \times 10^8 (\epsilon_r T)^{-1/2} \quad (5)$$

6.1.1. Conductivity Equations

Onsager limiting equation

Onsager applied Debye-Hückel theory for electrical conductance of unassociated electrolytes and developed the following equation, which proved the Kohlrausch empirical law.

$$\Lambda = \Lambda_0 - S\sqrt{C} \quad (6)$$

The slope S is given by the following equations:

$$S = \alpha\Lambda_0 + \beta \quad (7)$$

$$\alpha = \frac{e^2}{3\epsilon_r kT} \left(\frac{8\pi e^2 N}{1000\epsilon_r kT} \right)^{1/2} \left(\frac{0.5}{1 + \sqrt{0.5}} \right) = 8.205 \times 10^5 (\epsilon_r T)^{-3/2} \quad (8)$$

$$\beta = \frac{e^2 N}{3\pi\eta} \left(\frac{8\pi e^2 N}{1000\epsilon_r kT} \right)^{1/2} (10^{-11}/8.9876) = 82.49 \eta^{-1} (\epsilon_r T)^{-1/2} \quad (9)$$

, where the viscosity η is in poise, and terms α and β express the relaxation effect and the electrophoretic effect. The Onsager equation is of limited application for extrapolating Λ data to obtain Λ_0 , because it only yields the slope at infinite dilution.

Arrhenius-Ostwald equation

This relationship was deduced from the law of mass action, using the assumption that the degree of dissociation was equal to Λ/Λ_0 .

$$1/\Lambda = 1/\Lambda_0 + C\Lambda K_A/\Lambda_0^2 \quad (10)$$

A plot of $1/\Lambda_0$ vs $C\Lambda$ give rise to a straight line, from which Λ_0 and K_A can be derived. The Arrhenius-Ostwald equation is very useful to obtain approximate values of Λ_0 and K_A , without the need for rigorous computer analysis and to eliminate points that are obviously inaccurate.

Shedlovsky equation [10]

Shedlovsky modified Onsager limiting equation for associated electrolytes and proposed the following equation, which can reproduce conductivity data to significantly higher concentrations.

$$\Lambda = \gamma\Lambda_0 - S(\Lambda/\Lambda_0)\sqrt{C}\gamma \quad (11)$$

The solution of this equation is written as

$$\gamma = (\Lambda/\Lambda_0)S(z) \quad (12)$$

, where $S(z)$ is the Shedlovsky function defined by the following equation:

$$S(z) = [z/2 + \sqrt{1 + (z/2)^2}]^2 \quad (13)$$

$$z = S\Lambda_0^{-3/2}\sqrt{C\Lambda} \quad (14)$$

The substitution of γ in the mass action equation affords the final equation:

$$1/\Lambda S(z) = 1/\Lambda_0 + CAS(z)f_{\pm}^2 K_A/\Lambda_0^2 \quad (15)$$

This equation is regarded as a modification of the Arrhenius-Ostwald equation and a plot of $1/\Lambda S(z)$ vs $C\Lambda S(z)f_{\pm}^2$ can give Λ_0 and K_A . The Shedlovsky equation has the advantage that it can be applied in almost every case and is not dependent on data of high precision.

Fuoss-Onsager equation and other related equations [11-14]

Several extensions of the crude model of the Debye-Hückel theory have taken into account ionic size, employing the model of the ion considered as a sphere with its charge in the center moving in a continuum.

These are expressed by the following general formula for associated electrolytes:

$$\Lambda = \Lambda_0 - S(C\gamma)^{1/2} + E(C\gamma)\ln(C\gamma) + J_1(C\gamma) - J_2(C\gamma)^{3/2} - K_A(C\gamma)f_{\pm}^2\Lambda \quad (16)$$

, where the coefficients E_1 , J_1 and J_2 depend on the solvent properties (ϵ , η), and J_1 and J_2 also depend on so-called ion size parameter R .

The expressions of these coefficients are given in the following equations and various expressions are proposed as listed in Table 1 [14].

$$E = E_1\Lambda_0 - E_2 \quad (17)$$

$$E_1 = \frac{b^2 R^2}{24} (\kappa/c^{1/2})^2 = 2.943 \times 10^{12} (\epsilon_r T)^{-3} \quad (18)$$

$$E_2 = \frac{bR\beta}{16} (\kappa/c^{1/2}) = 4.332 \times 10^7 \eta^{-1} (\epsilon_r T)^{-2} \quad (19)$$

$$J_1 = \sigma_1\Lambda_0 + \sigma_2 \quad (20)$$

$$J_2 = \sigma_3\Lambda_0 + \sigma_4 \quad (21)$$

$$\sigma_1 = 2E_1[\Delta_1 + \ln(R\kappa/c^{1/2})] \quad (22)$$

$$\sigma_2 = 2E_2[\Delta_2 - \ln(R\kappa/c^{1/2})] \quad (23)$$

$$\sigma_3 = 4E_1 bR(\kappa/c^{1/2})\Delta_3 \quad (24)$$

$$\sigma_4 = 2E_2 bR(\kappa/c^{1/2})\Delta_4 - \Delta_5 \quad (25)$$

$$b = e^2 / \epsilon_r kTR \quad (26)$$

$$\kappa/c^{1/2} = \left(\frac{8\pi e^2 N}{1000 \epsilon_r kT} \right)^{1/2} = 50.29 \times 10^8 (\epsilon_r T)^{-1/2} \quad (27)$$

Table 1. Expressions for the Δ_i terms.

Theory	Δ_1	Δ_2
Fuoss-Onsager (Kraeft)	$2.2125/b + 0.75/b^2 - 1/b^3 + 1.1020$	$7.75/b + 1/b^2 - 0.7897$
Fuoss-Hsia	$2/b + 2/b^2 - 1/b^3 + 0.9074$	$7.3333/b + 0.0142$
Pitts	$2/b + 1.7718$	$8/b + 0.01387$
	Δ_3	Δ_4
Fuoss-Hsia	$0.1523/b + 1.1187/b^2 - 0.9571/b^3$	$0.5738/b + 7.0572/b^2 - 0.6667/b^3 - 0.6461$
Pitts	$1.5732/b + 1.2929/b^2$	$1.4073/b + 8/b^2$
	Δ_5	
Fuoss-Hsia	$(E_2\beta/\Lambda_0)(1.3333/b - 2.2194)$	

Although the distance parameters R_{j1} and R_{j2} , which are derived from J_1 and J_2 , must be compatible with R_j in equation 2, there exists inconsistency between distance parameters. Justice recommended that R_{j1} and R_j be set equal to the Bjerrum critical distance q [15].

$$q = e^2/2\epsilon_r kTR \quad (28)$$

Fernández-Prini suggested further that the best results for slightly associated electrolytes are obtained by fixing these parameters, and they are set equal to q , when association is assumed to be of electrostatic nature [14].

The problem of which equation to use is questionable, but all the different equations yield approximately the same value of Λ_0 . However, it is advisable to use the same equation for the association constants K_A that are being compared, because the different equations give various values of K_A .

In this thesis, Fuoss-Hsia equation was used by adopting the assumption that R_{j1} , R_{j2} and R_j are equal to q . A two-parameter equation was solved by an iterative least square method similar to that described by Kay [16]. The standard error of estimate σ_Λ is defined by the following equation:

$$\sigma_\Lambda = \left[\frac{\sum (\Lambda_{\text{obsd}} - \Lambda_{\text{calcd}})^2}{(n-2)} \right]^{1/2} \quad (29)$$

, where n is the number of data points.

6.1.2. Single Ion Limiting Molar Conductivity and Stokes Law

In order to compare the ionic mobilities, a limiting molar conductivity Λ_0 must be assigned to those of cation and anion, λ_0^+ and λ_0^- . Several approaches are used to generate the single ion molar conductivity.

The direct measurement of transference number is the first one. In the second approach, the conductivity of an electrolyte composed of large ions is divided equally between the cation and anion. The typical example of this reference electrolyte salt is *iso*-Am₄N *iso*-Am₄B. The third approach makes use of Walden rule, where the Walden product is assumed to remain constant in different solvents, that is $\lambda_0\eta = \text{const}$.

The Walden product arises from Stokes law:

$$\lambda_0\eta = \frac{Ne^2}{6\pi r_s} (10^{-11}/8.9876) = 0.8201 \times 10^{-8} / r_s \quad (30)$$

, where r_s is the hydrodynamic radius of a spherical particle moving through a continuous fluid of viscosity η . If the boundary between the particle and the fluid is slippy, a numerical factor becomes 4.

$$\lambda_0\eta = \frac{Ne^2}{4\pi r_s} (10^{-11}/8.9876) = 1.2302 \times 10^{-8} / r_s \quad (31)$$

However, Stokes equation must be modified by using a numerical factor x less than 6, when applied to very small molecules ($r < 0.5$ nm) [2].

6.1.3. Ionic Association Theories

The experimental values of K_A can be compared to the values calculated from several coulombic ionic association theories.

One approach is Bjerrum equation:

$$K_B = 4\pi N \int_{a_B}^q \exp(-e^2/\epsilon_r kT R) R^2 dR \quad (32)$$

, where distance a_B represents the contact distance for two spherical ions and q is Bjerrum critical distance at which ion pairing no longer is regarded as exist.

The another approach is Fuoss equation:

$$K_F = \frac{4\pi N a_F^3}{3000} \exp(-e^2/\epsilon_r kT a_F) \quad (33)$$

, where the ions are separated by the same distance a_F , generally taken as the sum of crystallographic radii of cation and anion.

On comparing the experimental values of K_A with the values calculated from theory, one can distinguish ion pairs as a contact ion pair or a solvent-separated ion pair shown in Fig. 1. However, this kind of argument is difficult for slightly associated electrolytes, because the present conductance theories do not have the completeness to afford an exact association constant.

List of Physical Constants

e : electronic charge, 4.80324×10^{-10} esu

k : Boltzmann constant, 1.38066×10^{-16} erg deg $^{-1}$

N : Avogadro number, 6.02205×10^{23} mol $^{-1}$

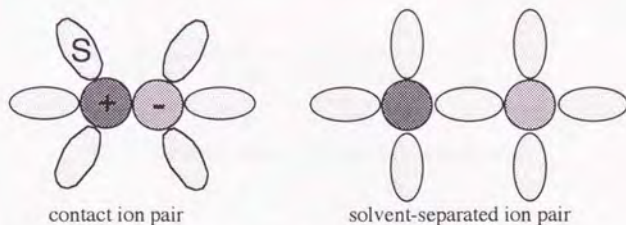


Fig. 1. The structure of electrolyte solution.

6.2. Examples of Conductivity Fitting

Conductivity analysis was carried out using the various conductivity equations in order to compare the fitting results. The conductivity data of tetraethylammonium biphthalate (Et_4NPA) and triethylammonium biphthalate (Et_3NHPA) in γ -butyrolactone were selected as examples of a strong electrolyte and a weak electrolyte.

The conductivity curves and derived parameters are given in Fig 2 and Table 2, respectively. The corrected values using the data of perchlorate salts are given in parentheses, because it is inevitable to get lower limiting molar conductivities for strongly associated electrolytes. All the equations yielded approximately the same values within about 1% of deviation. However, the difference in the association constants was very large particularly for the slightly associated electrolyte.

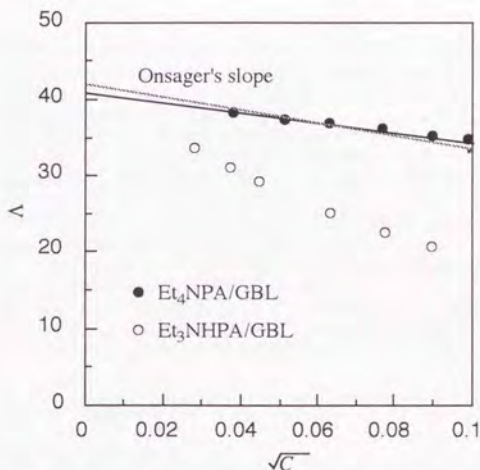


Fig. 2. Conductivity curves for GBL electrolytes.

Table 2. Derived parameters for GBL electrolytes.

Solute	Shedlovsky		Fuoss-Onsager		Fuoss-Hsia		Pitts	
	Λ_0	K_A	Λ_0	K_A	Λ_0	K_A	Λ_0	K_A
Et_3NH <chem>C1=CC=C(C(=O)O)C=C1C(=O)O</chem>	39.47 (41.72)	216	39.87 (42.11)	234	39.72 (41.90)	228	39.63 (41.67)	226
Et_4N <chem>C1=CC=C(C(=O)O)C=C1C(=O)O</chem>	40.59	1.7	41.03	12.0	40.78	7.3	40.53	4.2

Λ_0 in $\text{S cm}^2 \text{ mol}^{-1}$, K_A in $\text{dm}^3 \text{ mol}^{-1}$

6.3. Program for Conductivity Analysis

The conductivity analysis was carried out by an original BASIC program written in N88-BASIC on NEC PC-9801BX (Nippon Electric Co.). The list of this program is given below. This program covers Shedlovsky equation, Modified Fuoss-Onsager equation (including viscosity correction), Fuoss-Hsia equation and Pitts equation. The number of data points is limited to less than 10. All parameters are those given by R. Fernández-Prini [1], where the coefficient E is expressed by $E = E_1\Lambda_0 - E_2$, not $E = E_1\Lambda_0 - 2E_2$. All calculations require an initial value of Λ_0 and, sometimes K_A , when three parameters are optimized, therefore, an automatic Λ_0 calculation routine by Arrhenius-Ostwald equation is included in Shedlovsky method. One can get initial values of Λ_0 and K_A by Shedlovsky method and then proceed to the elaborate methods. Iterations were continued until the errors in γ , Λ_0 and K_A became less than 10^{-5} , 10^{-4} , and 10^{-3} , respectively.

```
10000 '*****
10010 '* *** Program for conductivity analysis *** *
10020 '* [COND.BAS Ver. 1.0 1994. 3.30] *
10030 '* Programmed by Makoto Ue *
10040 '* (Mitsubishi Petrochemical Co.) *
10050 '* Original Fuoss-Onsager program was *
10060 '* provided by Prof. M. Ueno & K. Ibuki *
10070 '* at Dohshisya University. *
10080 '* Fuoss-Hsia, Pitts equations were added. *
10090 '* All parameters are cited from *
10100 '* R. Fernandez-Prini in Physical Chemistry *
10110 '* of Organic Solvent Systems, *
10120 '* A. K. Convington and T. Dickinson (Eds.) *
10130 '* Ch. 5. 1. Prenum Press, London (1973) *
10140 '*****
10150 '
10160 CLEAR:CLS 3
10170 ON ERROR GOTO *DERRO
10180 CONSOLE , , 0, 1
10190 DIM EQUAS(10), DDNO$(5)
10200 DIM PRES(7), COMP(7), DIEL(7), YETA(7), DENS(7), LZ(7), AZ(7),
KZ(7), QZ(7)
10210 DIM
SCON(7,10), ACON(7,10), LAMD(7,10), LCAL(7,10), DIFF(7,10),
GG(7,10), FF(7,10)
10220 DIM THIT(10), XI(10), YI(10), ZI(10)
10230 DIM LP(7), AP(7), KP(7)
10240 DIM FA(7), FB(7), FS(7), FE1(7), FE2(7), FE(7)
10250 DIM FS1(7), FS2(7), FJ1(7), FS3(7), FS4(7), FJ2(7)
10260 DIM FSDL(7), FSDLZ(7), FSDK(7), FSDA(7), FLAG(7)
10270 '
10280 EQUAS(10)="Shedlovsky"
10290 EQUAS(1)="Fuoss-Onsager (Non association, 2-parameter)"
10300 EQUAS(2)="Fuoss-Onsager (Association, 2-parameter)"
10310 EQUAS(3)="Fuoss-Onsager (Association, 3-parameter)"
10320 EQUAS(4)="Fuoss-Hsia (Non association, 2-parameter)"
10330 EQUAS(5)="Fuoss-Hsia (Association, 2-parameter)"
10340 EQUAS(6)="Fuoss-Hsia (Association, 3-parameter)"
10350 EQUAS(7)="Pitts (Non association, 2-parameter)"
10360 EQUAS(8)="Pitts (Association, 2-parameter)"
```

```

10370 EQUAS(9)="Pitts          (Association, 3-parameter)"
10380
DDNOS(1)="A:\":DDNOS(2)="B:\":DDNOS(3)="C:\":DDNOS(4)="D:\":
10390 '
10400 PAI=3.14159:CHRG=4.80324E-10:BOLZ=1.38066E-16:
AVGD=6.02205E+23
10410 DNM=1:DRS=DDNOS(DNM)
10420 '
10430 'Main
10440 COLOR 5:PRINT "PROGRAM FOR CONDUCTIVITY ANALYSIS"
10450 PRINT
10460 COLOR 6:PRINT " *DATA INPUT*"
10470 COLOR 6:PRINT "   Select input mode?":PRINT
10480 COLOR 7:PRINT "   1. Keyboard"
10490     PRINT "   2. Disk":COLOR 7
10500 C$=INKEY$:IF C$<>" " THEN GOTO 10500
10510 C$=INKEY$:IF C$=" " THEN GOTO 10510 ELSE NO=ASC(C$)
10520 IF NO=&H31 THEN GOSUB *DINPU:GOTO 10550
10530 IF NO=&H32 THEN GOSUB *DLOAD:IF CC$="" THEN GOTO 10530
ELSE 10550
10540 GOTO 10500
10550 GOSUB *DPLOT
10560 '
10570 COLOR 6:LOCATE 1,1:PRINT "Title:"
10580 COLOR 7:LOCATE 13,1:PRINT TITL$
10590 COLOR 6:LOCATE 1,2:PRINT "Solute:"
10600 COLOR 7:LOCATE 13,2:PRINT SOLU$
10610 COLOR 6:LOCATE 1,3:PRINT "Solvent:"
10620 COLOR 7:LOCATE 13,3:PRINT SOLV$
10630 COLOR 6:LOCATE 1,4:PRINT "File:"
10640 COLOR 7:LOCATE 13,4:PRINT FLNM$
10650 IF NFIT=0 THEN GOTO 10780
10660 COLOR 4:LOCATE 1,6:PRINT EQUAS(NFIT)
10670 COLOR 6
10680 FOR IP=1 TO NP
10690 IF FLG(IP)=1 THEN LOCATE 1,8:PRINT "Fail":GOTO 10710
10700 LOCATE 1,8:PRINT USING "NO.=# L0=###.### KA=###.### A=#.###
SD(L)=#.##^";NP;LP(IP);KP(IP);AP(IP)*1E+08;FSDL(IP)
10710 NEXT IP
10720 COLOR 2
10730 IF AFLG<>0 THEN LOCATE 1,13:PRINT "Negative a value!";AFLG
10740 IF KFLG<>0 THEN LOCATE 1,14:PRINT "Negative KA
value!";KFLG
10750 IF GFLG<>0 THEN LOCATE 1,15:PRINT "Negative G value!";GFLG
10760 IF NFLG<>0 THEN LOCATE 1,16:PRINT "Not convergent!";NFLG
10770 IF EFLG<>0 THEN LOCATE 1,17:PRINT "Other error!";EFLG
10780 COLOR 5
10790 LOCATE 1,21:PRINT "1. Input  2. Correct  3. Save  4. Fit
5. Print  6. Quit"
10800 COLOR 6:LOCATE 1,22:PRINT " Select number?":COLOR 7
10810 C$=INKEY$:IF C$<>" " THEN GOTO 10810
10820 C$=INKEY$:IF C$=" " THEN GOTO 10820 ELSE NO=ASC(C$)
10830 IF NO=&H31 THEN RUN "COND"
10840 IF NO=&H32 THEN GOSUB *DCORR:GOTO 10550
10850 IF NO=&H33 THEN GOSUB *DSAVE:GOTO 10550
10860 IF NO=&H34 THEN GOSUB *DFITT:GOTO 10550
10870 IF NO=&H35 AND NFIT>0 THEN GOSUB *DPRIN:GOTO 10550
10880 IF NO=&H36 THEN CLS 3:END
10890 GOTO 10810
10900 '

```

```

10910 'Input data
10920 *DINPU
10930 CLS 3
10940 COLOR 6:LOCATE 1,1:PRINT "A. Title           ":COLOR 7
10950 COLOR 7:LOCATE 21,1:INPUT TITL$
10960 COLOR 6:LOCATE 1,2:PRINT "B. Solute           ":COLOR 7
10970 COLOR 7:LOCATE 21,2:INPUT SOLU$
10980 COLOR 6:LOCATE 1,3:PRINT "C. + Charge           ":COLOR 7
10990 COLOR 7:LOCATE 21,3:INPUT ZP:ZP=ABS(ZP)
11000 COLOR 6:LOCATE 1,4:PRINT "D. - Charge           ":COLOR 7
11010 COLOR 7:LOCATE 21,4:INPUT ZM:ZM=ABS(ZM)
11020 COLOR 6:LOCATE 1,5:PRINT "E. Solvent           ":COLOR 7
11030 COLOR 7:LOCATE 21,5:INPUT SOLV$
11040 COLOR 6:LOCATE 1,6:PRINT "F. Temp.(C):           ":COLOR 7
11050 COLOR 7:LOCATE 21,6:INPUT CTEMP
11060 COLOR 6:LOCATE 1,7:PRINT "G. B-factor:           ":COLOR 7
11070 COLOR 7:LOCATE 21,7:INPUT VB
11080 COLOR 6:LOCATE 1,8:PRINT "H. No. of series: ":COLOR 7
11090 COLOR 7:LOCATE 21,8:INPUT NP:IF NP>7 THEN NP=7
11100 COLOR 6:LOCATE 1,9:PRINT "I. No. of points: ":COLOR 7
11110 COLOR 7:LOCATE 21,9:INPUT NC:IF NC>10 THEN NC=10
11120 FOR IP=1 TO NP
11130   CLS 3
11140   LOCATE 1,0:COLOR 6
11150   PRINT "No. ";:COLOR 7:PRINT IP;:COLOR 6:PRINT " series"
11160   COLOR 6:LOCATE 1,1 :PRINT "A. Pressure (MPa):"
11170   COLOR 7:LOCATE 21,1:INPUT PRES(IP)
11180   COLOR 6:LOCATE 1,2 :PRINT "B. Compression:"
11190   COLOR 7:LOCATE 21,2:INPUT COMP(IP)
11200   COLOR 6:LOCATE 1,3 :PRINT "C. Permittivity:"
11210   COLOR 7:LOCATE 21,3:INPUT DIEL(IP)
11220   COLOR 6:LOCATE 1,4 :PRINT "D. Viscosity (cP):"
11230   COLOR 7:LOCATE 21,4:INPUT YETA(IP)
11240   COLOR 6:LOCATE 1,5 :PRINT "E. Density (g/cm3):"
11250   COLOR 7:LOCATE 21,5:INPUT DENS(IP)
11260   COLOR 6:LOCATE 1,6 :PRINT "F. Initial L0:"
11270   COLOR 7:LOCATE 21,6:INPUT LZ(IP):LAMDA(IP,0)=LZ(IP)
11280   COLOR 6:LOCATE 1,7 :PRINT "G. Initial a (A):"
11290   COLOR 7:LOCATE 21,7:INPUT AZ(IP)
11300   IF AZ(IP)=0 THEN AZ(IP)=ZP*ZM*CHRG^2*1E+08/
(2*DIEL(IP)*BOLZ*(CTEMP+273.15))
11310   LOCATE 21,7: PRINT AZ(IP)
11320   COLOR 6:LOCATE 1,8 :PRINT "H. Initial KA:"
11330   COLOR 7:LOCATE 21,8:INPUT KZ(IP)
11340   COLOR 6:LOCATE 1,9 :PRINT "I. q:":COLOR 7:LOCATE 21,9
11350   IF ZM=ZP THEN QZ(IP)=.5:PRINT QZ(IP) ELSE INPUT QZ(IP)
11360   COLOR 5:LOCATE 1,10
11370   IF IP>1 THEN PRINT "If concentrations are equal to prior
series, hit RET."
11380   COLOR 6:LOCATE 1,11
11390   PRINT "No.      Conc.(mM)          Lamda (Scm2mol-1)"
11400   FOR IC=1 TO NC
11410     Y=11+IC:IF IC=10 THEN ICR=0 ELSE ICR=IC
11420     COLOR 6:LOCATE 2,Y :PRINT ICR
11430     COLOR 7:LOCATE 9,Y:INPUT CC$
11440     IF IP=1 AND CC$="" THEN GOTO 11420
11450     IF CC$="" THEN SCON(IP,IC)=SCON(IP-1,IC):LOCATE
9,Y:PRINT SCON(IP,IC)*1000
11460     IF CC$<>"" THEN SCON(IP,IC)=VAL(CC$)/1000
11470     ACON(IP,IC)=SCON(IP,IC)*COMP(IP)

```

```

11480     LOCATE 23,Y:INPUT LAMD(IP,IC)
11490     NEXT IC
11500     NEXT IP
11510     LMMIN=LAMD(1,1):LMMAX=LAMD(1,1):CNMAX=ACON(1,1)
11520     FOR IP=1 TO NP
11530         FOR IC=0 TO NC
11540             IF LAMD(IP,IC)>LMMAX THEN LMMAX=LAMD(IP,IC)
11550             IF LAMD(IP,IC)<LMMIN THEN LMMIN=LAMD(IP,IC)
11560             IF ACON(IP,IC)>CNMAX THEN CNMAX=ACON(IP,IC)
11570         NEXT IC
11580     NEXT IP
11590     RETURN
11600     '
11610     'Correct data
11620     *DCORR
11630     CLS 3
11640     AFLG=0:KFLG=0:GFLG=0:NFLG=0:EFLG=0:NFIT=0
11650     IP=0
11660     IPMAX=NP
11670     IF IP=0 THEN GOSUB *REM1 ELSE GOSUB *REM2
11680     COLOR 6:LOCATE 1,22:PRINT " Select item?"
11690     COLOR 3:LOCATE 20,22:PRINT " Next/prev=arrow, OK=ESC":
COLOR 7
11700     IF IP=0 THEN GOTO 12610
11710     C$=INKEY$:IF C$<>" " THEN GOTO 11710
11720     C$=INKEY$:IF C$="" THEN GOTO 11720 ELSE NO=ASC(C$)
11730     IF NO=&H1B THEN RETURN
11740     IF NO=&H1E AND IP<>0 THEN IP=IP-1:GOTO 11670
11750     IF NO=&H1F AND IP<>IPMAX THEN IP=IP+1:GOTO 11670
11760     IF NO=&H41 OR NO=&H61 THEN GOTO 11880
11770     IF NO=&H42 OR NO=&H62 THEN GOTO 11940
11780     IF NO=&H43 OR NO=&H63 THEN GOTO 12010
11790     IF NO=&H44 OR NO=&H64 THEN GOTO 12070
11800     IF NO=&H45 OR NO=&H65 THEN GOTO 12130
11810     IF NO=&H46 OR NO=&H66 THEN GOTO 12190
11820     IF NO=&H47 OR NO=&H67 THEN GOTO 12250
11830     IF NO=&H48 OR NO=&H68 THEN GOTO 12310
11840     IF NO=&H49 OR NO=&H69 THEN GOTO 12370
11850     IF NO=>&H30 AND NO<=&H39 THEN ICR=VAL(C$):GOTO 12430
11860     GOTO 11710
11870     '
11880     COLOR 3:LOCATE 1,1 :PRINT "A. Pressure (MPa) : "
11890     LOCATE 21,1:PRINT PRES(IP)
11900     GOSUB *FORM
11910     IF CC$<>" " THEN PRES(IP)=VAL(CC$)
11920     GOTO 11670
11930     '
11940     COLOR 3:LOCATE 1,2 :PRINT "B. Compression      : "
11950     LOCATE 21,2:PRINT COMP(IP)
11960     GOSUB *FORM
11970     IF CC$<>" " THEN COMP(IP)=VAL(CC$)
11980     FOR IC=1 TO NC:ACON(IP,IC)=SCON(IP,IC)*COMP(IP):NEXT IC
11990     GOTO 11670
12000     '
12010     COLOR 3:LOCATE 1,3 :PRINT "C. Permittivity    : "
12020     LOCATE 21,3:PRINT DIEL(IP)
12030     GOSUB *FORM
12040     IF CC$<>" " THEN DIEL(IP)=VAL(CC$)
12050     GOTO 11670
12060     '

```

```

12070 COLOR 3:LOCATE 1,4 :PRINT "D. Viscosity (cP) :"
12080 LOCATE 21,4:PRINT YETA(IP)
12090 GOSUB *FORM
12100 IF CCS<>" THEN YETA(IP)=VAL(CCS)
12110 GOTO 11670
12120 '
12130 COLOR 3:LOCATE 1,5 :PRINT "E. Density (g/cm3):"
12140 LOCATE 21,5:PRINT DENS(IP)
12150 GOSUB *FORM
12160 IF CCS<>" THEN DENS(IP)=VAL(CCS)
12170 GOTO 11670
12180 '
12190 COLOR 3:LOCATE 1,6 :PRINT "F. Initial L0      :"
12200 LOCATE 21,6:PRINT LZ(IP)
12210 GOSUB *FORM
12220 IF CCS<>" THEN LZ(IP)=VAL(CCS):LAMDA(IP,0)=LZ(IP)
12230 GOTO 13290
12240 '
12250 COLOR 3:LOCATE 1,7 :PRINT "G. Initial a (A)  "
12260 LOCATE 21,7:PRINT AZ(IP)
12270 GOSUB *FORM
12280 IF CCS<>" THEN AZ(IP)=VAL(CCS)
12290 GOTO 11670
12300 '
12310 COLOR 3:LOCATE 1,8 :PRINT "H. Initial KA      "
12320 LOCATE 21,8:PRINT KZ(IP)
12330 GOSUB *FORM
12340 IF CCS<>" THEN KZ(IP)=VAL(CCS)
12350 GOTO 11670
12360 '
12370 COLOR 3:LOCATE 1,9 :PRINT "I. q              "
12380 LOCATE 21,9:PRINT QZ(IP)
12390 GOSUB *FORM
12400 IF CCS<>" THEN QZ(IP)=VAL(CCS)
12410 GOTO 11670
12420 '
12430 IF ICR=0 THEN IC=10 ELSE IC=ICR
12440 IF IC>NC THEN GOTO 11710
12450 Y=IC+11:COLOR 3
12460 LOCATE 2,Y :PRINT ICR:LOCATE 9,Y:PRINT SCON(IP,IC)*1000
12470 LOCATE 23,Y:PRINT LAMD(IP,IC)
12480 LOCATE 1,21:PRINT SPACE$(70)
12490 LOCATE 1,22:PRINT SPACE$(70)
12500 COLOR 6:LOCATE 1,21
12510 PRINT "No.      Conc.(mM)          Lamda (Scm2mol-1)"
12520 COLOR 6:LOCATE 2,22 :PRINT ICR;
12530 COLOR 7:LOCATE 9,22:INPUT CCS
12540 IF CCS<>" THEN SCON(IP,IC)=VAL(CCS)/1000:GOTO 12560
12550 LOCATE 9,22:PRINT SCON(IP,IC)*1000
12560 ACON(IP,IC)=SCON(IP,IC)*COMP(IP)
12570 LOCATE 23,22:INPUT CCS
12580 IF CCS<>" THEN LAMD(IP,IC)=VAL(CCS)
12590 GOTO 13290
12600 '
12610 C$=INKEY$:IF C$<>" THEN GOTO 12610
12620 C$=INKEY$:IF C$="" THEN GOTO 12620 ELSE NO=ASC(C$)
12630 IF NO=&H1B THEN RETURN
12640 IF NO=&H1E AND IP<>0 THEN IP=IP-1:GOTO 11670
12650 IF NO=&H1F AND IP<>IPMAX THEN IP=IP+1:GOTO 11670
12660 IF NO=&H41 OR NO=&H61 THEN GOTO 12760

```

```

12670 IF NO=&H42 OR NO=&H62 THEN GOTO 12820
12680 IF NO=&H43 OR NO=&H63 THEN GOTO 12880
12690 IF NO=&H44 OR NO=&H64 THEN GOTO 12940
12700 IF NO=&H45 OR NO=&H65 THEN GOTO 13000
12710 IF NO=&H46 OR NO=&H66 THEN GOTO 13060
12720 IF NO=&H47 OR NO=&H67 THEN GOTO 13120
12730 IF NO=&H48 OR NO=&H68 THEN GOTO 13180
12740 IF NO=&H49 OR NO=&H69 THEN GOTO 13240
12750 '
12760 COLOR 3:LOCATE 1,1 :PRINT "A. Title" : "
12770 LOCATE 21,1:PRINT TITL$
12780 GOSUB *FORM
12790 IF CC$<>" THEN TITL$=CC$
12800 GOTO 11670
12810 '
12820 COLOR 3:LOCATE 1,2 :PRINT "B. Solute" : "
12830 LOCATE 21,2:PRINT SOLU$
12840 GOSUB *FORM
12850 IF CC$<>" THEN SOLU$=CC$
12860 GOTO 11670
12870 '
12880 COLOR 3:LOCATE 1,3 :PRINT "C. + Charge" : "
12890 LOCATE 21,3:PRINT ZP
12900 GOSUB *FORM
12910 IF CC$<>" THEN ZP=VAL(CC$):ZP=ABS(ZP)
12920 GOTO 11670
12930 '
12940 COLOR 3:LOCATE 1,4 :PRINT "D. - Charge" : "
12950 LOCATE 21,4:PRINT ZM
12960 GOSUB *FORM
12970 IF CC$<>" THEN ZM=VAL(CC$):ZM=ABS(ZM)
12980 GOTO 11670
12990 '
13000 COLOR 3:LOCATE 1,5 :PRINT "E. Solvent" : "
13010 LOCATE 21,5:PRINT SOLV$
13020 GOSUB *FORM
13030 IF CC$<>" THEN SOLV$=CC$
13040 GOTO 11670
13050 '
13060 COLOR 3:LOCATE 1,6 :PRINT "F. Temp. (C)" : "
13070 LOCATE 21,6:PRINT CTEMP
13080 GOSUB *FORM
13090 IF CC$<>" THEN CTEMP=VAL(CC$)
13100 GOTO 11670
13110 '
13120 COLOR 3:LOCATE 1,7 :PRINT "G. B-factor" : "
13130 LOCATE 21,7:PRINT VB
13140 GOSUB *FORM
13150 IF CC$<>" THEN VB=VAL(CC$)
13160 GOTO 11670
13170 '
13180 COLOR 3:LOCATE 1,8 :PRINT "H. No. of series" : "
13190 LOCATE 21,8:PRINT NP
13200 GOSUB *FORM
13210 IF CC$<>" THEN NP=VAL(CC$)
13220 GOTO 13290
13230 '
13240 COLOR 3:LOCATE 1,9 :PRINT "I. No. of points" : "
13250 LOCATE 21,9:PRINT NC
13260 GOSUB *FORM

```

```

13270 IF CC$<>" THEN NC=VAL(CC$)
13280 '
13290 LMMIN=LAMD(1,1):LMMAX=LAMD(1,1):CNMAX=ACON(1,1)
13300 FOR I=1 TO NP
13310   FOR J=0 TO NC
13320     IF LAMD(I,J)>LMMAX THEN LMMAX=LAMD(I,J)
13330     IF LAMD(I,J)<LMMIN THEN LMMIN=LAMD(I,J)
13340     IF ACON(I,J)>CNMAX THEN CNMAX=ACON(I,J)
13350   NEXT J
13360 NEXT I
13370 GOTO 11660
13380 '
13390 *FORM
13400 LOCATE 1,22:PRINT SPACES(70)
13410 COLOR 6:LOCATE 1,22:PRINT "Input data!";
13420 COLOR 7:INPUT CC$
13430 RETURN
13440 '
13450 *REM1
13460 CLS 3
13470 COLOR 6:LOCATE 1,1 :PRINT "A. Title           :"
13480 COLOR 7:LOCATE 21,1:PRINT TITL$
13490 COLOR 6:LOCATE 1,2 :PRINT "B. Solute           :"
13500 COLOR 7:LOCATE 21,2:PRINT SOLU$
13510 COLOR 6:LOCATE 1,3 :PRINT "C. + Charge        :"
13520 COLOR 7:LOCATE 21,3:PRINT ZP
13530 COLOR 6:LOCATE 1,4 :PRINT "D. - Charge        :"
13540 COLOR 7:LOCATE 21,4:PRINT ZM
13550 COLOR 6:LOCATE 1,5 :PRINT "E. Solvent         :"
13560 COLOR 7:LOCATE 21,5:PRINT SOLV$
13570 COLOR 6:LOCATE 1,6 :PRINT "F. Temp. (C)      :"
13580 COLOR 7:LOCATE 21,6:PRINT CTEMP
13590 COLOR 6:LOCATE 1,7 :PRINT "G. B-factor       :"
13600 COLOR 7:LOCATE 21,7:PRINT VB
13610 COLOR 6:LOCATE 1,8 :PRINT "H. No. of series  :"
13620 COLOR 7:LOCATE 21,8:PRINT NP
13630 COLOR 6:LOCATE 1,9 :PRINT "I. No. of points  :"
13640 COLOR 7:LOCATE 21,9:PRINT NC
13650 RETURN
13660 '
13670 *REM2
13680 CLS 3
13690 COLOR 6:LOCATE 1,1 :PRINT "A. Pressure (MPa)  :"
13700 COLOR 7:LOCATE 21,1:PRINT PRES(IP)
13710 COLOR 6:LOCATE 1,2 :PRINT "B. Compression     :"
13720 COLOR 7:LOCATE 21,2:PRINT COMP(IP)
13730 COLOR 6:LOCATE 1,3 :PRINT "C. Permittivity    :"
13740 COLOR 7:LOCATE 21,3:PRINT DIEL(IP)
13750 COLOR 6:LOCATE 1,4 :PRINT "D. Viscosity (cP)  :"
13760 COLOR 7:LOCATE 21,4:PRINT YETA(IP)
13770 COLOR 6:LOCATE 1,5 :PRINT "E. Density (g/cm3):"
13780 COLOR 7:LOCATE 21,5:PRINT DENS(IP)
13790 COLOR 6:LOCATE 1,6 :PRINT "F. Initial L0     :"
13800 COLOR 7:LOCATE 21,6:PRINT LZ(IP)
13810 COLOR 6:LOCATE 1,7 :PRINT "G. Initial a (A)  :"
13820 COLOR 7:LOCATE 21,7:PRINT AZ(IP)
13830 COLOR 6:LOCATE 1,8 :PRINT "H. Initial KA     :"
13840 COLOR 7:LOCATE 21,8:PRINT KZ(IP)
13850 COLOR 6:LOCATE 1,9 :PRINT "I. q              :"
13860 COLOR 7:LOCATE 21,9:PRINT QZ(IP)

```

```

13870 COLOR 6:LOCATE 1,11
13880 PRINT "No.      Conc.(mM)      Lamda (Scm2mol-1)"
13890 FOR IC=1 TO NC
13900   Y=11+IC:IF IC=10 THEN ICR=0 ELSE ICR=IC
13910   COLOR 6:LOCATE 2,Y :PRINT ICR
13920   COLOR 7:LOCATE 9,Y:PRINT SCON(IP,IC)*1000
13930   COLOR 7:LOCATE 23,Y:PRINT LAMD(IP,IC)
13940 NEXT IC
13950 RETURN
13960 '
13970 'Load data
13980 *DLOAD
13990 CLS 3
14000 COLOR 6:LOCATE 1,1 :PRINT " *LOAD DATA*"
14010 COLOR 6:LOCATE 1,3 :PRINT " Disk drive:";
14020 COLOR 3:PRINT DR$;
14030 LOCATE 1,5
14040 PRINT " OK? y=RET, n=SPC"
14050   C$=INKEY$:IF C$<>" " THEN GOTO 14050
14060   C$=INKEY$:IF C$=" " THEN GOTO 14060 ELSE NO=ASC(C$)
14070   IF NO=&H20 THEN DNM=DNM+1 ELSE GOTO 14100
14080   IF DNM=5 THEN DNM=1
14090   DR$=DDNO$(DNM):GOTO 14010
14100   IF NO=&HD THEN GOTO 14120
14110   GOTO 14050
14120 COLOR 7:PRINT:FILES DR$+"*.CND"
14130 COLOR 6:PRINT:PRINT " File name:";
14140 COLOR 7:INPUT CC$
14150   IF CC$="" THEN RETURN
14160   IF LEN(CC$)>8 THEN FLNM$=RIGHT$(CC$,8) ELSE FLNM$=CC$
14170   FFNM$=DR$+FLNM$+"*.CND"
14180 CLS 3:COLOR 3:LOCATE 1,22:PRINT FFNM$;" Now loading!"
":COLOR 7
14190 OPEN FFNM$ FOR INPUT AS #1
14200 INPUT #1,TITL$
14210 INPUT #1,SOLU$
14220 INPUT #1,ZP
14230 INPUT #1,ZM
14240 INPUT #1,SOLV$
14250 INPUT #1,CTEMP
14260 INPUT #1,NP
14270 INPUT #1,NC
14280 INPUT #1,VB
14290 FOR IP=1 TO NP
14300   INPUT #1,PRES(IP)
14310   INPUT #1,COMP(IP)
14320   INPUT #1,DIEL(IP)
14330   INPUT #1,YETA(IP)
14340   INPUT #1,DENS(IP)
14350   INPUT #1,LZ(IP):LAMD(IP,0)=LZ(IP)
14360   INPUT #1,AZ(IP)
14370   INPUT #1,KZ(IP)
14380   INPUT #1,QZ(IP)
14390   FOR IC=1 TO NC
14400     INPUT #1,SCON(IP,IC)
14410     ACON(IP,IC)=SCON(IP,IC)*COMP(IP)
14420     INPUT #1,LAMD(IP,IC)
14430   NEXT IC
14440 NEXT IP
14450 LMMIN=LAMD(1,1):LMMAX=LAMD(1,1):CNMAX=ACON(1,1)

```

```

14460 FOR IP=1 TO NP
14470   FOR IC=0 TO NC
14480     IF LAMD(IP,IC)>LMMAX THEN LMMAX=LAMD(IP,IC)
14490     IF LAMD(IP,IC)<LMMIN THEN LMMIN=LAMD(IP,IC)
14500     IF ACON(IP,IC)>CNMAX THEN CNMAX=ACON(IP,IC)
14510   NEXT IC
14520 NEXT IP
14530 CLOSE #1
14540 RETURN
14550 '
14560 'Save data
14570 *DSAVE
14580 CLS 3
14590 COLOR 6:LOCATE 1,1 :PRINT " *SAVE DATA*"
14600 COLOR 6:LOCATE 1,3 :PRINT " Disk drive:";
14610 COLOR 3:PRINT DR$;
14620 LOCATE 1,5 :
14630 PRINT " OK? y=RET, n=SPC"
14640   C$=INKEY$:IF C$<>" " THEN GOTO 14640
14650   C$=INKEY$:IF C$=" " THEN GOTO 14650 ELSE NO=ASC(C$)
14660   IF NO=&H20 THEN DNM=DNM+1 ELSE GOTO 14690
14670   IF DNM=5 THEN DNM=1
14680   DR$=DDNO$(DNM):GOTO 14600
14690   IF NO=&HD THEN GOTO 14710
14700   GOTO 14640
14710 COLOR 7:PRINT:FILES DR$+"*.CND"
14720 COLOR 6:PRINT:PRINT " File name:";
14730 COLOR 7:INPUT CC$
14740   IF CC$="" THEN RETURN
14750   IF LEN(CC$)>8 THEN FLNM$=RIGHT$(CC$,8) ELSE FLNM$=CC$
14760   FFMN$=DR$+FLNM$+".CND"
14770 COLOR 3:PRINT:PRINT " OK? y=RET, n=ESC":COLOR 7
14780   C$=INKEY$:IF C$<>" " THEN GOTO 14780
14790   C$=INKEY$:IF C$=" " THEN GOTO 14790 ELSE NO=ASC(C$)
14800   IF NO=&H1B THEN GOTO 14580
14810   IF NO=&HD THEN GOTO 14830
14820   GOTO 14780
14830 CLS 3:COLOR 3:LOCATE 1,22:PRINT FFMN$;" Now saving!
":COLOR 7
14840 OPEN FFMN$ FOR OUTPUT AS #1
14850 PRINT #1,TITL$
14860 PRINT #1,SOLU$
14870 PRINT #1,ZP
14880 PRINT #1,ZM
14890 PRINT #1,SOLV$
14900 PRINT #1,CTEMP
14910 PRINT #1,NP
14920 PRINT #1,NC
14930 PRINT #1,VB
14940 FOR IP=1 TO NP
14950   PRINT #1,PRES(IP)
14960   PRINT #1,COMP(IP)
14970   PRINT #1,DIEL(IP)
14980   PRINT #1,YETA(IP)
14990   PRINT #1,DENS(IP)
15000   PRINT #1,LZ(IP)
15010   PRINT #1,AZ(IP)
15020   PRINT #1,KZ(IP)
15030   PRINT #1,QZ(IP)
15040   FOR IC=1 TO NC

```

```

15050     PRINT #1,SCON(IP,IC)
15060     PRINT #1,LAMD(IP,IC)
15070     NEXT IC
15080     NEXT IP
15090     CLOSE #1
15100     RETURN
15110     '
15120     'Kohlrausch plot
15130     *DPLOT
15140     CLS 3
15150     LOWC=0:HIGC=SQR(CNMAX)*1.1:RNGC=HIGC-LOWC
15160     LOWL=INT(LMMIN-.3):HIGL=INT(LMMAX)+3 :RNGL=HIGL-LOWL
15170     SCREEN 3
15180     WINDOW (0,-300)-(300,0)
15190     VIEW (300,0)-(600,300)
15200     LINE (0,-300)-(300,0),7,B
15210     FOR IP=1 TO NP
15220         FOR IC=1 TO NC
15230             X=(SQR(ACON(IP,IC))-LOWC)/RNGC*300:X=INT(X)
15240             Y=(LAMD(IP,IC)-LOWL)/RNGL*300           :Y=-INT(Y)
15250             CIRCLE (X,Y),2,IP
15260         NEXT IC
15270     NEXT IP
15280     LOCATE 30,0 :PRINT USING "###.#";HIGL
15290     LOCATE 31,5 :PRINT "Lamda"
15300     LOCATE 30,18:PRINT USING "###.#";LOWL
15310     LOCATE 36,19:PRINT USING "###.#";LOWC
15320     LOCATE 49,19:PRINT "SQR(C)"
15330     LOCATE 67,19:PRINT USING "#.###^";HIGC
15340     IF NFIT=0 THEN RETURN
15350     '
15360     GM=1
15370     FOR IP=1 TO NP
15380         IF FLG(IP)=1 THEN GOTO 15640
15390         X=(0-LOWC)/RNGC*300:X=INT(X)
15400         Y=(LZ(IP)-LOWL)/RNGL*300:Y=-INT(Y)
15410         PSET(X,Y),IP
15420         FOR IC=1 TO 100
15430             X1=X:Y1=Y
15440             RTC=3*IC/300*HIGC:C=RTC*RTC
15450         '
15460         GM1=GM:IF GM<0 THEN GM=.0001
15470         CG=C*GM:RTCG=SQR(CG)
15480         DBT=DIEL(IP)*BOLZ*TEMP
15490         KAP2=8*PAI*CHRG^2*AVGD*ZZ2/(DBT*1000)
15500         KAP=SQR(KAP2)
15510         F=EXP(-KAP*RTCG*CHRG^2*ZP*ZM/
(2*DBT*(1+KAP*RTCG*AP(IP))))
15520         GM=1-KP(IP)*GM*CG*F*F
15530         IF GM>1 THEN GM=1
15540         IF ABS(GM-GM1)>.0001 THEN GOTO 15460
15550         IF NFIT=10 THEN L=GM*LP(IP)^2/
(LP(IP)+FS(IP)*SQR(C*GM)):GOTO 15590
15560         L=LP(IP)-FS(IP)*RTCG+FE(IP)*CG*LOG(CG)
15570         L=(L+(FJ1(IP)-VB*LP(IP))*CG-FJ2(IP)*CG*RTCG)/
(1+KP(IP)*F*F*CG)
15580         '
15590         X=3*IC
15600         Y=(L-LOWL)/RNGL*300:Y = -INT(Y)
15610         LINE(X1,Y1)-(X,Y),IP

```

```

15620 IF L<LOWL OR L>HIGL THEN GOTO 15640
15630 NEXT IC
15640 NEXT IP
15650 RETURN
15660 '
15670 'Print data
15680 *DPRIN
15690 COLOR 3:LOCATE 1,22: PRINT " Now printing!"
":COLOR 7
15700 LPRINT:LPRINT:LPRINT:LPRINT
15710 LPRINT " *** Results for conductivity analysis ***"
15720 LPRINT:LPRINT " ";EQUAS(NFIT)
15730 LPRINT
15740 LPRINT " Data File : ";FLNMS$+".CND"
15750 LPRINT " Title : ";TITL$
15760 LPRINT " Solute : ";SOLUS$;" ";
15770 LPRINT USING "z(+)=## z(-)=##";ZP;ZM
15780 LPRINT " Solvent : ";SOLVS
15790 LPRINT USING " Temperature: ##.# C";CTEMP
15800 LPRINT USING " B-factor : #.####";VB
15810 LPRINT USING " Series : ## Points : ##";NP;NC
15820 FOR IP=1 TO NP
15830 LPRINT
15840 LPRINT USING " Pressure : ##.####
MPa";PRES(IP)
15850 LPRINT USING " Compression factor :
##.####";COMP(IP)
15860 LPRINT USING " Relative permittivity:
##.####";DIEL(IP)
15870 LPRINT USING " Viscosity : ##.####
cP";YETA(IP)
15880 LPRINT USING " Density : ##.#### g/
cm3";DENS(IP)
15890 LPRINT
15900 IF FLG(IP)=0 THEN GOTO 16000
15910 LPRINT " Failed to fit!"
15920 LPRINT
15930 LPRINT " Conc.(mM) Adjusted L(obs)"
15940 FOR IC=1 TO NC
15950 LPRINT USING " ##.#### ##.####
##.####";SCON(IP,IC)*1000; ACON(IP,IC)*1000;LAMD(IP,IC)
15960 NEXT IC
15970 LPRINT:LPRINT:LPRINT:LPRINT:LPRINT:LPRINT:LPRINT:LPRINT
15980 GOTO 16290
15990 LPRINT USING " q :
#.####";QZ(IP)
16000 IF NFIT<>10 THEN GOTO 16120
16010 LPRINT " LOi LO KA"
16020 LPRINT USING " ##.####";LZ(IP);LP(IP);KP(IP)
16030 LPRINT
16040 LPRINT " C L Z S G F
X Y"
16050 FOR IC=1 TO NC
16060 C=1000*SCON(IP,IC):L=LAMD(IP,IC):Z=ZI(IC):SH=THIT(IC)
16070 G=GG(IP,IC):F=FF(IP,IC):X=XI(IC):Y=YI(IC)
16080 LPRINT USING " ##.#### ##.#### #.#### #.#### #.####
#.#### #.#### #.####";C;L;Z;SH;G;F;X;Y
16090 NEXT IC
16100 LPRINT:LPRINT:LPRINT:LPRINT:LPRINT
16110 GOTO 16240

```

```

16120 LPRINT USING "      iL0 = ###.###      iKA = ###.###
ia = ##.###";LZ(IP);KZ(IP);AZ(IP)
16130 LPRINT USING "      L0 = ###.###      KA = ###.###
a = ##.###";LP(IP);KP(IP);AP(IP)*1E+08
16140 LPRINT
16150 LPRINT USING "      AL = #.#####      BE = #.#####
S = #.#####";FA(IP);FB(IP);FS(IP)
16160 LPRINT USING "      E1 = #.#####      E2 = #.#####
E = #.#####";FE1(IP);FE2(IP);FE(IP)
16170 LPRINT USING "      S1 = #.#####      S2 = #.#####
J1 = #.#####";FS1(IP);FS2(IP);FJ1(IP)
16180 LPRINT USING "      S3 = #.#####      S4 = #.#####
J2 = #.#####";FS3(IP);FS4(IP);FJ2(IP)
16190 LPRINT
16200 LPRINT "      Conc.(mM)   Adjusted   L(obs)   L(calc)
Error      G      F"
16210 FOR IC=1 TO NC
16220 LPRINT USING "      ##.#####   ##.#####   ##.###
###.###   ###.###   #.#####   #.#####"
;SCCN(IP,IC)*1000;ACCN(IP,IC)*1000;LAMD(IP,IC);LCAL(IP,IC);DIEF(IP,IC);GG(IP,IC);FF(IP,IC)
16230 NEXT IC
16240 LPRINT
16250 LPRINT USING "      SD(L)= #.#####";FSDL(IP);
16260 LPRINT USING "      SD(L0)= #.#####";FSDLZ(IP);
16270 LPRINT USING "      SD(KA)= #.#####";FSDK(IP);
16280 LPRINT USING "      SD(a)= #.#####";FSDA(IP)*1E+08
16290 NEXT IP
16300 LPRINT:LPRINT:LPRINT
16310 RETURN
16320 '
16330 'Fitting
16340 *DFIT
16350 CLS 3:COLOR 6
16360 AFLG=0:KFLG=0:GFLG=0:NFLG=0:EFLG=0
16370 LOCATE 1,1 :PRINT "Select a fitting equation?":COLOR 5
16380 LOCATE 1,3 :PRINT "0. ";EQUAS(10)
16390 LOCATE 1,4 :PRINT "1. ";EQUAS(1)
16400 LOCATE 1,5 :PRINT "2. ";EQUAS(2)
16410 LOCATE 1,6 :PRINT "3. ";EQUAS(3)
16420 LOCATE 1,7 :PRINT "4. ";EQUAS(4)
16430 LOCATE 1,8 :PRINT "5. ";EQUAS(5)
16440 LOCATE 1,9 :PRINT "6. ";EQUAS(6)
16450 LOCATE 1,10 :PRINT "7. ";EQUAS(7)
16460 LOCATE 1,11 :PRINT "8. ";EQUAS(8)
16470 LOCATE 1,12 :PRINT "9. ";EQUAS(9)
16480 LOCATE 1,13 :PRINT "Quit=ESC":COLOR 7
16490 C$=INKEY$:IF C$<>" " THEN GOTO 16490
16500 C$=INKEY$:IF C$=" " THEN GOTO 16500 ELSE NO=ASC(C$)
16510 IF NO=&H30 THEN NFIT=10:GOTO 16810
16520 IF NO=&H31 THEN NFIT=1:GOTO 16630
16530 IF NO=&H32 THEN NFIT=2:GOTO 16630
16540 IF NO=&H33 THEN NFIT=3:GOTO 16630
16550 IF NO=&H34 THEN NFIT=4:GOTO 16630
16560 IF NO=&H35 THEN NFIT=5:GOTO 16630
16570 IF NO=&H36 THEN NFIT=6:GOTO 16630
16580 IF NO=&H37 THEN NFIT=7:GOTO 16630
16590 IF NO=&H38 THEN NFIT=8:GOTO 16630
16600 IF NO=&H39 THEN NFIT=9:GOTO 16630
16610 IF NO=&H1B THEN RETURN
16620 GOTO 16490

```

```

16630 COLOR 6:LOCATE 1,22:PRINT " Replace with a new L0? n=RET,
y=SPC ":COLOR 7
16640 C$=INKEY$:IF C$<>" THEN GOTO 16640
16650 C$=INKEY$:IF C$="" THEN GOTO 16650 ELSE NO=ASC(C$)
16660 IF NO=&HD THEN GOTO 16690
16670 IF NO=&H20 THEN GOSUB *REPL:GOTO 16690
16680 GOTO 16640
16690 COLOR 6:LOCATE 1,22:PRINT " Replace with new a? n=RET,
y=SPC ":COLOR 7
16700 C$=INKEY$:IF C$<>" THEN GOTO 16700
16710 C$=INKEY$:IF C$="" THEN GOTO 16710 ELSE NO=ASC(C$)
16720 IF NO=&HD THEN GOTO 16750
16730 IF NO=&H20 THEN GOSUB *REPA:GOTO 16750
16740 GOTO 16700
16750 COLOR 6:LOCATE 1,22:PRINT " Replace with a new KA? n=RET,
y=SPC ":COLOR 7
16760 C$=INKEY$:IF C$<>" THEN GOTO 16760
16770 C$=INKEY$:IF C$="" THEN GOTO 16770 ELSE NO=ASC(C$)
16780 IF NO=&HD THEN GOTO 16810
16790 IF NO=&H20 THEN GOSUB *REPK:GOTO 16810
16800 GOTO 16760
16810 COLOR 3:LOCATE 1,22:PRINT " Now fitting!
":COLOR 7
16820 FOR IP=1 TO NP
16830 D=DIEL(IP):H=YETA(IP)*.01:TEMP=CTEMP+273.15
16840 L0=LZ(IP):A=AZ(IP)*1E-08:K=KZ(IP):Q=QZ(IP)
16850 ZZ2=(ZP*ZP+ZM*ZM)/2:DTRT=SQR(D*TEMP):DBT=D*BOLZ*TEMP
16860 KAP2=8*PAI*CHRG^2*AVGD*ZZ2/(DBT*1000)
16870 KAP=SQR(KAP2)
16880 ALPH=ZP*ZM*CHRG^2*KAP*Q/(3*DBT*(1+SQR(Q)))
16890 BETA=CHRG^2*AVGD*(ZP+ZM)*KAP*1E-11/(6*8.98755*PAI*H)
16900 '
16910 IF NFIT=10 THEN GOSUB *SHED
16920 IF NFIT<>10 THEN GOSUB *FUOS
16930 '
16940 LP(IP)=L0
16950 AP(IP)=A
16960 KP(IP)=K
16970 FA(IP)=ALPH:FB(IP)=BETA:FS(IP)=ONSS
16980 FE1(IP)=E1:FE2(IP)=E2:FE(IP)=E
16990 FS1(IP)=SIG1:FS2(IP)=SIG2:FJ1(IP)=J1
17000 FS3(IP)=SIG3:FS4(IP)=SIG4:FJ2(IP)=J2
17010
FSDL(IP)=SDL:FSDLZ(IP)=SDLZ:FSDK(IP)=SDK:FSDA(IP)=SDA:FLG(IP)=FFLG
17020 NEXT IP
17030 RETURN
17040 '
17050 'Shedlovsky equation
17060 *SHED
17070 FFLG=0
17080 E1=0:E2=0:E=0:SIG1=0:SIG2=0:J1=0:SIG3=0:SIG4=0:J2=0
17090 'Arrhenius-Ostwald
17100 FOR IC=1 TO NC
17110 C=ACON(IP,IC):L=LAMD(IP,IC)
17120 XI(IC)=C*L
17130 YI(IC)=1/L
17140 NEXT IC
17150 SX=0:SY=0:SXX=0:SYY=0:SXY=0
17160 FOR IC=1 TO NC
17170 SX=SX+XI(IC)

```

```

17180 SY=SY+YI(IC)
17190 SXX=SXX+XI(IC)*XI(IC)
17200 SYI=SYI+YI(IC)*YI(IC)
17210 SXY=SXY+XI(IC)*YI(IC)
17220 NEXT IC
17230 NSS=NC*SXX-SX*SX
17240 L0=NSS/(SXX*SY-SX*SXY):LZ(IP)=L0
17250 K=L0^2*(NC*SXY-SX*SY)/NSS
17260 KAI=0
17270 'Iteration Start
17280 K1=K:L01=L0
17290 ONSS=ALPH*L0+BETA
17300 FOR IC=1 TO NC
17310 C=ACON(IP,IC):RTC=SQR(C):L=LAMD(IP,IC)
17320 ZI(IC)=ONSS*SQR(C*L/L0^3):Z=ZI(IC)
17330 THIT(IC)=(Z/2+SQR(1+Z*Z/4))^2:SH=THIT(IC)
17340 GG(IP,IC)=L*SH/L0
17350 IF GG(IP,IC)<0 THEN GFLG=GFLG+1
17360 IF GG(IP,IC)>1 THEN GG(IP,IC)=1
17370 CG=C*GG(IP,IC):RTCG=SQR(CG)
17380 F=EXP(-KAP*RTCG*CHRG^2*ZP*ZM/(2*DBT*(1+KAP*RTCG*A)))
17390 FF(IP,IC)=F
17400 XI(IC)=C*L*SH*F*F
17410 YI(IC)=1/(L*SH)
17420 NEXT IC
17430 '
17440 SX=0:SY=0:SXX=0:SYI=0:SXY=0
17450 FOR IC=1 TO NC
17460 SX=SX+XI(IC)
17470 SY=SY+YI(IC)
17480 SXX=SXX+XI(IC)*XI(IC)
17490 SYI=SYI+YI(IC)*YI(IC)
17500 SXY=SXY+XI(IC)*YI(IC)
17510 NEXT IC
17520 NSS=NC*SXX-SX*SX
17530 L0=NSS/(SXX*SY-SX*SXY):DL=L0-L01
17540 K=L0*L0*(NC*SXY-SX*SY)/NSS:DK=K-K1
17550 KAI=KAI+1
17560 IF KAI>100 THEN NFLG=NFLG+1:FFLG=1:RETURN
17570 IF ABS(DL)>.0001 THEN GOTO 17270
17580 IF ABS(DK)>.001 THEN GOTO 17270
17590 IF K<0 THEN KFLG=KFLG+1
17600 '
17610 SDL=0
17620 FOR IC=1 TO NC
17630 RTCG=SQR(ACON(IP,IC)*GG(IP,IC))
17640 LCAL(IP,IC)=GG(IP,IC)*L0*L0/(L0+ONSS*RTCG)
17650 DIFF(IP,IC)=LAMD(IP,IC)-LCAL(IP,IC)
17660 SD=DIFF(IP,IC)
17670 SDL=SDL+SD*SD
17680 NEXT IC
17690 SDL=SQR(SDL/(NC-2))
17700 SDK=SDL*SQR(NC/NSS)*L0*L0
17710 SDLZ=SDL*SQR(SXX/NSS)*L0*L0
17720 SDA=0
17730 RETURN
17740 '
17750 'Fuoss-Onsager, Fuoss-Hsia & Pitts equation
17760 *FUOS
17770 FFLG=0

```

```

17780 AB=ZP*ZM*CHRG^2/DBT
17790 E1=KAP2*AB*AB/24
17800 E2=KAP*AB*BETA/16
17810 KAI=0
17820 'Iteration Start
17830 K1=K:L01=L0:A1=A
17840 IF A<0 THEN AFLG=AFLG+1:FFLG=1:RETURN
17850 ONSS=ALPH*L0+BETA
17860 B=AB/A
17870 FOR IC=1 TO NC
17880 C=ACON(IP,IC):RTC=SQR(C):L=LAMD(IP,IC)
17890 IF NFIT=1 OR NFIT=4 OR NFIT=7 THEN G0=1:F=1:K=0:GOTO
17920
17900 G0=L/(L0-ONSS*RTC*SQR(L/L0))
17910 IF G0<0 THEN GFLG=GFLG+1:FFLG=1:RETURN
17920 CG=C*G0:RTCG=SQR(CG)
17930 E=E1*L0-E2
17940 IF NFIT>=1 AND NFIT<=3 THEN GOSUB *ONSA
17950 IF NFIT>=4 AND NFIT<=6 THEN GOSUB *HSIA
17960 IF NFIT>=7 AND NFIT<=9 THEN GOSUB *PITT
17970 J1=SIG1*L0+SIG2
17980 J2=SIG3*L0+SIG4
17990 JJ1=(J1-VB*L0)/A:JJ2=J2/A
18000 IF NFIT=1 OR NFIT=4 OR NFIT=7 THEN
GG(IP,IC)=G0:FF(IP,IC)=F:XI(IC)=JJ1*C-JJ2*C*RTC:GOTO 18090
18010 GG(IP,IC)=L/(L0-ONSS*RTCG+E*CG*LOG(CG)+(J1-VB*L0)*CG-
J2*CG*RTCG)
18020 IF GG(IP,IC)>1 THEN GG(IP,IC)=1:GOTO 18060
18030 DG=GG(IP,IC)-G0
18040 IF ABS(DG)>.00001 THEN G0=GG(IP,IC):GOTO 17910
18050
18060 F=EXP(-KAP*RTCG*CHRG^2*ZP*ZM/(2*DBT*(1+KAP*RTCG*A)))
18070 FF(IP,IC)=F
18080 XI(IC)=-L*F*F*CG
18090 YI(IC)=L-L0+ONSS*RTCG-E*CG*LOG(CG)-(J1-
VB*L0)*CG+J2*CG*RTCG+K*F*F*L*CG
18100 ZI(IC)=JJ1*CG-JJ2*CG*RTCG
18110 NEXT IC
18120
18130 SX=0:SY=0:SZ=0:SXX=0:SYX=0:SZZ=0:SXY=0:SYZ=0:SZX=0
18140 FOR IC=1 TO NC
18150 SX=SX+XI(IC)
18160 SY=SY+YI(IC)
18170 SXX=SXX+XI(IC)*XI(IC)
18180 SYX=SYX+YI(IC)*YI(IC)
18190 SXY=SXY+XI(IC)*YI(IC)
18200 IF NFIT=3 OR NFIT=6 OR NFIT=9 THEN GOTO 18210 ELSE GOTO
18250
18210 SZ=SZ+ZI(IC)
18220 SZZ=SZZ+ZI(IC)*ZI(IC)
18230 SYZ=SYZ+YI(IC)*ZI(IC)
18240 SZX=SZX+ZI(IC)*XI(IC)
18250 NEXT IC
18260 IF NFIT=3 OR NFIT=6 OR NFIT=9 THEN GOTO 18270 ELSE GOTO
18370
18270 NSS=(SZZ-SZ*SZ/NC)*(SXX-SX*SX/NC)-(SZX-SZ*SX/NC)^2
18280 DA=(SYZ-SZ*SY/NC)*(SXX-SX*SX/NC)/NSS
18290 DA=DA-(SXY-SY*SX/NC)*(SZX-SZ*SX/NC)/NSS
18300 DK=(SZZ-SZ*SZ/NC)*(SXY-SX*SY/NC)/NSS
18310 DK=DK-(SYZ-SY*SZ/NC)*(SZX-SZ*SX/NC)/NSS

```

```

18320 DL=(SY-DA*SZ-DK*SX)/NC
18330 A=DA+A1
18340 K=DK+K1
18350 L0=DL+L01
18360 GOTO 18420
18370 NSS=NC*SXX-SX*SX
18380 IF NFIT=1 OR NFIT=4 OR NFIT=7 THEN DA=(NC*SXY-SX*SY)/
NSS:A=DA+A1
18390 IF NFIT=2 OR NFIT=5 OR NFIT=8 THEN DK=(NC*SXY-SX*SY)/
NSS:K=DK+K1
18400 DL=(SXX*SY-SX*SXY)/NSS:L0=DL+L01
18410 '
18420 KAI=KAI+1
18430 IF KAI>100 THEN NFLG=NFLG+1:FFLG=1:RETURN
18440 IF ABS(DL)>.0001 THEN GOTO 17820
18450 IF NFIT=1 OR NFIT=4 OR NFIT=7 THEN GOTO 18480
18460 IF NFIT=2 OR NFIT=5 OR NFIT=8 THEN GOTO 18500
18470 IF NFIT=3 OR NFIT=6 OR NFIT=9 THEN GOTO 18530
18480 IF ABS(DA)>1E-11 THEN GOTO 17820
18490 GOTO 18570
18500 IF ABS(DK)>.001 THEN GOTO 17820
18510 IF K<0 THEN KFLG=KFLG+1
18520 GOTO 18570
18530 IF ABS(DK)>.001 THEN GOTO 17820
18540 IF K<0 THEN KFLG=KFLG+1
18550 IF ABS(DA)>1E-11 THEN GOTO 17820
18560 '
18570 SDL=0
18580 FOR IC=1 TO NC
18590 CG=ACON(IP,IC)*GG(IP,IC):RTCG=SQR(CG):F=FF(IP,IC)
18600 LCAL(IP,IC)=(L0-ONSS*RTCG+E*CG*LOG(CG)+(J1-VB*L0)*CG-
J2*CG*RTCG)/(1+K*F*F*CG)
18610 DIFF(IP,IC)=LAMD(IP,IC)-LCAL(IP,IC)
18620 SD=DIFF(IP,IC)
18630 SDL=SDL+SD*SD
18640 NEXT IC
18650 IF NFIT=3 OR NFIT=6 OR NFIT=9 THEN SDL=SQR(SDL/(NC-3))
18660 SDL=SQR(SDL/(NC-2))
18670 IF NFIT=1 OR NFIT=4 OR NFIT=7 THEN SDA=SDL*SQR(NC/NSS)
ELSE SDA=0
18680 IF NFIT=2 OR NFIT=5 OR NFIT=8 THEN SDK=SDL*SQR(NC/NSS)
ELSE SDK=0
18690 IF NFIT=3 OR NFIT=6 OR NFIT=9 THEN GOTO 18720
18700 SDLZ=SDL*SQR(SXX/NSS)
18710 GOTO 18780
18720 DA=(SXX-SX*SX/NC)/NSS
18730 DK=(SZZ-SZ*SZ/NC)/NSS
18740 DLZ=(NC+DA*SZ*SZ+DK*SX*SX+2*SZ*SX*(SZ*SX/NC-SZX)/NSS)/NC/
NC
18750 SDA=SDL*SQR(DA)
18760 SDK=SDL*SQR(DK)
18770 SDLZ=SDL*SQR(DLZ)
18780 RETURN
18790 '
18800 *ONSA
18810 SIG1=2*E1*(LOG(KAP*A)+1.102+2.2125/B+3/4/B/B-1/B/B/B)
18820 SIG2=2*E2*(-LOG(KAP*A)-.7897+7.75/B+1/B/B)
18830 SIG3=0:SIG4=0
18840 RETURN
18850 '

```

```

18860 *HSIA
18870 SIG1=2*E1*(.90735+2/B+2/B/B-1/B/B/B+LOG(KAP*A))
18880 SIG2=2*E2*(.0142+22/3/B-LOG(KAP*A))
18890 SIG3=4*E1*KAP*A*B*(.1523/B+1.1187/B/B+.9571/B/B/B)
18900 SIG4=2*E2*KAP*A*B*(-.6461+.5738/B+7.0572/B/B-2/3/B/B/B)
18910 SIG4=SIG4-BETA*E2*(4/3/B-2.2194)/L0
18920 RETURN
18930 '
18940 *PITT
18950 SIG1=2*E1*(1.7718+2/B+LOG(KAP*A))
18960 SIG2=2*E2*(.01387+8/B-LOG(KAP*A))
18970 SIG3=4*E1*KAP*A*B*(1.5732/B+1.2929/B/B)
18980 SIG4=2*E2*KAP*A*B*(1.4073/B+8/B/B)
18990 RETURN
19000 '
19010 *REPL
19020 FOR IP=1 TO NP
19030 LZ(IP)=LP(IP)
19040 NEXT IP
19050 RETURN
19060 '
19070 *REPA
19080 FOR IP=1 TO NP
19090 AZ(IP)=AP(IP)
19100 NEXT IP
19110 RETURN
19120 '
19130 *REPK
19140 FOR IP=1 TO NP
19150 KZ(IP)=KP(IP)
19160 NEXT IP
19170 RETURN
19180 '
19190 *DERRO
19200 IF ERL>=18800 AND ERL<=18830 THEN
EFLG=EFLG+1:FFLG=1:RESUME 18840
19210 IF ERL>=18860 AND ERL<=18910 THEN
EFLG=EFLG+1:FFLG=1:RESUME 18920
19220 IF ERL>=18940 AND ERL<=18980 THEN
EFLG=EFLG+1:FFLG=1:RESUME 18990
19230 IF ERL>=17060 AND ERL<=17720 THEN
EFLG=EFLG+1:FFLG=1:RESUME 17730
19240 IF ERL>=17760 AND ERL<=18770 THEN
EFLG=EFLG+1:FFLG=1:RESUME 18780
19250 CLOSE #1
19260 '
19270 END

```

6.4. References

1. R. M. Fuoss and F. Accascina, *Electrolytic Conductance*, Wiley-Interscience, New York (1959).
2. R. A. Robinson and R. H. Stokes, *Electrolyte Solutions*, 2nd ed. rev., Butterworths, London (1970).
3. A. K. Convington and T. Dickinson, Editors, *Physical Chemistry of Organic Solvent Systems*, Plenum Press, London (1973).
4. S. I. Smedley, *The Interpretation of Ionic Conductivity in Liquid*, Plenum Press, New York (1980).
5. O. Popovych and R. P. T. Tomkins, *Nonaqueous Solution Chemistry*, Wiley-Interscience, New York (1981).
6. J. C. Justice, "Conductance of Electrolyte Solutions", in *Comprehensive Treatise of Electrochemistry*, B. E. Conway, J. O'M. Bockris and E. Yeager, Editors, Vol. 5, Chap. 3, Plenum Press, New York (1983).
7. M. Spiro, "Conductance and Transference Determination", in *Physical Methods of Chemistry*, 2nd ed., B. M. Rossiter and J. F. Hamilton, Editors, Vol. 2, Chap. 8, Wiley-Interscience, New York (1986).
8. K. Miyoshi, *Kagaku no Ryoiki*, **26**, 847, 898 (1972).
9. M. Hojo, *Denki Kagaku*, **62**, 119 (1994).
10. R. M. Fuoss and T. Shedlovsky, *J. Amer. Chem. Soc.*, **71**, 1496 (1949).
11. E. Pitts, *Proc. Roy. Soc.*, **217A**, 43 (1953).
12. R. M. Fuoss and L. Onsager, *J. Phys. Chem.*, **61**, 668 (1957).
13. R. M. Fuoss and K. L. Hsia, *Proc. Nat. Acad. Sci.*, **57**, 1550 (1967).
14. R. Fernández-Prini, in Ref. 3, Ch. 5.1.
15. J. C. Justice, *Electrochim. Acta*, **16**, 701 (1971).
16. R. L. Kay, *J. Amer. Chem. Soc.*, **82**, 2099 (1960).

7. Conclusions

The preparation and properties of organic electrolytes for electrochemical devices including aluminum electrolytic capacitors, electrical double layer capacitors and lithium batteries were presented. Among organic electrolytes described in this thesis, quaternary ammonium salts of carboxylic acids have acquired a potential application in aluminum electrolytic capacitors.

Quaternary ammonium salts have been very popular substances for both synthetic chemists and electrochemists as a phase transfer catalyst or a supporting electrolyte salt. However, as far as quaternary ammonium carboxylate salts are concerned, one cannot find them except acetate salts in common reagent catalogues. This is presumably because they had no industrial application.

The author feels that this great success came from selecting a research theme in the interdisciplinary area between synthetic chemistry and electrochemistry.

Recently, the organic electrolytes for the rechargeable lithium ion battery became one of the major concerns for chemical companies, because this battery is regarded as one of the strategic products for many portable electronic appliances. The author feels more synthetic challenges are being required in finding new materials for organic electrolytes, because a technological breakthrough has been expected.

Finally, there are many books which deal with fundamentals of nonaqueous solution chemistry as listed in Chap. 1.6, however, there are few books, which concentrate on the industrial application of organic electrolytes. This thesis provides the technical application of the organic electrolytes and furnishes a good example to understand how the basic chemistry is applied to the real industry.

8. List of Publications

8.1. Papers

[Chapter 2]

1. Makoto Ue, Tomohiro Sato, Hitoshi Asahina, Kazuhiko Ida and Shoichiro Mori, "Anodic Oxidation of Aluminum in Quaternary Ammonium Carboxylate/ γ -Butyrolactone Electrolytes", *Denki Kagaku*, **60**, 480 (1992).
2. Makoto Ue, Tomohiro Sato and Masayuki Takeda, "Conductivities and Ion Association of Quaternary Ammonium Carboxylates in γ -Butyrolactone", *Denki Kagaku*, **61**, 1080 (1993).
3. Makoto Ue, Kuniyoshi Shima and Shoichiro Mori, "Electrochemical Properties of Quaternary Ammonium Borodiglycolates and Borodioxalates", *Electrochim. Acta*, **39**, in press.
4. Makoto Ue, Sachie Sekigawa, Masayuki Takeda and Shoichiro Mori, "Comparison of Ionic Association between Tertiary and Quaternary Ammonium Carboxylates in γ -Butyrolactone", *Denki Kagaku*, **63**(1), in press.
5. Makoto Ue, Hitoshi Asahina and Shoichiro Mori, "Anodic Oxidation of Aluminum in Organic Electrolytes under Nearly Anhydrous Condition", *Oxide Films on Metals and Alloys VII*, The Electrochemical Society Proceedings Series, Pennington, NJ, in press.
6. Makoto Ue, Hitoshi Asahina and Shoichiro Mori, "Anodic Oxidation of Aluminum in Organic Electrolytes under Nearly Anhydrous Condition", *J. Electrochem. Soc.*, submitted.
7. Makoto Ue, Masayuki Takeda, Yoko Suzuki and Shoichiro Mori, "Chemical Stability of γ -Butyrolactone-based Electrolytes for Aluminum Electrolytic Capacitors", *J. Power Sources*, to be submitted.
8. 宇恵 誠、
「アルミ電解コンデンサ用新規高性能電解液の研究開発および工業化」、
TCSC News Letters, **23**, 89 (1993).
9. 宇恵 誠、井田 和彦、森 彰一郎、
「アルミ電解コンデンサ用電解液」、
ケミトピア, **12**, 2 (1993).

10. 宇恵 誠、森 彰一郎、
「カルボン酸第四級アンモニウム／ガンマーブチロラクトン系電解液の電気化学的特性」、
電解蓄電器評論, **45**, 1 (1994).
11. 宇恵 誠、
「ガンマーブチロラクトン系電解液の電気伝導率解析」、
電解蓄電器評論, **45**, 166 (1994).

[Chapter 3]

1. Makoto Ue,
"Conductivities and Ion Association of Quaternary Ammonium Tetrafluoroborates in Propylene Carbonate",
Electrochim. Acta, **39**, 2083 (1994).
2. Makoto Ue, Kazuhiko Ida and Shoichiro Mori,
"Electrochemical Properties of Organic Liquid Electrolytes Based on Quaternary Onium Salts for Electrical Double Layer Capacitors",
J. Electrochem. Soc., **141**, 2989 (1994).
3. 宇恵 誠、井田 和彦、森 彰一郎、
「電気二重層コンデンサ用電解液の開発」、
ニューキャパシタ研究会, **2**, 投稿中.

[Chapter 4]

1. Makoto Ue,
"Conductivities and Ion Association of LiCF_3SO_3 , $\text{Li}(\text{CF}_3\text{SO}_2)_2\text{N}$ and $\text{LiC}_4\text{F}_9\text{SO}_3$ in Propylene Carbonate",
Denki Kagaku, **64**, 620 (1994).
2. Makoto Ue,
"Mobility and Ionic Association of Lithium and Quaternary Ammonium Salts in Propylene Carbonate and γ -Butyrolactone",
J. Electrochem. Soc., **141**, 3336 (1994).
3. Makoto Ue and Shoichiro Mori,
"Mobility and Ionic Association of Lithium Salts in Aprotic Solvents",
Rechargeable Lithium and Lithium Ion (RCT) Batteries, The Electrochemical Society Proceedings Series, Pennington, NJ, in press.
4. Makoto Ue and Shoichiro Mori,
"Mobility and Ionic Association of Lithium Salts in a Propylene Carbonate-Ethyl Methyl Carbonate Mixed Solvent",
J. Electrochem. Soc., submitted.

5. Makoto Ue,
"Mobility and Ionic Association of Lithium Salts in Aprotic Solvents",
Prog. Batteries Battery. Materials, **14**, submitted.
6. 宇恵 誠、森 彰一郎、
「リチウム電池用有機溶媒」、
機能材料、**15**, 投稿中.

[Chapter 5]

1. Makoto Ue, Mitsumasa Kaitoh, Eiki Yasukawa and Shoichiro Mori,
"A New Gelling Agent and its Application as A Solid Electrolyte for Lithium Batteries",
Electrochim. Acta, **38**, 1301 (1993).
2. Michael M. Lerner, Steven J. Visco, Makoto Ue, Merca M. Doeff and Lutgard C.
De Jonghe,
"Preparation and Discharge Characteristics of Solid Redox Polymerization Electrodes
Employing Disulfide Polymers and Copolymers",
Mat. Res. Sym. Proc., **210**, 81 (1991).
3. Makoto Ue, Steven J. Visco and Lutgard C. De Jonghe,
"Comparison of Cathode Utilization between Polymeric Organodisulfide and Titanium
Disulfide in Solid Polymer Electrolyte Rechargeable Lithium Cells",
Denki Kagaku, **61**, 1409 (1993).
4. Steven J. Visco, Lutgard C. De Jonghe and Makoto Ue,
「新しい概念のエネルギー貯蔵材料 (ジスルフィドポリマー)」
電気化学、**62**, 300 (1994).

8.2. Society Meetings

[Chapter 2]

1. 宇恵 誠、佐藤智洋、
「有機電解液中でのアルミ陽極酸化皮膜の絶縁破壊電圧」、
電気化学協会第59回大会、1B06 (1992).
2. 佐藤智洋、朝比奈 均、宇恵 誠、
「 γ -ブチロラクトン系電解液中で形成したアルミ陽極酸化皮膜」、
電気化学協会第59回大会、1B07 (1992).
3. Makoto Ue, Tomohiro Sato, Kazuhiko Ida and Shoichiro Mori,
"A High Performance Electrolyte for Aluminum Electrolytic Capacitors",
The First West Pacific Electrochemistry Symposium, 1A-11 (1992).
4. Tomohiro Sato, Makoto Ue, Hitoshi Asahina and Shoichiro Mori,
"Anodic Oxidation of Aluminum in γ -Butyrolactone Based Organic Electrolytes",
The First West Pacific Electrochemistry Symposium, 2P-14 (1992).
5. 宇恵 誠、佐藤智洋、武田政幸、
「アルミ電解コンデンサ用 γ -ブチロラクトン系電解液の電気伝導度」、
電気化学協会'92秋季大会、2H14 (1992).
6. 朝比奈 均、横戸清美、佐藤智洋、宇恵 誠、
「有機電解質溶液によるアルミニウムの陽極酸化皮膜の解析」、
表面技術協会第86回講演大会、15A-2 (1992).
7. 宇恵 誠、
「カルボン酸第四級アンモニウム/ガンマーブチロラクトン系電解液の
電気化学的特性」、
平成4年12月度電解蓄電器研究会 (1992).
8. 宇恵 誠、佐藤智洋、朝比奈 均、横戸清美、
「有機電解液中でのアルミニウムの陽極酸化」、
表面技術協会第87回講演大会、18D-1 (1993).
9. 武田政幸、佐藤智洋、宇恵 誠、鈴木葉子、山崎静悦、
「アルミ電解コンデンサ用 γ -ブチロラクトン系電解液の熱安定性」、
電気化学協会第60回大会、3G05 (1993).
10. 武田政幸、宇恵 誠、鈴木葉子、山崎静悦、
「アルミ電解コンデンサ用 γ -ブチロラクトン系電解液の熱安定性(2)」、
電気化学協会'93秋季大会、2D08 (1993).
11. 藤見 正、宇恵 誠、直井勝彦、
「in-situ FFTインピーダンス、EQCM法によるアルミ電解酸化膜の成長過程」、
電気化学協会'93秋季大会、2D08 (1993).
12. 宇恵 誠、
「ガンマーブチロラクトン系電解液の電導度解析」、
平成6年3月度電解蓄電器研究会 (1994).

13. 直井勝彦、藤見 正、宇恵 誠、
「in-situ EQCM法によるアルミ電解酸化膜の成長過程のモニタリング」、
電気化学協会第61回大会、3K20(1994).
14. 大浦 靖、吉澤篤志、宇恵 誠、直井勝彦、
「in-situ EQCM法によるアルミ電解酸化膜成長過程の評価 (III)」、
電気化学協会'94秋季大会、2J17(1994).
15. Makoto Ue, Hitoshi Asahina and Shoichiro Mori,
"Anodic Oxidation of Aluminum in Organic Electrolytes under Nearly Anhydrous
Condition",
Abstract 187, The Electrochemical Society Extended Abstracts, Vol. 94-2, Miami Beach,
Florida, Oct. 9-14 (1994).
16. 宇恵 誠、
「コンデンサ用誘電体皮膜の生成と電解液の特性」、
第11回A R S鳥羽コンファレンス、56(1994).

[Chapter 3]

1. 井田 和彦、宇恵 誠、森 彰一郎、
「電解液成分の電気化学特性」、
電気化学協会第59回大会、2A19(1992).
2. 宇恵 誠、
「四級アンモニウム塩系電解液の電導度解析」、
電気化学協会'93秋季大会、2D26(1993).
3. 宇恵 誠、関川佐千江、武田政幸、森 彰一郎、
「四級アンモニウム塩系電解液の電導度解析 (2)」、
電気化学協会第61回大会、1E24(1994).
4. Makoto Ue, Kazuhiko Ida and Shoichiro Mori,
"Electrochemical Properties of Organic Liquid Electrolytes for Electrical Double Layer
Capacitors",
Abstract 508, The Electrochemical Society Extended Abstracts, Vol. 94-2, Miami Beach,
Florida, Oct. 9-14 (1994).

[Chapter 4]

1. Makoto Ue, Kazuhiko Ida and Shoichiro Mori,
"Molecular Design of the Solvent for Electrolytes",
IBA Los Angeles Meeting, May 12-13 (1989).
2. 宇恵 誠、
「濃厚溶液の電気伝導率と希薄溶液の電気伝導率パラメータとの相関性」、
電気化学協会'94秋季大会、2D06(1994).

3. Makoto Ue and Shoichiro Mori,
"Mobility and Ionic Association of Lithium Salts in Aprotic Solvents",
Abstract 124, The Electrochemical Society Extended Abstracts, Vol. 94-2, Miami Beach,
Florida, Oct. 9-14 (1994).

8.3. Patents

[Chapter 2]

1. Shoichiro Mori and Makoto Ue,
"Electrolyte Solution for Electrolytic Capacitor",
USP4,715,976 (1987).
2. Shoichiro Mori, Makoto Ue and Kazuhiko Ida,
"Electrolyte for Aluminum Electrolytic Capacitor",
USP4,774,011 (1988).
3. Shoichiro Mori, Makoto Ue and Kazuhiko Ida,
"Electrolyte for Aluminum Electrolytic Capacitor",
USP4,786,429 (1988).
4. Shoichiro Mori, Kazuhiko Ida and Makoto Ue,
"Process for Producing Quaternary Salts",
USP4,892,944 (1990).
5. Shoichiro Mori and Makoto Ue,
"Electrolyte Solution of Quaternary Ammonium Salt for Electrolytic Capacitor",
EP0227433B (1992).
6. Shoichiro Mori, Makoto Ue and Kazuhiko Ida,
"Quaternary Salt Solution Electrolyte for Electrolytic Capacitors",
EP0246825B (1991).
7. Shoichiro Mori, Makoto Ue and Kazuhiko Ida,
"Ammonium Salt Solution as Electrolyte for Electrolytic Capacitors",
EP0221577B (1993).
8. Shoichiro Mori, Kazuhiko Ida and Makoto Ue,
"Process for Producing Quaternary Salts",
EP0291074B (1992).
9. 森 彰一郎、宇恵 誠、
「電解コンデンサ用電解液」、
特公平 3- 6646.
10. 森 彰一郎、宇恵 誠、
「電解コンデンサ用電解液」、
特公平 3- 8092.
11. 森 彰一郎、宇恵 誠、
「電解コンデンサ用電解液」、
特公平 5- 56846.
12. 森 彰一郎、宇恵 誠、
「電解コンデンサ用電解液」、
特公平 6- 11021.

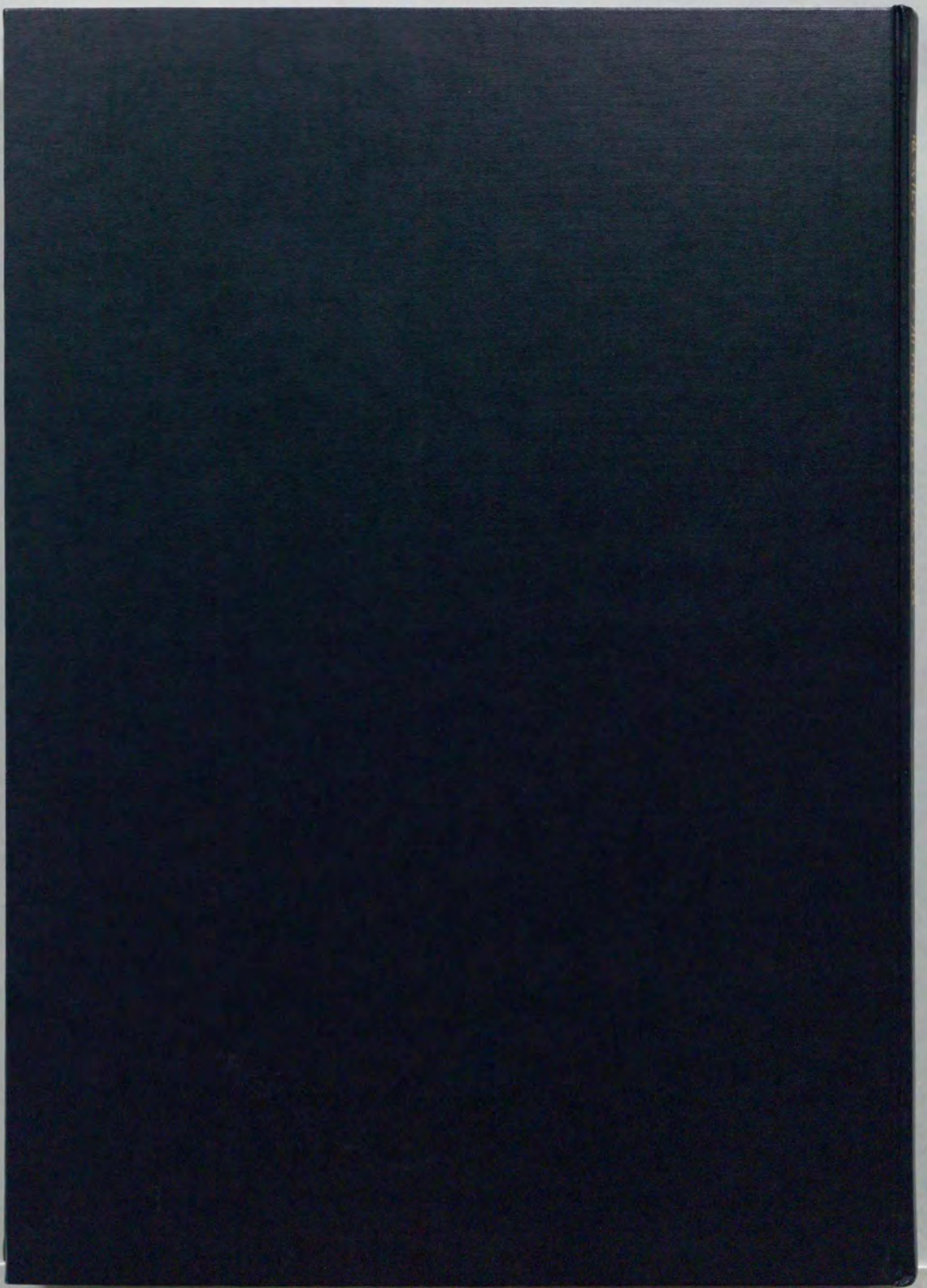
13. 森 彰一郎、井田和彦、宇恵 誠、四級アンモニウム有機酸塩の製造方法、特開昭 63- 280045.
14. 森 彰一郎、井田和彦、宇恵 誠、四級アンモニウム無機酸塩の製造方法、特開昭 63- 284148.
15. 森 彰一郎、井田和彦、宇恵 誠、四級ホスホニウム有機酸塩の製造方法、特開昭 63- 290889.
16. 森 彰一郎、井田和彦、宇恵 誠、四級ホスホニウム無機酸塩の製造方法、特開昭 63- 290890.
17. 宇恵 誠、島 邦久、井田和彦、森 彰一郎、電解コンデンサ用電解液、特開平 1- 194313.
18. 森 彰一郎、井田和彦、宇恵 誠、四級アンモニウム有機酸塩の製造方法、特開平 1- 197462.
19. 宇恵 誠、佐藤智洋、朝比奈 均、アルミニウム酸化皮膜の形成方法及びそれに用いる電解液、特開平 5- 271992.
20. 宇恵 誠、佐藤智洋、朝比奈 均、アルミニウム酸化皮膜の形成方法及びそれに用いる電解液、特開平 5- 271994.

[Chapter 3]

1. 森 彰一郎、宇恵 誠、井田和彦、四級アンモニウムヨウ化物のアニオン交換方法、特開昭 63- 30453.
2. 森 彰一郎、宇恵 誠、井田和彦、四級アンモニウム塩のイオン交換方法、特開昭 63- 30454.
3. 森 彰一郎、井田和彦、宇恵 誠、ホウフッ化脂環式アルキルアンモニウム塩、特開昭 63- 115876.
4. 森 彰一郎、宇恵 誠、井田和彦、小湊あさを、テトラアルキル四級無機酸塩の製造方法、特開昭 63- 174954.

[Chapter 5]

1. 安川栄起、森 彰一郎、皆藤光雅、宇恵 誠、高分子ゲル電解質組成物、特開平 1- 309205.
2. 皆藤光雅、宇恵 誠、森 彰一郎、ゲル状電解液、特開平 2- 14506.

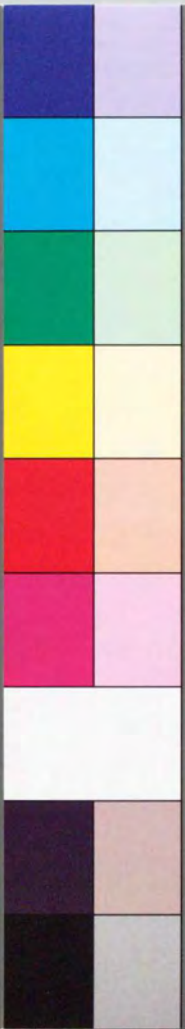


1 2 3 4 5 6 7 8 9 10 11 12 13 14 15 16 17 18 19
inches
1 2 3 4 5 6 7 8 9
cm

Kodak Color Control Patches

© Kodak, 2007 TM Kodak

Blue Cyan Green Yellow Red Magenta White 3/Color Black



Kodak Gray Scale



© Kodak, 2007 TM Kodak

A 1 2 3 4 5 6 M 8 9 10 11 12 13 14 15 B 17 18 19

